Aus dem Institut für Neurobiologie

Direktor: Prof. Dr. rer. nat. Henrik Oster

Optogenetic manipulation
of circadian rhythms

Inauguraldissertation

zur Erlangung der Doktorwürde

der Universität zu Lübeck

- aus der Sektion Medizin –

vorgelegt von

Christopher Matthias Blaum

aus Krefeld

Hamburg 2021

1. Berichterstatter/Berichterstatterin: Prof. Dr. rer. nat. Henrik Oster

2. Berichterstatter/Berichterstatterin: Prof. Dr. rer. nat. Jens Mittag

Tag der mündlichen Prüfung: 2.3.2022

Zum Druck genehmigt. Lübeck, den 2.3.2022

Promotionskommission der Sektion Medizin

meinen Eltern

Tables and Figures

Abbreviations

(k)bp	(kilo)basepairs
(m/mi/si)RNA	(messenger/micro/short interfering) Ribonucleic acid
5-HT	5-hydroxytriptamine (serotonin)
AAV	Adeno-associated virus
AMPA	α-amino-3-hydroxy-5-methylisoxazole-4-propionic acid
AVP	Arginine vasopressin
BMAL1	Brain and Muscle ARNTL-like 1
bPAC	*Beggiatoa* photoactivated adenylyl cyclase
Ca^{2+}	Calcium
CaM	Calmodulin
CaMKII	Ca^{2+}/calmodulin-dependent protein kinase II
cAMP	Cyclic adenosine monophosphate
CBP	CREB-binding protein
CCG	Clock controlled gene
cGMP	Cyclic guanosine monophosphate
CK1	Casein kinase 1
CLOCK	Circadian Locomotor Output Cycle Kaput
CRE(B)	Ca2+/cAMP response element (binding protein)
CRY	Cryptochrome
DMEM	Dulbecco's Modified Eagle's Medium
DMSO	Dimethyl sulfoxide
DNA	Deoxyribonucleic acid
ELISA	Enzyme-linked Immunosorbent assay
ERK	Extracellular signal regulated kinase
GABA	Gamma aminobutyric acid
GFP	Green fluorescent protein
GHT	Geniculohypothalamic tract
GRE	Glucocorticoid receptor element
GTPase	G-protein binding guanosine triphosphate
HEPES	(4-(2-hydroxyethyl)-1-piperazineethanesulfonic acid)
LED	Light emitting diode
MAPK	Mitogen-activated protein kinase
NMDA	N-methyl-D-aspartate
NO(S)	Nitric oxide (synthase)
NPY	Neuropeptide Y
PACAP	Pituitary adenylyl cyclase activating polypeptide
PCR	Polymerase chain reaction
PDE	Phosphodiesterase
PER	Period
PKA/C/G	Protein kinase A/C/G
PLC	Phospholipase C
RHT	Retinohypothalamic tract
RORE	Retinoic acid-related orphan receptor response element
SCN	Suprachiasmatic nucleus
TTL	Transcriptional-translational feedback loop
U2OS cells	Human bone osteosarcoma cell line
VGCC	Voltage gated calcium channel
VIP	Vasointestinal polypeptide

1 Introduction

1.1 Life on earth and circadian rhythms

Life on earth is under the influence of rhythmic environmental changes. The earth's rotation around its own axis with a period of 24 h causes the daily light-dark cycle, whilst the gravitational pull of the moon around the earth causes the tides. On a longer time scale, the change of the tilt of the earth's axis relative to the sun over the course of a year gives rise to the seasons.

To this inherently rhythmic and hence predictable habitat life has adapted through the development of molecular mechanisms that function as time keepers and can generate endogenous rhythms. These molecular mechanisms, also called clocks, enable species to anticipate the cyclic environmental changes they are exposed to. This allows the optimal timing of physiological processes such as metabolism (e.g. separating over time counteracting metabolic pathways) or behaviour (e.g. feeding, sleep, reproduction) to the external rhythm, thereby conferring an advantage to species that possess clocks[1–5]. It should thus not be surprising that in both the prokaryotic as well as the eukaryotic domain of life such clocks can be found[6,7]. The existence of human endogenous rhythms were first comprehensively demonstrated by Jürgen Aschoff, who is therefore regarded as one of the founding fathers of chronobiology[8]. The discovery of the underlying molecular mechanisms in the fruitfly *drosophila* was later rewarded with the 2017 Nobel Prize in Physiology or Medicine[9].

The dominant rhythm governing life on earth is the daily light-dark cycle. Endogenous clocks therefore display oscillatory periods of approximately 24 h and are termed *circadian*, deriving from the Latin words *circa* (around) and *dies* (day). External cues that synchronise endogenous clocks to the environment are termed *Zeitgeber*. Light is the most important *Zeitgeber*, others being for example locomotor activity or food intake.

The key properties of a circadian clock are:

- It continues oscillating with a period of approximately 24 h in the absence of environmental cues such as light. This is called "free-running" behaviour, and can be observed under continuous conditions such as continuous darkness
- Its oscillatory period is unaffected by temperature fluctuations in the physiological range (unlike many other biological processes)
- It can adapt to changes in the oscillation of environmental cues such as light or feeding, a process called entrainment

1.2 Anatomical and functional organisation of the mammalian circadian clock

In mammals, the presence of circadian clocks has been demonstrated in many organs and tissues, ranging from the heart, the liver, the pancreas, the adrenal gland, the gut and the lung to adipose tissue, fibroblasts as well as immune cells[10–13]. Rhythmic oscillations can be observed persisting over days in tissue explants of many organs, however without a master synchroniser, the synchrony between individual organs within an organism is lost[10]. Furthermore, single-cell oscillations within a tissue lose synchrony *in vitro*, although persisting phase coherence in the liver has recently been demonstrated *in vivo* in mice with a functional clock present only in hepatocytes[14,15]. The task of coordinating peripheral tissue clocks, aligning them with the daily light-dark cycle, and thus timekeeping on the scale of the whole organism is achieved by a circadian pacemaker residing in the suprachiasmatic nucleus (SCN).

The SCN is a bilateral structure of the ventral hypothalamus located below the III. ventricle and above the optic chiasma[16,17]. Each nucleus consists of a network of approximately 10,000 neurons, where each neuron displays individual cell autonomous molecular and electrical rhythms with intrinsic periods varying from 22 to 30 h[18,19]. The neurons communicate via gap junctions, synaptic transmission and paracrine signaling, creating a complex network[20–25]. This neuronal network oscillates with a much more precise period than single SCN neurons or SCN tissue slices and is robust to external noise, fluctuations of body temperature as well as mutations of clock genes within the network[26–28]. These network properties are a unique feature of the SCN and key to its physiological function[29].

Anatomically the SCN is subdivided into a retinorecipient ventral core region and a dorsal shell region, which differ in their neuronal projections and their expressed neurotransmitters[30–32]. Gamma aminobutyric acid (GABA) is the principal neurotransmitter of SCN neurons, with core and shell neurons also expressing vasointestinal polypeptide (VIP) and arginine vasopressin (AVP), respectively. The SCN core region receives input concerning the environmental light-dark state via the retinohypothalamic tract (RHT), a monosynaptic neuronal connection originating from the retina[33,34]. This is the key input pathway conferring photic information to the SCN[35]. The principal neurotransmitters co-stored in the neurons of the RHT are glutamate and pituitary adenylyl cyclase activating polypeptide (PACAP), which are released upon light exposure[36,37]. An additional multisynaptic input pathway conferring photic information involves the geniculohypothalamic tract (GHT)[38–40]. This pathway modulates SCN responses to retinal input and has been implicated in adjustment to environmentally occurring light regimes and seasonal photoperiod changes[41–43].

It furthermore confers information on non-photic stimuli to the SCN, a role also assumed by the third major input pathway to the SCN originating from the median raphe nuclei[44–46]. The GHT uses GABA and neuropeptide Y (NPY) as its neurotransmitters, whilst the projections from the median raphe nuclei are serotoninergic.

SCN neurons project mainly to hypothalamic and thalamic brain regions, where they act by rhythmic release of neurotransmitters such as GABA or glutamate as well as peptides such as AVP or prokineticin 2[47–51]. Non-neuronal output signals such as diffusible factors are equally able to convey signals from the SCN, governing locomotor activity but not endocrine rhythms[52–54]. The output signals then directly and indirectly drive circadian rhythms and physiology of the organism[55]. The paraventricular nucleus of the hypothalamus assumes an important role in many of these direct pathways[56]: it links the SCN to the autonomous nervous system and thus to peripheral organs such as the adrenal gland, pancreas and the liver[57–62]. It furthermore links the SCN to the pituitary gland and thus the hypothalamic-pituitary-adrenal gland (HPA) axis, with rhythmic glucocorticoid signaling a potent synchronising agent for peripheral clocks throughout the body[63,64]. Finally, it connects the SCN to the pineal gland, which synthesises the hormone melatonin[65,66]. Melatonin in turn has been implicated in the circadian rhythm of blood glucose by acting on the pancreas, whilst also affecting the sleep-wake cycle and mediating seasonal changes in mammals[67,68]. Indirect influences on peripheral tissue clocks are mediated via the SCN-controlled sleep-wake cycle. This applies to the *Zeitgeber* locomotor-activity and feeding, both of which can only occur during an awake state. Locomotor-activity rhythms affect body temperature which in turn affects circadian rhythms in peripheral organs[28,69]. Food intake rhythms are equally able to influence circadian rhythms in the liver and other peripheral organs[70,71]. Thus signaling between the SCN and peripheral clocks involves many pathways, which in their entirety and in their interplay are still incompletely understood, with the importance of each signaling pathway likely to vary between different tissue clocks.

In summary the SCN is anatomically uniquely positioned, connecting the retina, the brain and peripheral organs. Combined with its precise and robust circadian oscillation, this enables the SCN to act as the principle timekeeper of the organism and to reliably control and coordinate physiological function and peripheral circadian rhythms. The significance of the SCN is demonstrated by experiments involving rodents with a completely lesioned SCN: these animals display abolished circadian rhythms, which can be rescued by transplantation of SCN tissue[16,72]. Crucially, the period of newly observed rhythms in the lesioned animal matches the oscillating period of the donor SCN, demonstrating its hierarchy in relation to downstream tissue clocks[73].

1.3 Circadian time keeping: the molecular mechanisms

The molecular mechanism of circadian clocks in mammals consists of transcriptional-translational feedback loops (TTL), the basis of which is similar in both SCN neurons as well as peripheral tissues (**Fig. 1.1**)[74–76].

The positive arm of the TTL consists of the protein products of the clock genes *Bmal1* and *Clock*[77,78]. BMAL1 (Brain and Muscle Arnt-like Protein-1) and CLOCK (Circadian Locomotor Output Cycle Kaput) heterodimerise facilitated by the presence of PAS (Per-Arnt-Sim) domains. The heterodimer acts as a transcription factor by binding to E-boxes, palindromic DNA-regulatory sequences containing the sequence 5'-CACGTG-3' upstream of target genes, via basic helix-loop-helix domains (bHLH) in both proteins[79–81]. Target genes include the clock genes *Per1*[82,83], *Per2*[84–86] and *Per3*[87,88] (*Period* 1-3) as well as *Cry1* and *Cry2* (*Cryptochrome* 1-2)[89,90]. The BMAL/CLOCK1 heterodimer activates their transcription beginning in the early morning hours. The protein products of these activated genes form the negative arm of the TTL: PER and CRY accumulate in the cytosol over the course of the day and heterodimerise themselves, thereby stabilising each other[90]. Once a threshold concentration of the PER/CRY heterodimer is reached towards the end of daytime, it translocates into the nucleus and represses the transcription of its constituents driven by the BMAL1/CLOCK heterodimer[91–93]. As a consequence the concentrations of PER and CRY fall due to both their inhibited transcription as well as their proteasomal degradation over the course of the night. This allows BMAL1 and CLOCK to initiate *Per* and *Cry* transcription from anew at the start of the day. Due to the time delay associated with transcription, translation, dimerisation and nuclear translocation, inhibitory feedback is not immediate and hence a molecular oscillation results, with PER/CRY cycling in antiphase to BMAL1/CLOCK.

A second accessory TTL exists, functioning to stabilise the period of the "core" TTL. The CLOCK/BMAL1 heterodimer also binds to E-boxes upstream of *Rev-erbα* and *Rorα*, genes encoding the retinoic acid receptor-related orphan receptors REV-ERBα und RORα. These transcription factors bind directly to retinoic acid-related orphan receptor response elements (ROREs) in the *Bmal1* promoter, leading to an upregulation (RORα) or downregulation (REV-ERBα) of *Bmal1* transcription[94–97]. The PER/CRY heterodimer represses the transcription of *Rev-erbα*, so that with falling concentrations of REV-ERBα suppression of *Bmal1* transcription is lifted, resulting in higher BMAL1 concentrations as the cycle starts again. As a result BMAL1 oscillates in antiphase to PER and CRY.
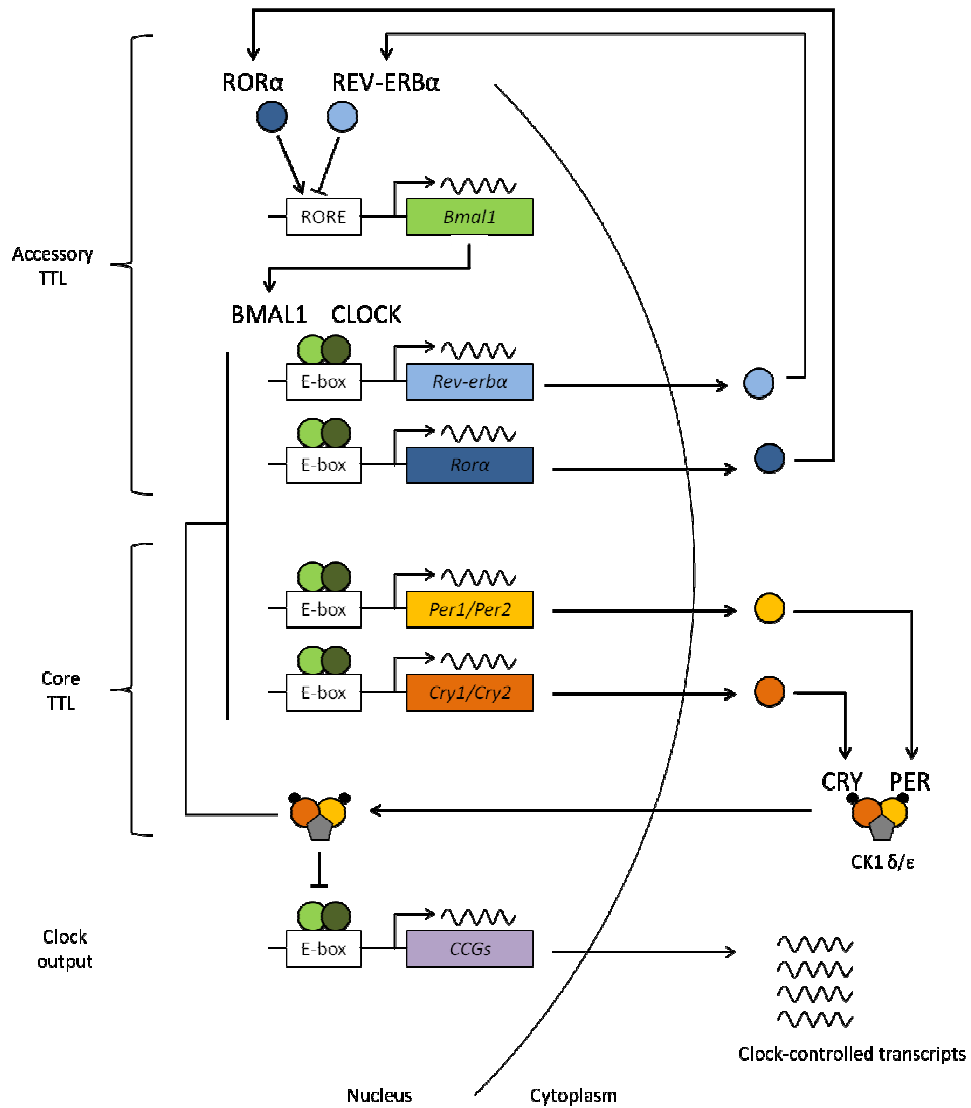
Fig. 1.1: Overview of the core mammalian circadian oscillator

Transcriptional/translational loops (TTLs) result in molecular oscillations driving downstream rhythms. The positive arm of the core TTL consists of the CLOCK/BMAL1 heterodimer, which acts via E-box mediated transcription of *Per* and *Cry*. PER and CRY form the negative arm of the TTL by heterodimerising and repressing the CLOCK/BMAL1 transcription complex upon translocation into the nucleus. Phosphorylation of CRY and PER by CK1δ/ε and AMPK (the latter not shown) as signified by black dots determines protein stability and turnover. An accessory TTL involving REV-ERBα and RORα stabilises the core TTL. Clock controlled genes, e.g. driven by E-box mediated transcription, form the output of the TTL. For further details see section 1.4. Adapted and simplified from Takahashi (2017)[98]

Abbreviations: AMPK, Adenosine monophosphate-activated protein kinase; BMAL1, Brain and Muscle Arnt-like Protein-1; *CCG*, clock controlled gene; CK1, casein kinase 1; CLOCK, Circadian Locomotor Output Cycle Kaput; CRY, Cryptochrome; PER, Period; REV-ERB*α*, Reverse erythroblastic leukemia viral oncogene homolog alpha; ROR*α*, Retinoic acid-related orphan receptor alpha; RORE, retinoic acid-related orphan receptor response elements

The period length of the core TTL is determined by the stability of the repressor proteins PER and CRY, which are influenced by dimerisation, and post-translational modifications, particularly via alterations in phosphorylation state and ubiquitination. Phosphorylation events both sustain and set the rate of circadian oscillations[99–102]. The casein kinases 1ε/δ (CK1ε/δ) associate with the PER/CRY dimer and phosphorylate the PER proteins, thereby governing both their subcellular localisation (nuclear vs. cytoplasmic) as well as their turnover, since phosphorylation marks the proteins for proteasomal degradation[103–106]. Adenosine monophosphate-activated protein kinase (AMPK) in turn phosphorylates CRY, equally targeting it for degradation[107]. Ubiquitination precedes proteosomal degradation and is thus a second key event governing PER/CRY stability[108–110]. Delayed nuclear entry or delayed degradation of the PER proteins both lead to prolonged circadian periods, with converse effects observed if these processes are accelerated[111–114].

Concerning clock "output", E-box mediated transcription drives the expression of the so-called clock-controlled genes, for example the D-site albumin promoter binding protein (DBP)[115]. DBP acts as a transcription factor at D-box-enhancer elements, in turn generating rhythmic expression of downstream genes and regulating circadian behaviour[116,117]. ROREs have also been implicated in mediating circadian transcription of target genes[118]. Thus, both the core as well as the accessory TTL are involved in regulating behaviour and circadian physiology. More than 40% of mammalian protein coding genes display circadian rhythms in at least one tissue, with around 10% of genes displaying circadian rhythms in a given organ [119–121]. In the liver, for example, key genes of glucose metabolism, steroid biosynthesis and detoxification are under circadian control[121].

Finally, it has to be stressed that the molecular mechanisms underlying circadian oscillations are far more complex than outlined here. Studies in recent years have elucidated transcriptional, post-transcriptional, translational and post-translational processes regulating both the core TTL as well as the circadian-controlled transcriptome/translatome. Examples include chromatin remodeling, RNA splicing, mRNA polyadenylation and mRNA regulation by miRNAs, as well as further phosphorylation, acetylation and sumoylation steps of the clock proteins[74,98,122]. The significance of these discoveries is that non-rhythmic mRNA transcripts can yet yield rhythmic proteins, or that proteins with no circadian variation in concentration can yet display circadian functionality by rhythmic modification, highlighting a multi-layered control of molecular circadian mechanisms[123,124].

1.4 Mechanisms of clock resetting

As stated earlier, the ability to adapt to changes in the oscillations of environmental cues is a fundamental property of a circadian clock. The clock in the SCN is most responsive to changes in the light/dark cycle. Light phase-shifts the clock in the SCN in a temporally restricted manner: exposure in the early night causes a phase delay, exposure in the late night causes a phase advance, and exposure during the day has no effect on phase[125,126]. **Fig. 1.2** schematically illustrates phase advances and delays for a nocturnal rodent exposed to a light pulse either in the early or late night.
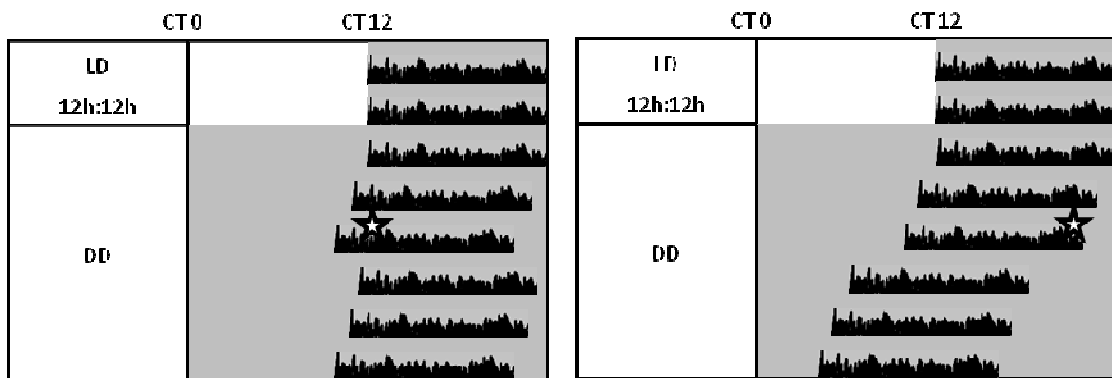
Fig. 1.2: Light pulses cause phase shifts in nocturnal rodents.

Schematically depicted actogram of a nocturnal rodent subjected to a nocturnal light pulse under constant darkness conditions (DD). Activity bouts of the rodent are represented by black bars. Each row represents 24 h, CT denoting circadian time. Initially, the rodent is entrained to a 24 h light-dark (LD) cycle (CT 0 = lights on, CT 12 = lights off). Upon release into darkness, the rodent begins to free-run at its intrinsic period, which in this case is less than 24 h. Stimulation with a 15 min light pulse (marked by a star) during the early night and the late subjective night causes phase delays (left) and advances (right) respectively.

The following sections will discuss the physiological and molecular mechanisms underlying this phase-response relationship. It will discuss how photic input as well as signals from other pathways converge on the SCN, initiating a complex cascade of intracellular signaling which leads to both the induction of clock genes as well as posttranslational effects on the proteins expressed by clock genes. As a result the phase of the molecular clock machinery in the SCN is shifted.

1.5 Light causes the upregulation of intracellular signaling cascades in the SCN

Photic input is first registered by intrinsically photosensitive retinal ganglion cells expressing the photopigment melanopsin[127–129]. This information is passed on via the retinohypothalamic tract (RHT), which releases the neurotransmitters glutamate and PACAP upon light exposure[36,37]. The integrity of this input pathway to the SCN, from melanopsin via the RHT to neurotransmitter secretion, is essential for physiological phase shifting[35,130,131]. Glutamate is regarded as the primary neurotransmitter of the RHT, whilst PACAP is assigned a modulatory function, although its role is less clearly understood (cf. section 1.9)[132]. Glutamate binds to postsynaptic NMDA- and AMPA receptors in the neurons of the ventrolateral region of the SCN, causing a depolarisation of the neuronal membrane[133–135]. This leads to an influx of calcium, which further depolarises the membrane, thus enabling more calcium influx via voltage-gated calcium channels (VGCCs)[136,137]. Cytosolic calcium levels can also be augmented by release from intracellular calcium stores, but only during the early night[138]. The increased cytosolic calcium levels lead to the activation of a host of intracellular signaling cascades, partly mediated by the calcium/calmodulin complex. In the SCN, several key pathways have been implicated in the signal transduction of photic stimuli:

- calcium/calmodulin-dependent protein kinase II (CaMKII) phosphorylates neuronal nitric oxide synthase (nNOS), which in turn activates soluble guanylyl cyclase (sGC), leading to an increase in cGMP, thus activating protein kinase G (PKG)[139–142]
- via the small GTPase Ras, the p44/p42 mitogen-activated protein kinase (MAPK) pathway is activated, the cascade itself potentially also being a downstream target of CaMKII [143–146]
- the activation of adenylyl cyclase causes an increase in cAMP, in turn activating protein kinase A (PKA)[147]
- calcium and diacylglycerol activate protein kinase C (PKC)[148–150]

Negative regulators of these pathways exert control by limiting signal duration or intensity. As examples concerning the MAPK pathway, Raf kinase inhibitor protein (RKIP), the phosphatase PHLPP1 and the light-inducible MAP kinase phosphatase 1 (MKP1) all contribute to physiological phase shifting and/or are likely to act via a negative feedback mechanism[151–153].

1.6 Light-induced gene expression in the SCN

The calcium-triggered signaling cascades lead to an induction of gene expression[154]. The different cascades converge on a common target, which is the Ca^{2+}/cAMP response element binding protein (CREB)[155,156]. This transcription factor binds to Ca^{2+}/cAMP response elements (CREs), short DNA binding sites containing the palindromic sequence 5'-TGACGTCA-3' in the promoter region of target genes. Once phosphorylated, pCREB in association with other proteins such as CREB binding protein (CBP) then induces gene transcription, which in the SCN is restricted to the subjective night[157]. In the SCN, phosphorylation of CREB at Ser133 and at Ser142 has been shown to regulate light-induced phase shifting[158–160]. The critical nature of CREB/CRE driven transcription is highlighted by the observation that CRE-decoy oligodeoxynucleotides can block light induced phase advances *in vivo*[161]. Similarly to the upstream signaling cascades, CREB/CRE-driven transcription is regulated by a negative feedback loop involving CRTC1 (CREB-regulated transcription coactivator)[162,163]. A further regulator of CREB/CRE driven transcription is the cAMP-responsive element modulator ICER (inducible cAMP early repressor), which is light-inducible in the SCN and has been implicated in control of peripheral clocks, although its exact role in SCN resetting remains to be elucidated[164–166].

Several genes have been demonstrated to be light-inducible in the SCN in a phase-restricted manner at night, amongst them the *Period* genes *Per1* and *Per2*, but also immediate early genes like *cFos* and *junB*[167–169]. In the case of *cFos* the transcriptional response to light is rapid, mRNA levels rising within minutes after a light pulse and peaking as soon as 30 min later[84,168]. Of the *Period* genes, only *Per1* and *Per2* are transiently light-inducible, however with different response kinetics, different phase responsiveness and with a different spatial distribution within the SCN[170,171]. In response to a light pulse in the late night (i.e. a phase-advancing light pulse) *Per1* mRNA quickly rises and peaks after 60-90 min. Expression is initially confined to the retinorecipient core region of the SCN, later spreading throughout the SCN to the shell region[84,171]. In response to a light pulse in the early night (i.e. a phase-delaying light pulse) *Per1* mRNA displays similar induction kinetics in the core SCN, but no significant expression in the shell at any time point[171,172]. *Per2* mRNA, on the other hand, is only inducible by a light pulse in the early night (i.e. a phase delaying light pulse), maximum transcript levels being observed after 120 min in both the core and shell of the SCN. Prolonged raised *Per2* mRNA-levels in response to a phase-delaying light pulse have also been reported, potentially reflecting a posttranscriptional mechanism augmenting mRNA stability[173].

The reported expression patterns of the proteins PER1 and PER2 in the SCN after a light pulse largely match those of the respective mRNAs: PER1 expression is augmented in both the core and the shell of the SCN in response to phase-advancing and -delaying light pulses, whilst PER2 expression is only raised by a phase-delaying, early-night light pulse[174].

Due to its robust response to phase-shifting light pulses, the induction of *Per1* appears to be a critical step determining phase-shifts[170]: *Per1* is only inducible by light at times when a light-pulse causes a phase shift of the organism, the threshold of light intensity for *Per1* induction matches that required for phase shifts, the speed of induction is consistent with an initiating role in the process of a phase shift and the magnitude of the observed phase shifts correlates with the amount of *Per1* induction[172]. Furthermore, *Per1* antisense oligodeoxynucleotides can block light- or glutamate-induced phase shifts in the SCN[175]. The role of *Per2* appears to be confined to mediating phase delays, supported by its time-restricted inducibility in the early night. At this time, *Per1* and *Per2* assume additive roles, since phase delays can be blocked completely by simultaneous application of both *Per1* and *Per2* oligodeoxynucleotides[176]. Further evidence for the different roles of the *Period* genes is derived from experiments involving *Per* mutant mice: *Per1* mutants fail to phase advance in response to a light pulse in the late night, whilst *Per2* mutants fail to phase delay in response to a light pulse in the early night[177]. Thus, *Per1* is the principal gene involved in phase advances, whilst also being implemented in phase delays. *Per2* is involved in mediating phase delays, but does not seem to be involved in phase advances. Mechanistically, upregulation of *Per1* in the late night initiates the circadian cycle prematurely, thus drawing forward the phase of the clock. Induction of *Per1* and *Per2* during the falling arm of their mRNA cycle is thought to cause prolonged levels of PERIOD proteins, thus sustained BMAL/CLOCK repression and, hence, a phase delay.

As for the immediate early genes, *cFos* and *junB* antisense oligodeoxynucleotides can block light-induced phase shifts similarly to their *Per1* and *Per2* counterparts[178]. A strong correlation also exists between the light threshold required for phase shifts and *cFos* induction, although the correlation between the magnitude of the phase shift and the amount of *cFos* induction is less clear[179,180]. The corresponding proteins heterodimerise, forming the transcription factor activator protein 1 (AP-1). AP-1 can act at CRE and AP-1 consensus sites, thus a possible link between the immediate early genes and *Period* gene transcription exists[181]. Light has furthermore been shown to alter the composition of AP-1 and its binding activity in the SCN, particularly the retinorecipient ventrolateral region[169,182,183].

However, the induction of *Per1* by light occurs more quickly than synthesis of e.g. cFOS, meaning that, at least for induction by light, a direct role for the immediate early genes in *Period* gene transcription is rather unlikely[172]. Furthermore, whilst there is evidence that cFOS can modulate BMAL1/CLOCK-driven *Per1* transcription, the same has not been demonstrated for CREB-driven transcription[184].

The role of the immediate early genes and their possible interplay with *Period* genes in phase shifting is, thus, incompletely understood. The currently accepted view is that the induction of the *Period* genes is the primary event required for light-induced phase shifts, whilst induction of the immediate early genes reflects unspecific transcriptional activation.

1.7 Light-induced posttranslational changes in the SCN

As described in section 1.3, the concentration and stability of PER proteins are key variables determining the speed of the molecular circadian cycle. Posttranslational modifications influencing these variables thus offer a second mechanism by which activated signaling cascades can implement phase shifts.

For example, activated protein kinase C α (PKCα) transiently interacts with and phosphorylates PER2. As a result, PER2 is retained in the cytoplasm, delaying the negative arm of the TTL[149]. Similarly, PKC modulates PER1 stability by a posttranslational hitherto unknown mechanism, possibly by preventing its degradation[150]. Discrepant results exist concerning the exact role of protein kinase C *in vivo*: mice lacking PKCα display attenuated phase delays in response to a light pulse in the early night, whilst application of a broad-spectrum PKC blocker has been shown to either attenuate or enhance phase delays depending on the experimental set-up[150,185]. This might reflect different roles in photic entrainment for different isoforms of PKC present in the SCN[186]. Importantly, posttranslational modifications affecting PERIOD stability and intracellular distribution enable a rapid impact of photic signals on the molecular clock due to circumventing the need for *de-novo* protein synthesis. Intriguingly, *CKIε* and *CKIδ* have been shown to be weakly upregulated in response to a light pulse in the early night[187]. Combined with altered phase shift responses, particularly phase delays, observed in hamsters carrying a homozygous mutation in *CKIε*, this points towards an involvement of the casein kinases not only in setting the period of circadian rhythms but also in mediating phase shifts[188,189].

The relative contributions of transcription and posttranslational modifications to mediating phase shifts are unknown. It is likely that they depend on circadian time, the exact input pathway to the SCN, and the upregulated intracellular signaling cascade. Phase advances have been shown to depend on protein synthesis, which however does not preclude an additional role for posttranslational modifications[190]. The evidence available points to both mechanisms being involved in phase delays.

1.8 Multiple neurotransmitters and receptors for multiple input pathways

The principal role of glutamate receptors mediating photic input to the SCN has already been described. The following section will briefly expand on the neurotransmitters and corresponding receptors of the further direct and indirect as well as non-photic input pathways to the retinorecipient core of the SCN.

PACAP is the main co-transmitter of the RHT[37]. This neuropeptide from the VIP family binds to two G protein-coupled receptors in the SCN, a PACAP preferring type-1 receptor (PAC1) and a VIP/PACAP preferring type-2 receptor (VPAC2). Its role as ascertained by pharmacological studies depends on the timing of release and its concentration: at low concentrations it causes phase shifts in a similar fashion as light or glutamate and induces expression of the *Period* genes[191,192]. At high concentrations it causes phase advances during the daytime and modulates glutamate-induced phase shifts and upregulation of the *Period* genes during the night[192–194]. Experiments with mice lacking the PAC1 receptor or PACAP have yielded conflicting results, however recent results point towards an integral role for PACAP in glutamate-induced phase advances[195]. The effects of PACAP are mediated via the cAMP/PKA and the MAPK pathways[196,197].

GABA and NPY are the neurotransmitters of the GHT. GABA released by GHT projections binds to $GABA_A$ receptors (ionotropic receptors serving as ligand-gated anion channels) and $GABA_B$ receptors (metabotropic receptors coupled to G_i proteins), thereby acting in an inhibitory manner on SCN neurons and modulating their response to photic input via the RHT[41]. NPY acts via Y_2 and Y_5 receptors, both G_i-coupled receptors inhibiting the adenylyl cyclase pathway, although the PKC pathway has also been implicated[198,199]. Stimulation of the GHT or exposure of the SCN to NPY *in vitro* and *in vivo* results in phase advances during the daytime, an effect remarkably associated with downregulation of the *Period* genes[200–203].

Serotonin is the neurotransmitter of projections from the median raphe nuclei to the SCN and acts via 5-HT$_{1A/1B/7}$ receptors, which are G-coupled receptors with inhibiting (1A, 1B) or stimulating (7) effects on the adenylyl cyclase pathway[204]. 5-HT$_{1B}$ receptors located presynaptically on RHT neurons and 5-HT$_7$ receptors located postsynaptically on SCN neurons are involved in modulating retinal input to the SCN[204,205]. Exposure of the SCN to serotonin or serotonin receptor agonists results in phase advances during the daytime which, similarly as observed with NPY-mediated phase shifts, are associated with downregulation of the *Period* genes[206–208].

Melatonin, whose circadian rhythm is a peripheral output of the SCN, can feed back on the SCN by binding to the G protein-coupled MT$_1$ and MT$_2$ receptors. The latter are implicated in phase advances when melatonin is exogenously administered at dusk or dawn, mediated by the PKC pathway and induction of *Per1* and *Per2*[209–211]. The physiological significance of endogenous melatonin feedback under normal circumstances is little understood, however, sensitivity of the SCN to melatonin offers a therapeutic target for disorders such as jetlag syndrome or insomnia[68]. In blind people, exogenous melatonin administration has even been shown to be able to entrain free-running rhythms[212].

Finally, intercellular signaling between SCN neurons serves as critical input to the individual neuron. As will be discussed in section 1.11, VIP mediates network synchrony amongst core SCN neurons. Pharmacologically, VIP can effect phase shifts of the SCN *in vitro* as well as of rodents *in vivo* with a phase-response curve similar to light (i.e. phase delays in the early night, phase advances in the late night)[213,214]. Its effects are conferred by G$_s$-coupled VPAC2 receptor, and the cAMP/PKA-pathway has been demonstrated to be involved in the induction of the *Period* genes in the late night by VIP[215,216].

In summary, multiple input pathways with a multitude of neurotransmitters and their respective receptors converge on the core region of the SCN. This complexity at the membrane level is mirrored by the intricate web of intracellular signaling cascades influencing circadian processes via transcription and posttranslational modifications. This creates the potential for counteracting signals to impinge simultaneously on SCN neurons, such that phase shifts can be potentiated or attenuated depending on the combination of signals.

1.9 Integrating input signals to the SCN

Nighttime photic phase shifts mediated by glutamate released from the RHT lead to an upregulation of *Per1* and *Per2*. Conversely, daytime non-photic cues such as locomotor activity or feeding lead to downregulation of the *Period* genes[217]. Indeed, suppressing *Per1* expression during the daytime using antisense oligodeoxynucleotides results in phase advances mimicking non-photic phase shifts[218]. As described in sections 1.2 and 1.8, non-photic phase shifts *in vivo* are mediated by NPY and serotonin released by the GHT and projections from the median raphe nuclei, respectively.

The SCN integrates these incoming signals, which share intracellular signaling cascades and a transcriptional target and are thus entwined. For example, when applied to SCN slices *in vitro*, glutamate and NPY can cancel each other's phase shifts, with NPY capable of suppressing glutamate-induced upregulation of *Per1* and *Per2*[219,220]. *In vivo*, photic phase shifts are blocked by the administration of serotonin receptor agonists and modulated by administration of NPY[199,221]. Consistent with these pharmacological manipulations, photic phase response curves are altered by hypocaloric feeding[222].

Integration of photic signals in the SCN is likely to occur on many levels. As an example, on the level of the signaling cascades, different input pathways stimulating G_s- and G_i-coupled receptors could modulate adenylyl cyclase activity in a counteracting manner, the net activity determining the strength of further signal transduction. On the transcriptional level, the *Per1* promotor serves as the integrator for diverse signaling cascades, such as the PKA and the MAPK-pathways which converge separately on CREB/CRE-driven transcription[223]. The *Per1* promotor furthermore integrates E-box driven with CRE-driven transcription, which are independent of one another[223]. In peripheral tissues, the presence of glucocorticoid response elements (GREs) adds a further pathway for clockwork access. Finally, counteracting transcriptional and posttranslational effects could differentially regulate the circadian clockwork. For example, light can suppress serotonin-mediated phase shifts despite downregulation of the *Period* genes, pointing to an additional non-transcriptional mechanism[224]

The exact transcriptional or posttranslational response of the SCN thus not only depends on the circadian time, but also on the nature and multitude of active input pathways and the consecutively upregulated intracellular signaling cascades.

1.10 Different molecular mechanisms underlying phase advances and delays

Revisiting the mechanisms underlying photic phase shifts, differences between phase advances and phase delays emerge with respect to the neurotransmitters, calcium sources and signaling cascades implicated.

For phase advances during the late night, the initial calcium influx via NMDA receptors is augmented by L-type VGCCs[137,225]. The key activated signaling pathway is the NO/cGMP pathway, the effector kinase being PKG[139,140,142]. Both *in vitro* and *in vivo* disruption of this pathway can block light-induced phase advances, whilst inhibition of phosphodiesterases augments them[226–228]. In the SCN, endogenous rhythms of cGMP and PKG activity are observed, which peak at the night-day transition[229]. Phase advances in response to photic stimuli during the late night would therefore correspond to premature activation of this pathway. On a molecular level, the PKG isoform I has been shown to be able to phosphorylate CREB in cell culture experiments, thus CREB/CRE-driven transcription of the *Period* genes is a likely target in the SCN[230]. Conversely, mice deficient for the isoform II display normal phase advances in response to light pulses in the late night and have unaltered levels of *Per1* and *Per2* mRNA compared to wildtype mice[231]. Interestingly in these mice it is the phase delays which are attenuated, with differentially modulated levels of *Per1* and *Per2* mRNA observed in the SCN, an effect that is independent of CREB/CRE-drive transcription. The exact mechanism of action of PKGs in the SCN therefore remains to be elucidated. Additionally the cGMP/PKG pathway is counteracted by the cAMP/PKA pathway in the late night[147].

For phase delays during the early night, the initial calcium influx via NMDA receptors is augmented by T-type VGCCs as well as by release from the endoplasmic reticulum[137,138]. In addition to signaling downstream of the glutamate receptor, PACAP is involved in mediating phase delays[193,195]. This is consistent with *in vitro* data demonstrating the cAMP/PKA pathway to augment glutamate-induced signaling[147]. The further pathways/kinases implicated in mediating phase delays are CaMK isoform II, MAPK and PKG isoform II (acting at the transcriptional level via CREB/CRE) and PKC (acting at the posttranslational level)[141,146,149,150,231].

In summary, the mechanisms of phase advances and delays involve distinct signaling cascades which differentially affect the *Period* genes and PERIOD proteins (cf. sections 1.6 and 1.7). **Fig. 1.3** provides an overview of photic input pathways and signaling in the core SCN.
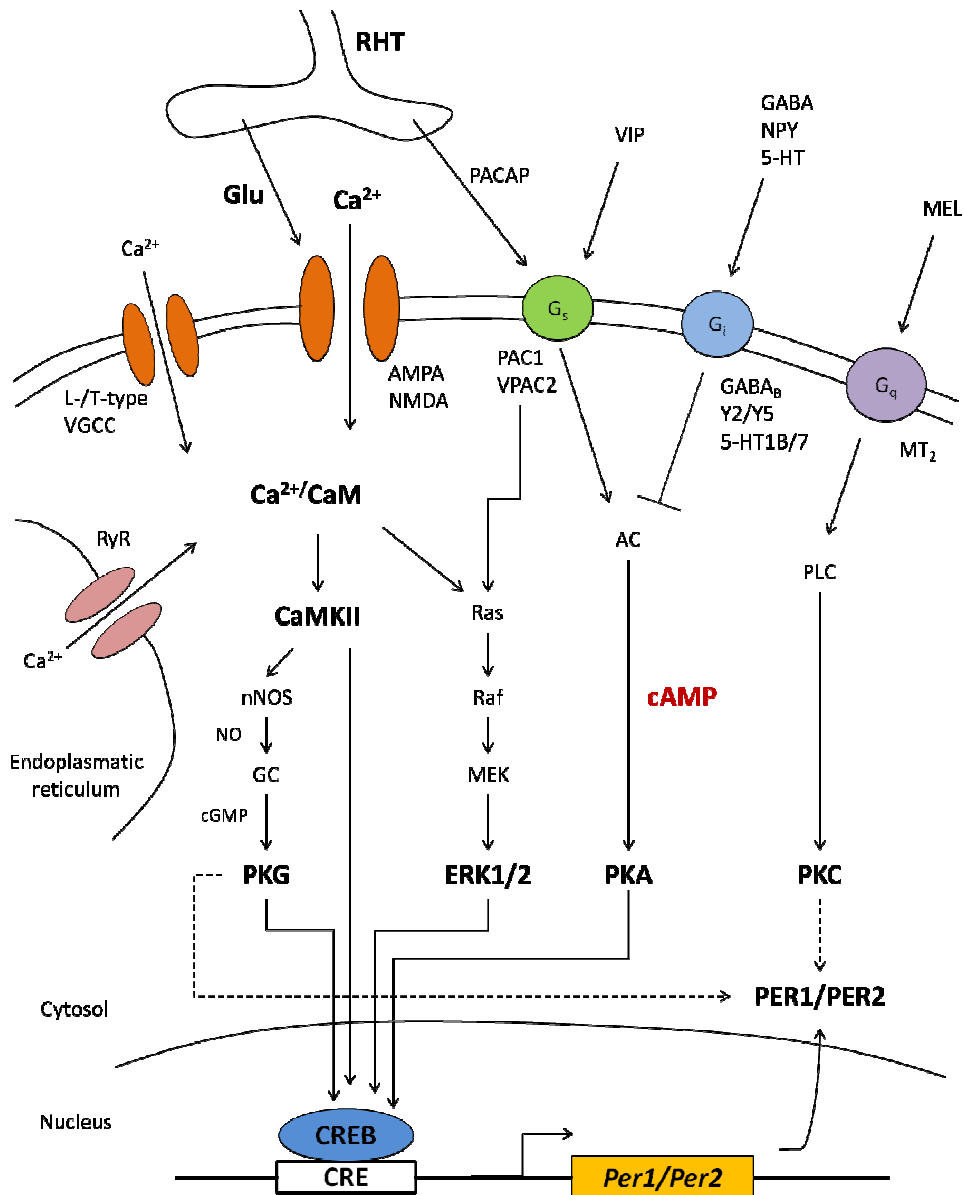
Fig. 1.3: Overview of signaling pathways in the core SCN

Multiple neurotransmitters impinge on the core SCN, eliciting intracellular signaling cascades which activate effector kinases. These converge on CREB, which upon phosphorylation initiates CRE-driven transcription of *Per1* and *Per2*. Furthermore, phosphorylation of PER proteins (dotted lines) conveys posttranslational control of the molecular clock. Note the direct access of the cAMP/PKA pathway on transcriptional regulation of the *Period* genes. Abbreviations: 5-HT, serotonin; AC/GC, adenylyl/guanylyl cyclase; AMPA, α-amino-3-hydroxy-5-methyl-4-isoxazolepropionic acid receptor; cAMP/cGMP, cyclic adenosine/guanosine monophosphate; CaM, calmodulin; CaMKII, Ca^{2+}/calmodulin-dependent protein kinase II; CRE(B), Ca^{2+}/cAMP response element (binding protein); ERK, extracellular signal regulated kinase; GABA, gamma butyric acid; Glu, glutamate; MEL, melatonin; NMDA, N-methyl-D-aspartate receptor; NPY, neuropeptide Y; NO(S), nitric oxide synthase; PACAP, pituitary adenylyl cyclase activating peptide; *Per1/2*, *Period 1/2*; PKA/C/G, protein kinase A/C/G; PLC, phospholipase C; RHT, retinohypothalamic tract; RyR, Ryanodine receptor; VGCC, voltage gated calcium channel; VIP, vasointestinal polypeptide.

16

1.11 Gating mechanisms in the SCN

As briefly touched upon in section 1.4, the SCN displays a marked circadian variation in sensitivity to incoming signals. Photic stimuli are able to cause phase shifts during the subjective night only. The exact mechanism by which photosensitivity of the SCN is temporally gated is unknown, although a promising line of enquiry points towards gating at the level of the glutamate receptors. NMDA receptors in the SCN display an increased conductance during the night, potentially related to altered subunit composition and phosphorylation state of the receptor over the course of the day, leading to altered receptor properties[232,233]. In recent years, posttranscriptional modifications of glutamate receptor mRNA by RNA-editing or alternative splicing have been investigated as sources of temporal gating[234,235]. However, gating at the level of the intracellular signaling cascades is likely to contribute to the observed phase response curves[236].

1.12 Phase shifting the SCN

The previously delineated input pathways impinge on the retinorecipient "core" neurons of the SCN, whose molecular clockwork is the first to be perturbed, leading to their phase resetting. However the number of neurons which are immediately reset is small (<25%)[237]. In order for the whole organism to adapt to the phase-shifting stimulus, first the whole SCN network has to be reset, which can then convey the new phase to peripheral oscillators. Intercellular communication between SCN neurons is paramount for this process – first amongst the group of retinorecipient neurons in order to reinforce the new phase, secondly between retinorecipient and the non-retinorecipient neurons in order to transmit the new phase.

Rhythmic release of neuropeptides, neurotransmitters as well as paracrine signals are implicated in this process[25,238]. Several layers of evidence point to VIP signaling being a crucial component required for intra-SCN synchrony[214,215,239–243]. On an intracellular level, the signal transduction has been described to be dependent on the cAMP/PKA , the MAPK and the PLC/PKC pathways[244–246]. A further role in synchronising cells has been described for GABA, which appears to be of particular significance for core-shell communication[247,248]. Signaling by diffusible molecules such as NO is also discussed as a possible synchronising agent[249].

Resetting of the SCN in response to a single light pulse is thought to be rapid (within 2 h)[250,251]. Consistent with the principal role of *Per1* in mediating phase shifts, *Per1* promotor activity is phase-shifted within a similar time scale in response to a brief phase-shifting stimulus[252]. Conversely, resetting the SCN to a new light-dark cycle shifted by several hours as tested in a jetlag paradigm takes several days. During this time, the core and shell SCN are desynchronised, with the core shifting quickly whilst the shell lagging behind in adapting to the new light regime[253–255]. This internal desynchrony within the SCN and the resulting desynchrony between organs throughout the body is believed to be the cause for jet lag syndrome.

1.13 Optogenetics

The field of optogenetics is concerned with the manipulation of cellular processes by light. The key components to achieve this are light-sensitive proteins. These possess a light-sensing domain and an effector domain, which changes its functionality upon illumination. Once the genes coding for these proteins are delivered to their target cells, intracellular processes can be influenced in a non-invasive, light-dependent manner.

Numerous light-sensitive proteins exist, the family of microbial opsins with their cofactor retinal being the most extensively studied[256,257]. The characterisation of channelrhodopsin 1 and 2 triggered the development of many optogenetic tools for application in the neurosciences[258,259]. Upon insertion of channelrhodopsin into cultured neurons or neuronal tissue *in vitro*, these light-sensitive ion channels allow for the manipulation of neuronal firing rates via light-dependent changes in the membrane potential[260]. Opsin-mediated optogenetic manipulation of behaviour has been demonstrated in *Drosophila* as well as in higher organisms[261,262]. Beyond opsins, other naturally occurring or synthetic light-sensitive proteins exist. Commonly found naturally occurring photoreceptors are the LOV (light-oxygen-voltage-sensitive) domain, which is receptive to blue light via the chromophore flavin mononucleotide (FMN), the BLUF domain (blue light sensor using flavin adenine dinucleotide, FAD) and cryptochrome 2 (CRY2), also requiring FAD[263].

The function of the light-sensitive protein is dependent on the light-induced change in the effector domain. Whilst the channelrhodopsins are light-sensitive ion channels, other effector functionalities are possible. Mechanistically, these are conferred by light-triggered conformational changes or dimerisation/oligomerisation events. The simplest functional consequence is an altered enzymatic activity of the effector domain.

Adenylyl cyclases or guanylyl cyclases that become activated by light, for example, offer control of intracellular signalling via the second messengers cAMP and cGMP, respectively[264,265]. By binding to signalling proteins or kinases, other signalling cascades such as the MAPK pathway can be modulated[266]. Furthermore, optogenetic systems offering control on individual gene transcription have been developed[267,268]. Thus a vast array of intracellular processes has become accessible for manipulation or investigation in a light-sensitive manner. By modifying specific residues, naturally existing light-sensitive proteins can be engineered to display a different absorption spectrum or use a different substrate, further broadening possibilities for manipulating cells[269,270].

Challenges in optogenetics concern the precise delivery of the optogenetic tool to the specific organ/cell/subcellular compartment. Here it has to be sufficiently expressed, and offer sufficient effector strength. From a technical viewpoint, the illumination setup must be able to produce lighting signals with the timing precision required by the target cells (e.g. milliseconds for neurons). If these conditions are met, optogenetics offers non-invasive manipulation of cellular function unrivalled in its high spatial and tight temporal control.

<u>1.14 bPAC – a light-sensitive adenylyl cyclase</u>

In the optogenetic experiments carried out for this work, bPAC (*Beggiatoa* photoactivated adenylyl cyclase) served as the optogenetic tool. It was first isolated in 2011 from the marine and freshwater-dwelling bacterium *Beggiatoa*, which colonises its environment in large microbial mats and has the ability to use hydrogen sulfide as its energy source, thereby displaying a chemolithoautotrophic metabolism[271]. The physiological role of bPAC is unclear, however it was found to be a functional ca. 350-amino acid protein that consists of an N-terminal photoreceptive BLUF domain coupled to a C-terminal catalytic adenylyl cyclase domain. In its purified form it displays an absorption spectrum with maximum absorbance at 411 nm. It is highly light-sensitive, with as little as ca. 4 µW/mm² of light intensity required for half-maximum cAMP production rates, and displays a large dynamic range, with a low dark activity and up to 300-fold increase in cyclase activity upon illumination. Furthermore it has fast kinetic properties, with a time constant of τ = 23 seconds for rise in cAMP after a light burst, as well as a quick recovery from the signaling (active) state to the dark state, with a half-life of τ = 12 seconds after lights-off. These characteristics make it an ideal tool for tight temporal control of cAMP-mediated intracellular processes. Another advantageous property is its small size, enabling it to be incorporated into many vector systems for delivery to target cells.

bPAC has thus far been studied in a variety of settings and in different species. Whilst early uses focused, for example, on affecting grooming behavior of *Drosophila* or studying the regulatory role of cAMP in host-cell invasion and parasite differentiation of *Toxoplasma gondii*, more recent uses have employed a transgenic mouse line expressing bPAC to study synaptic function in the hippocampus[271–273]. The appeal of bPAC as an optogenetic tool is demonstrated by more than 100 citations of the original report describing its use as of September 2021.

1.15 cAMP – second messenger and component of the circadian clock system

cAMP is a ubiquitous second messenger for intracellular signal transduction found throughout the kingdoms of life[274]. Its intracellular concentration is controlled by its rate of synthesis by adenylyl cyclases and its degradation by phosphodiesterases. The classical signaling pathway involving cAMP is initiated by G-protein coupled receptors, which upon extracellular ligand binding activate G_s or G_i proteins. These stimulate and inhibit adenylyl cyclases, thus raising or lowering the concentration of cAMP, respectively. cAMP exerts its effects via three routes: firstly (and most importantly) by activating the regulatory subunit of PKA, which in turn phosphorylates proteins, other kinases or transcription factors such as CREB and therefore influences many intracellular processes. Secondly by binding to cyclic nucleotide gated ion channels, thereby influencing membrane potential. Thirdly by binding to Epac proteins (exchange factor directly activated by cAMP), which act as nucleotide exchange factors for small GTPases that then affect downstream intracellular processes.

In circadian physiology, the cAMP/PKA pathway has long been recognised as an important regulator of CREB/CRE-driven transcription of the *Period* genes and as capable of shifting the phase of the molecular clock[147,157,223,275,276]. Beyond this role in signal transduction in response to external stimuli, a more fundamental function of cAMP as a key constituent of the molecular mechanism of the circadian clock has been proposed. cAMP displays circadian oscillations *in vitro* and *in vivo* in the SCN, peaking towards the end of the night[277,278]. The peak of cAMP precedes that of PER2 rhythms, suggesting the latter are caused by the former via rhythmic CRE-driven transcription. Both a sufficient concentration as well as rhythmicity of cAMP have been shown *in vitro* to be necessary to sustain circadian oscillations in the SCN[279]. Rather than cAMP rhythms representing solely a clock output, these rhythms would also feed back as clock input contributing to core oscillator properties such as period, phase and amplitude[280]. On the other hand, mice with arrhythmic cAMP in the SCN due to the genetic disruption of a circadian regulator which

modulates G_i retain circadian rhythmicity in *Per1* as well as in locomotor activity, although with a lengthened period[281]. Therefore a more nuanced role of cAMP is likely, cytosolic cAMP rhythms interlocking with the TTL to finetune timekeeping in the SCN.

1.16 Optogenetic manipulation of peripheral tissue clocks

Peripheral tissue cells harbor circadian clocks that share the molecular clockwork of their SCN counterparts[13,76]. Analogous to SCN neurons, multiple signaling pathways can induce *Period* genes in peripheral cells, including the cAMP/PKA, the PKC and the MAPK pathways[282,283]. The stimuli reported to induce circadian genes or maintain circadian rhythms in these cells range from treatment with a serum shock, dexamethasone or forskolin to temperature oscillations[13,63,69,284]. Peripheral cells can equally be phase-shifted in a manner similar to SCN neurons, displaying phase advances and delays depending on the time of stimulation[63,285]. Finally, the central role of *Per1* induction in mediating phase shifts in peripheral cells was demonstrated using an artificial zinc finger transcriptional regulator targeted specifically to the distal GRE of *Per1*[286]. Peripheral tissue clocks thus represent valid and easy-to-handle substitutes for experiments investigating circadian clocks, in this case an attempt to induce phase-shifts by optogenetic manipulation. At the time the presented experiments were carried out, no previous reports on optogenetically-mediated phase shifts of circadian rhythms had been published. Since then phase shifts in fibroblasts caused by optogenetic manipulation of the G_s signaling pathway have been reported[287]. Furthermore, optogenetic manipulation of SCN neuron firing rates via a channelrhodopsin has been demonstrated to cause phase shifts both *in vitro* and *in vivo*[288]. These findings will later be discussed in the context of the presented results.

1.17 Summary and aims

Increases in intracellular cAMP can cause phase shifts in cells, the direction of the response depending on the phase of the clock during stimulation. Upregulation of clock genes is a crucial mediator of this process. The aim of this work was therefore:
1. to manipulate intracellular cAMP concentrations in peripheral mammalian cells using an optogenetic tool
2. to investigate changes in circadian oscillations in response to optogenetic stimulation
3. to investigate transcriptional changes, particularly changes in clock gene expression, in response to optogenetic stimulation

2 Methods

2.1 Cells

The U2OS cell line derives from a human osteosarcoma patient and was chosen due to its intact and precise molecular clock machinery[289,290]. Due to the unavailability of U2OS wildtype cells, U2OS cells containing the Tet-On knock-in[291] were used as a surrogate in the experiments investigating optogenetic control of intracellular cAMP concentration and clock gene expression.

U2OS *Bmal1-Luc* cells stably expressing the firefly Luciferase protein under the control of the *Bmal1* promoter[292,293] were used in the experiment investigating the effect of optogenetic stimulation on circadian oscillations. Luciferase catalyses the oxidation of its substrate, D-luciferin, under the emission of light, the intensity of luminescence being proportional to luciferase and thus *Bmal1* concentration. These cells enable the real-time monitoring of the molecular clock over several days via the quantification of the luminescence signal.

2.2 Cell culture and media

Cells were kept in DMEM + GlutaMAX (Gibco) supplemented with 10 % foetal bovine serum (FBS) and penicillin (100 U/ml)/streptomycin (100 µg/ml) and grown in an incubator at 37 °C under an atmosphere of 5 % CO_2. For luminescence measurements the medium was changed immediately prior to transfer into the luminescence plate reader to colourless DMEM (i.e., without phenol red; Gibco) supplemented with stable glutamine (2 mM), HEPES buffer (10 mM), $NaHCO_3$ (352.5 µg/ml) and penicillin (100 U/ml)/streptomycin (100 µg/ml). Sodium-D-luciferin was added to a concentration of 1 µM.

2.3 Cloning and plasmids

The humanised *Beggiatoa* photoactivated adenylyl cyclase plasmid (*pGEM-HE-h_bPAC_cmyc*) was a gift from Peter Hegemann (Addgene plasmid # 28134)[294]. A 1.2-kbp segment containing the *bPAC* sequence was cloned into the *pAAV-GFP* control vector (Cell Biolabs Inc.) using the restriction sites for the *EcoRI* and *SalI* restriction enzymes (**Fig. 2.1**). This yielded the *pAAV-bPAC* plasmid (hereafter referred to as bPAC).
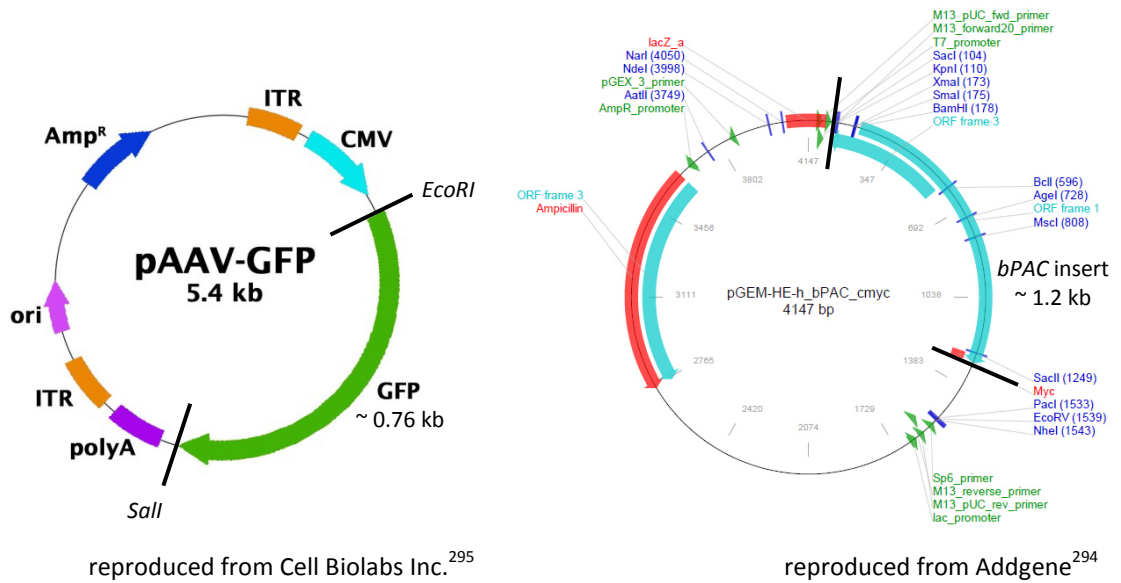
Fig. 2.1: Vector maps of *pAAV-GFP* (Cell Biolabs Inc.) and *pGEM-HE-h_bPAC_cmyc* (Addgene). Restriction sites (left) and amplified sequence (right) highlighted by black bars.

In detail, the *bPAC* sequence of *pGEM-HE-h_bPAC_cmyc* was amplified using the Phusion High Fidelity DNA Polymerase (New England Biolabs) and the primer pair in **Table 2.1**. The *EcoRI* restriction site was added upstream of the *SacI* restriction site to the 5' end of the forward primer, whilst the *SalI* restriction site was added to the 5' end of the reverse primer. An annealing temperature of 72 °C was used as calculated by the New England Biolabs T_m calculator[296], and a 2-step protocol applied (**Table 2.2**).

Primer pair used for amplification (5' – 3')		T_m /°C
Forward	AGTATA<u>GAATTC</u>GAGCTCGGTACCCAGC	66.6
Reverse	TGATA<u>GTCGAC</u>TTACAGGTCCTCCTCCG	68.0

Table 2.1: Primers used for the construction of *AAV-bPAC*.

EcoRI (forward primer) and *SalI* (reverse primer) restriction sites underlined.

98 °C	1x	30 sec
98 °C	30x	10 sec
72 °C		30 sec
72 °C	1x	10 min
4 °C	1x	∞

Table 2.2: 2-step PCR protocol used for amplification

23

The amplified sequence was purified using the QIAquick PCR purification kit (Qiagen). *pAAV-GFP* and the purified sequence coding for *bPAC* were then digested separately using *SalI*-HF and *EcoRI*-HF in CutSmart Buffer (all New England Biolabs) at 37 °C overnight. The digestion mixtures were separated on a 1-% agarose gel, the *bPAC* sequence and the *pAAV* backbone excised and then extracted using the QIAquick Gel Extraction kit (Qiagen). The *bPAC* insert sequence and the *pAAV* backbone were then ligated at 16 °C overnight using the T4 ligase (New England Biolabs). The ligation product, *pAAV-bPAC*, was transformed into *E.coli* strain STBL4 and its identity verified by restriction analysis (**Fig. 2.2**) and sequencing (**Table 2.3**). The unaltered *pAAV-GFP* plasmid (hereafter referred to as GFP) served as a control in the experiments.
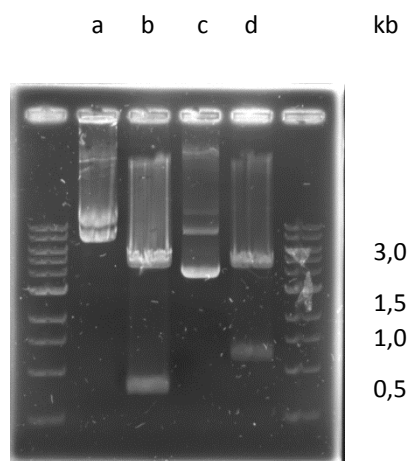
Fig. 2.2 (left): 1-% agarose gel showing restriction analysis of *pAAV-GFP* and *pAAV-bPAC*.

Undigested (a) and digested (b) *pAAV-GFP* showing the cut-out GFP band (760 bp). Undigested (c) and digested (d) *pAAV-bPAC* showing the heavier bPAC insert (1.2 kb). Digestion carried out using *EcoRI*-HF and *SalI*-HF in CutSmart Buffer at 37 °C for 1 h.

Table 2.3 (below): Sequencing analysis of *pAAV-bPAC*
EcoRI restriction site on *pAAV* and *SacI* restriction site on *pGEM-HE-h_bPAC_cmyc* underlined. GFP (green) and bPAC (red) sequences highlighted.

Plasmid (bp)	Sequence
pAAV-GFP (1311 – 1340)	ATTCGAACAT CGATTGAATT CTGAATGGTG
pGEM-HE-h_bPAC_cmyc (91 – 207)	AATTAATTCG AGCTCGGTAC CCAGCTTGCT TGTTCTTTTT GCAGAAGCTC AGAATAAACG CTCAACTTTG GCAGATCAAT TCCCCGGGGA TCCAAGCTTG CCACCATGAT GAAGCGG
pAAV-bPAC (1311 – 1440)	ATTCGAACAT CGATTGAATT CGAGCTCGG TACCCAGCTT GCTTGTTCTT TTTGCAGAAG CTCAGAATAA ACGCTCAACT TTGGCAGATC AATTCCCCGG GGATCCAAGC TTGCCACCAT GATGAAGCGG

Cells were transfected with the plasmids using Lipofectamine 3000 (Invitrogen/Life technologies). Transfection efficiency was estimated by fluorescence microscopy of GFP-transfected cells. Experiments were carried out 48 h post transfection at the earliest.

2.4 Optogenetic and pharmacological stimulation

All procedures carried out on transfected cells were undertaken in near-darkness, such as to tightly control the amount of illumination exposure. For optogenetic stimulation, cells were illuminated up to a maximum of 15 min using an array of white 3.6-mW LED sources whilst placed on a hotplate heated to a temperature of 37 °C. In the case of cells not meant for illumination being present on the same culture plate, these were shielded by opaque covers. Forskolin (10 µM) and dexamethasone (500 nM) were used as pharmacological stimulators, whilst dimethyl sulfoxide (DMSO) was used as a solvent control.

Forskolin, a diterpene derived from the roots of *Coleus forskohlii*, acts as a direct and rapid activator of adenylyl cyclase across a range of species and cell types studied. It is a potent activator even at low concentrations, with a half-maximum concentration in the range of 5 - 10 µM, and its effects are entirely reversible by washing treated cells[297]. Since a medium change itself can perturb circadian rhythms[13], it was deemed the most practicable solution to let forskolin remain in the media after treatment.

2.4.1 Optogenetic manipulation of intracellular cAMP concentration

U2OS cells were seeded into 24-well plates at a density of 10^5 cells/well and transfected 24 h later with 500 ng of either bPAC or GFP. 48 h post transfection cells were either stimulated by continuous illumination of varying duration (1, 5, 15 min), or were left untreated. GFP-transfected cells exposed to varying concentrations of forskolin for 30 min (1, 10, 100 µM) were used as positive controls. Immediately after the completion of treatment cells were lysed in 250 µl 0.1 M HCl for 10 min in darkness. The lysates were centrifuged and cAMP concentrations measured in the supernatant using a direct cAMP ELISA kit (Enzo Life Sciences). An acetylation step was included to increase sensitivity of the ELISA in the low concentration range. Optical densities at 405 nm were measured using a spectrophotometer plate reader (Epoch, Biotek). A standard curve was constructed from samples with known cAMP concentrations using the plate reader software (Gen5/BioTek, Version 2.00.17) and a 5-parameter logistic fit:

$$y(x) = \frac{A-D}{(1+\left(\frac{x}{C}\right)^B)^E} + D \quad \text{where y = OD}_{405\text{nm}} \text{ and } x = \text{[cAMP] /pmol/ml}$$

2.4.2 Optogenetic manipulation of clock gene expression

U2OS cells were seeded into 24-well plates at a density of 10^5 cells/well and transfected with 500 ng of either bPAC or GFP. 48 h post-transfection cells were either stimulated by illumination for 15 min, or were left untreated. GFP-transfected cells stimulated by addition of forskolin (10 µM) were used as positive controls. The cells were incubated and then lysed in 200 µl TRIzol (Ambion) 1, 2, 3 or 4 h after the commencement of treatment.

In a modification of the above procedure, the experiment was repeated with cells that were synchronised 48 h post transfection using dexamethasone (100 nM for 2 h) and stimulated a further 10-12 h later.

RNA Isolation

Total RNA was extracted from TRIzol by addition of 40 µl chloroform to the samples, shaking them for 15 s, leaving them on ice for 5 min, followed by centrifugation at 14,000 rpm for 20 min at 4 °C. The upper aqueous phase was carried forward and 200 µl isopropanol added. After incubation for 30 min at -20 °C the samples were centrifuged at 14,000 rpm for 30 min at 4 °C and the supernatant removed. The RNA pellet was washed with 100 µl pre-chilled 70-% ethanol, centrifuged at 14,000 rpm for 10 min at 4 °C and the supernatant removed. After air drying the pellet for 5-10 min, it was resuspended in 20 µl nuclease-free water. RNA concentration was determined by measuring the optical density of the samples at 260 and 280 nm using a spectrophotometer plate reader (Epoch, BioTek). RNA samples were stored at -80 °C.

Reverse Transcription (RT)

mRNA was transcribed into cDNA using the High-Capacity cDNA Reverse Transcription Kit (Applied Biosystems). 2-3 µg total RNA per sample were topped up to 10 µl with nuclease free water, and the samples heated to 65 °C for 10 min using a thermocycler (Analytik Jena). In the case of low RNA concentrations, the maximum amount of RNA possible (i.e. 10 µl) was carried forward. Subsequently, 10 µl of a reverse transcriptase master mix (**Table 2.4**) were added to each sample. The samples were mixed and the reverse transcription reaction initiated in the thermocycler using the program listed in **Table 2.5**. cDNA samples were diluted 1:20 with nuclease free water and stored at -20 °C.

MultiScribe Reverse Transcriptase	1 µl
25x dNTP mix	0.8 µl
10x RT random primers	2 µl
10x RT buffer	2 µl
Nuclease-free water	4.2 µl

Table 2.4: Reagents and volumes used for the reverse transcription (RT) master mix

25 °C	10 min
37 °C	120 min
85 °C	5 min
4 °C	∞

Table 2.5: Thermocycler program for reverse transcription

qPCR

mRNA levels were determined by quantitative real-time PCR using the GoTaq qPCR SYBR Green Pre-Mix (Promega) and a thermocycler (CFX-96 Touch, BioRad) and the primers in **Table 2.6**.

Primers used for qPCR		T_m /°C	Primer efficiency E (%)
β-*Actin*-f	TGC CGA CAG GAT GCA GAA G	58.8	1.848 (92.4%)
β-*Actin*-r	CTC AGG AGG AGC AAT GAT CTT GAT	61.0	
Per1-f	TCC ATT CGG GTT ACG AAG CT	57.3	1.938 (96.9%)
Per1-r	GCA GCC CTT TCA TCC ACA TC	59.4	
Per2-f	CGT GCC AAG CAG TTG ACT TA	57.3	2.022 (101.1%)
Per2-r	CAG CAA GGC TCA ACA AAT CA	55.3	
cFos-f	CCG GGG ATA GCC TCT CTC ACT	61.8	1.953 (97.6%)
cFos-r	CCA GGT CCG TGC AGA AGT C	61.0	

Table 2.6: Primer sequences (5' – 3'). Primer efficiencies and product specificity were determined by a dilution series and melt curve analysis, respectively.

5 µl of cDNA, 5 µl of the relevant primer mix (1.4 mM) containing the forward and reverse primer for the gene in question and 10 µl of SYBR Green Pre-Mix were mixed together and the amplification program detailed in **Table 2.7** run.

94 °C	1x	5 min
94 °C		15 sec
60 °C	40x	15 sec
72 °C		20 sec
72 °C	1x	5 min

Table 2.7: Amplification program for qPCR. N.B.: a lower annealing temperature (55 °C) was used to amplify *Per1* in order to account for the lower T_m of the *Per1* primers

Melt curves and threshold amplification (C_T) values were obtained via the thermocycler software. Gene expression of the gene of interest in a sample was calculated relative to the housekeeping gene β-*Actin* using the $\Delta\Delta C_T$ method[298]. The mean expression in non-stimulated cells served as the reference point for gene expression over time.

2.4.3 Optogenetic manipulation of endogenous cell rhythms

U2OS *Bmal1-Luc* cells were seeded into 96-well plates at a density of 2×10^4 cells/well and transfected with 100 ng of either bPAC or GFP. 48 h post transfection cells were synchronised with 100 nM dexamethasone (2 h), after which the medium was changed to colourless medium containing sodium D-Luciferin. The plate was transferred to a luminescence plate reader (TriStar LB941, Berthold) and endogenous *BMAL1* rhythms were observed by measuring the luminescence in each well every 5 min. After 24 - 48 h inside the plate reader the plate was removed from the measurement chamber at the appropriate phase in order to be subjected to 15 min of illumination, addition of 10 µM forskolin, DMSO or 500 nM dexamethasone, or to no treatment at all. Afterwards the cells were placed back in the plate reader and post-stimulation *BMAL1* rhythms recorded for a further 24 - 96 h. Oscillations relative to a 24-h running average were calculated and dampened sine fits obtained (**Fig. 2.3**) using Prism 5.00 (GraphPad) and the following formula:

$$y(t) = Ae^{-kt} \sin\left(2\pi \left(\frac{t}{\lambda} - \varphi \right) \right)$$

where

y = luminescence	t = time
A = amplitude	λ = wavelength
k = decay constant	φ = phase

In cases when the dampened formula failed to converge, a simple undampened sine fit was used. To ensure that a stable oscillatory signal was fitted to, the time cells spent acclimatising as judged by visual inspection was omitted from the analysis. A standard cut-off of 6 h after insertion into the plate reader was selected, which, if deemed insufficient was extended to 12 h. Pre-stimulation signals were fitted up to the point of stimulation, whilst post-stimulation signals were fitted for 24, 48 or 72 h depending on the stability of the signal. By comparison of the two signals, the phase response could be analysed (cf. section 3.4). For example, phase shifts (/h) were calculated at 24 and 48 h after stimulation as the time difference between peaks/nadirs of the pre- and post-stimulation sine fits, depending on the phase of stimulation as demonstrated in **Fig. 2.3** (e.g.: stimulation at a nadir → phase shifts calculated at the following nadirs).
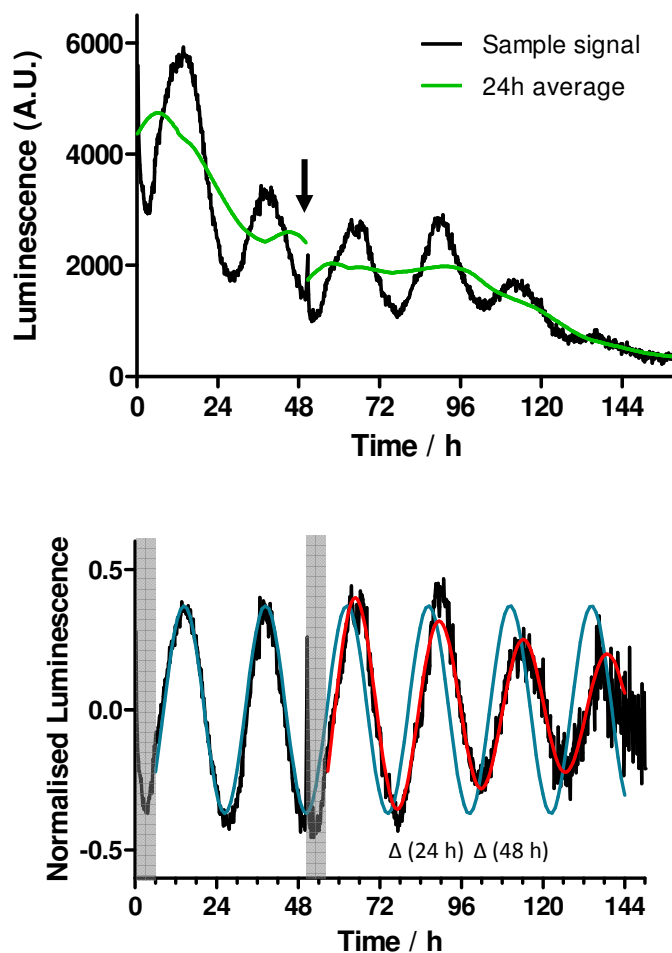
Fig. 2.3: *Above* luminescence signal of a representative sample containing cells transfected with bPAC (black) with a 24 h moving average (green) added. Stimulation time point marked by an arrow. *Below* the same signal divided by the moving average, with pre- and post-stimulation sine fits added (blue and red respectively). The first 6 h in the plate reader, during which cells acclimatised, were always discarded in the analysis (grey shading). Phase shifts denoted by Δ.

2.5 Analysis and statistics

Excel (Microsoft Office 2007) was used to process data. Prism 5.00 (GraphPad) was used for statistical analysis of the results. Numerical data are presented as mean ± standard deviation (SD) for means generated by replicates from the same experiment, or as mean ± error of the mean (SEM) for means of data generated in independent experiments. Means from two sample groups were compared using a two-tailed unpaired Student's t test. More than two groups were compared by 1- or 2-way ANOVA with Bonferroni post-tests. p-values < 0.05 were considered to be statistically significant. Results for Bonferroni post-tests are denoted as ns = p > 0.05, * = p < 0.05, ** = p < 0.01, *** = p < 0.001, unless otherwise stated. Statistical outliers were determined by the Grubbs outlier test (α = 0.05) and excluded from the analysis.

3 Results

3.1 Optogenetic stimulation leads to an increase in intracellular cAMP

The functionality of the *pAAV-bPAC* plasmid was tested by transient transfection of U2OS cells. These were subjected to illumination of varying duration, lysed, and the cAMP concentration in the cell lysates measured by an ELISA. Despite adding an acetylation step in order to increase the ELISA's sensitivity, some GFP control samples as well as non-illuminated bPAC samples were measured to have optical densities outside the range of the standard curve. Since it is not valid to extrapolate the standard curve in order to calculate the cAMP concentrations of samples, the concerned samples were assigned the value zero.

Fig. 3.1 left displays the cAMP concentrations in the cell lysates in response to varying illumination time. 2-way ANOVA showed a significant effect of plasmid used, illumination time and interaction on variance ($p < 0.0001$). Baseline cAMP levels in lysates of non-illuminated cells containing bPAC or GFP were not statistically different (0.037 ± 0.037 nM vs. 0.063 ± 0.038 nM, $p > 0.05$ for Bonferroni post-test). After illumination an increase in cAMP levels was only observed in the lysates of cells containing bPAC, cAMP levels rising to a maximum of 5.7 ± 1.3 nM after 5 min of illumination (vs. 0.048 ± 0.055 nM in the lysate of cells containing GFP, $p < 0.001$ for Bonferroni post-test). cAMP levels after 1 and 15 min of illumination were equally significantly elevated in lysates of cells transfected with bPAC compared to their GFP controls.
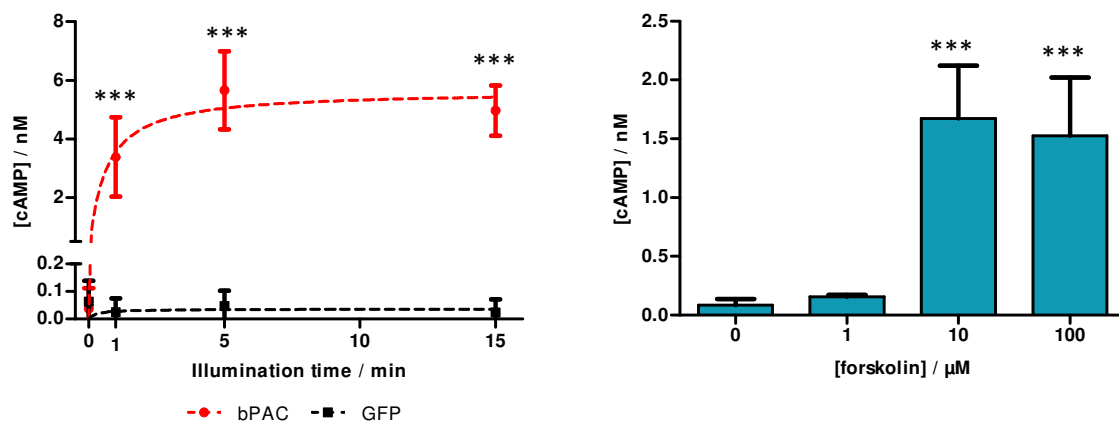
Fig. 3.1:

left: cAMP concentration in U2OS cell lysates in response to varying illumination time. Results plotted as mean ± SD, n = 4. Michaelis-Menten type fit added (dotted line), K_m = 35 s.

right: cAMP concentration in U2OS cell lysates in response to varying forskolin concentration. Results plotted as mean + SD, n = 4.

Bonferroni multiple comparisons testing showed no significant difference between mean cAMP levels at time points 1, 5 and 15 min in cell lysates of cells transfected with bPAC. The observed saturation kinetic was modeled with a Michaelis-Menten curve, yielding a half-saturation time of 35 s. 15 min was carried forward as the standard illumination time in the following experiments.

Fig. 3.1 right displays the cAMP concentrations in cell lysates in response to varying forskolin concentrations. 1-way ANOVA testing showed the means to be significantly different ($p < 0.0001$). Lysates of cells treated with forskolin displayed a significant increase in cAMP levels only for forskolin concentrations ≥ 10 µM ($p < 0.001$, Bonferroni multiple comparisons test vs. untreated cells). cAMP levels measured after stimulation with 10 µM forskolin (1.67 ± 0.22 nM) were of the same order of magnitude as those measured in lysates of illuminated cells containing bPAC. 10 µM forskolin was carried forward as the concentration used for positive controls in the following experiments.

3.2 Optogenetic stimulation leads to an upregulation of *Per1*

The next experiment investigated whether a light-induced cAMP burst would alter the expression of the clock genes *Per1* and *Per2*, since upregulation of these genes is considered a key step in causing phase shifts (cf. section 1.6). In order to understand the kinetics of transcriptional changes, a time profile of mRNA levels was constructed by lysing non-synchronised U2OS cells in hourly intervals up to a maximum of 4 h after illumination or pharmacological stimulation.

Fig. 3.2 displays the time profiles obtained for *Per1* **(left)** and *Per2* **(right)**. Concerning *Per1*, 2-way ANOVA showed a significant effect of treatment, time after stimulation and interaction on variance ($p < 0.0001$ for all). *Per1* was upregulated both in cells containing bPAC that were subjected to illumination as well as in control cells containing GFP that were stimulated with forskolin. 2 h after stimulation was identified as the time point with maximum *Per1* upregulation. At this time point relative expression of *Per1* in illuminated cells containing bPAC was significantly higher than in illuminated cells containing GFP ($p < 0.01$ for Bonferroni post-test). *Per1* expression was not found to differ at the other investigated time points for cells containing bPAC. In cells stimulated with forskolin the point of maximum *Per1* expression was similarly 2 h after stimulation, significantly elevated expression however persisting to 3 h and 4 h after stimulation vs. controls ($p < 0.001$ for all mentioned time points for Bonferroni post-tests).

Concerning *Per2*, the time profile yielded inconclusive results. At no time point after commencement of stimulation was *Per2* expression in stimulated cells different from control cells (p > 0.05 for Bonferroni post-tests). Considering cells transfected with bPAC in isolation, 1-way ANOVA showed *Per2* expression to be significantly higher at 2 h compared to 0 h (p < 0.001). However, given the lack of observed upregulation at this time point in cells stimulated with forskolin as well as the lack of a significant difference of *Per2* expression relative to non-stimulated cells, no clear conclusion about changes in *Per2* could be drawn. *Per2* was thus not investigated further in non-synchronised cells.
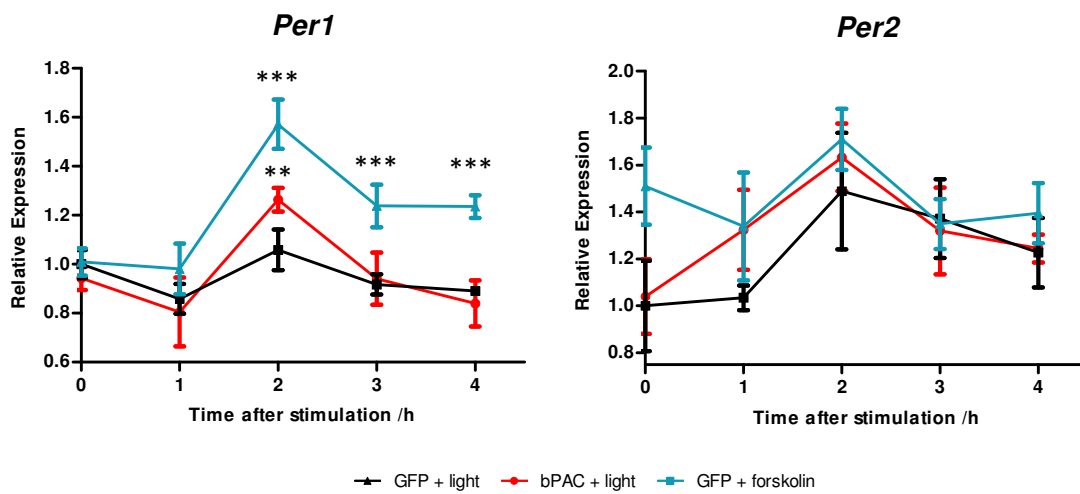
Fig. 3.2: Time profile of the expression of the clock gene *Per1* **(left)** and *Per2* **(right)** in non-synchronised U2OS cells. Expression calculated relative to non-stimulated cells (t = 0) containing the GFP plasmid. Results plotted as mean ± SD, n = 4.

The experiment was thus repeated focusing on the 0 and 2 h time points, and the resulting data pooled (**Fig. 3.3**). Again, 2-way ANOVA confirmed a significant effect of treatment (p < 0.01), time after stimulation (p < 0.001) and interaction (p < 0.01) on variance. Baseline *Per1* expression was not significantly different in non-stimulated cells irrespective of plasmid load (1.00 *vs.* 1.09 ± 0.14 for GFP and bPAC respectively, p > 0.05 for Bonferroni post-test), whilst *Per1* upregulation relative to control cells after 2 h was confirmed (1.02 ± 0.07 *vs.* 1.38 ± 0.09 and 1.68 ± 0.06 for illuminated cells containing GFP, illuminated cells containing bPAC and cells stimulated with forskolin, p < 0.05 and p < 0.001 for Bonferroni post-tests respectively).

Equally when comparing the 0 h and 2 h time points, a significant difference in *Per1* expression was shown for cells treated with forskolin (1.01 ± 0.003 *vs.* 1.68 ± 0.06, $p < 0.001$ for Bonferroni post-test). No significant difference was detected for illuminated cells containing bPAC (1.09 ± 0.14 *vs.* 1.38 ± 0.09, $p > 0.05$ for Bonferroni post-test), likely due to the higher variance of *Per1* expression in non-stimulated cells.
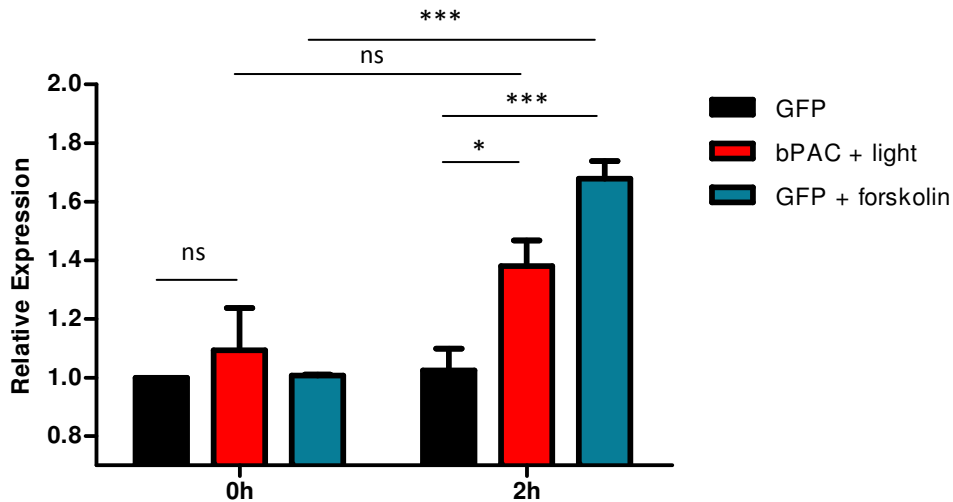
Fig. 3.3: Expression of *Per1* in non-synchronised U2OS cells, non-stimulated and 2 h after stimulation. Expression calculated relative to non-stimulated cells (t = 0) containing the GFP plasmid. Results plotted as mean + SEM, n = 3 independent experiments with 4 replicates each.

3.3 The circadian period is unchanged by bPAC in the absence of light

The previous experiments show that the bPAC plasmid was able to enact a rise in intracellular cAMP and thereby cause an upregulation in *Per1* upon illumination. Of equal importance is the finding that baseline cAMP levels and baseline *Per1* expression did not appear to be altered by the presence of the bPAC plasmid in non-stimulated cells. The next experiment investigated whether key parameters of circadian oscillation such as period and amplitude were affected by the presence of the bPAC plasmid. To this end, U2OS *Bmal1-Luc* cells were transfected with either bPAC or GFP, synchronised with dexamethasone, transferred to a luminescence plate reader and endogenous *Bmal1* rhythms were observed.

Fig. 3.4 displays the results obtained for period (left) and amplitude (right) of circadian oscillations. The period was not found to be different between non-stimulated cells transfected with either bPAC or GFP (23.64 ± 0.51 h vs. 23.56 ± 0.43 h, p = 0.91, unpaired t-test). A significant difference was however observed between the amplitudes of oscillations, which were lower in cells transfected with bPAC (0.34 ± 0.06 vs. 0.53 ± 0.05, p = 0.021, unpaired t-test).
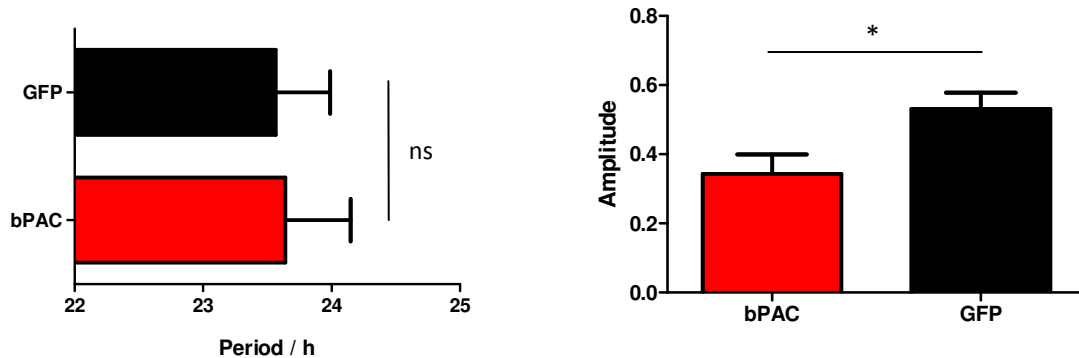
Fig. 3.4: Characterisation of circadian oscillations in U2OS *Bmal1-Luc* cells transfected with bPAC or GFP. **Left:** period, r**ight**: amplitude of oscillation. Results plotted as mean + SEM, n = 9 independent experiments containing a total of 105 bPAC replicates and 268 GFP replicates

3.4 Effect of optogenetic and pharmacological stimulation on circadian rhythms

Manipulating circadian rhythms by optogenetic stimulation was a key aim of the presented work. The next experiments thus investigated the effect of stimulating U2OS *Bmal1-Luc* cells transfected with either bPAC or GFP at different time points of the circadian cycle. For this purpose, cells that had acclimatised in a luminescence plate reader were stimulated by illumination or by addition of pharmacological substances and then transferred back into the plate reader for recording of post-stimulation signals. Nine stimulation experiments were carried out in total. Three experiments each at peak and nadir *Bmal1* expression formed the core analysis. An additional two experiments during the falling phase of *Bmal1* oscillation and one experiment during the rising phase of *Bmal1* oscillation were carried out, although the latter had to be discarded due to poor post-stimulation signal quality. In each experiment, 7 conditions were tested: bPAC cells with/without light, GFP cells with/without light, GFP cells treated with DMSO, forskolin and dexamethasone. This allowed for the analysis of the effects of the different modes of stimulation as well as unspecific effects associated with the stimulation procedure.

In order to demonstrate the data generated in these experiments, **Fig. 3.5** shows representative data from two experiments where cells were stimulated at nadir and peak concentrations of *Bmal1*. Cells containing bPAC were delayed in their circadian cycle when illuminated at nadir *Bmal1* compared to non-illuminated controls. Contrastingly, illumination at peak *Bmal1* caused cells containing bPAC to be advanced in their circadian cycle compared to non-illuminated controls. The rhythms of cells containing GFP were unaltered by illumination, whilst pharmacological stimulation (depicted here: dexamethasone) caused delays and advances to the circadian cycle in a similar fashion as for illuminated cells containing bPAC.
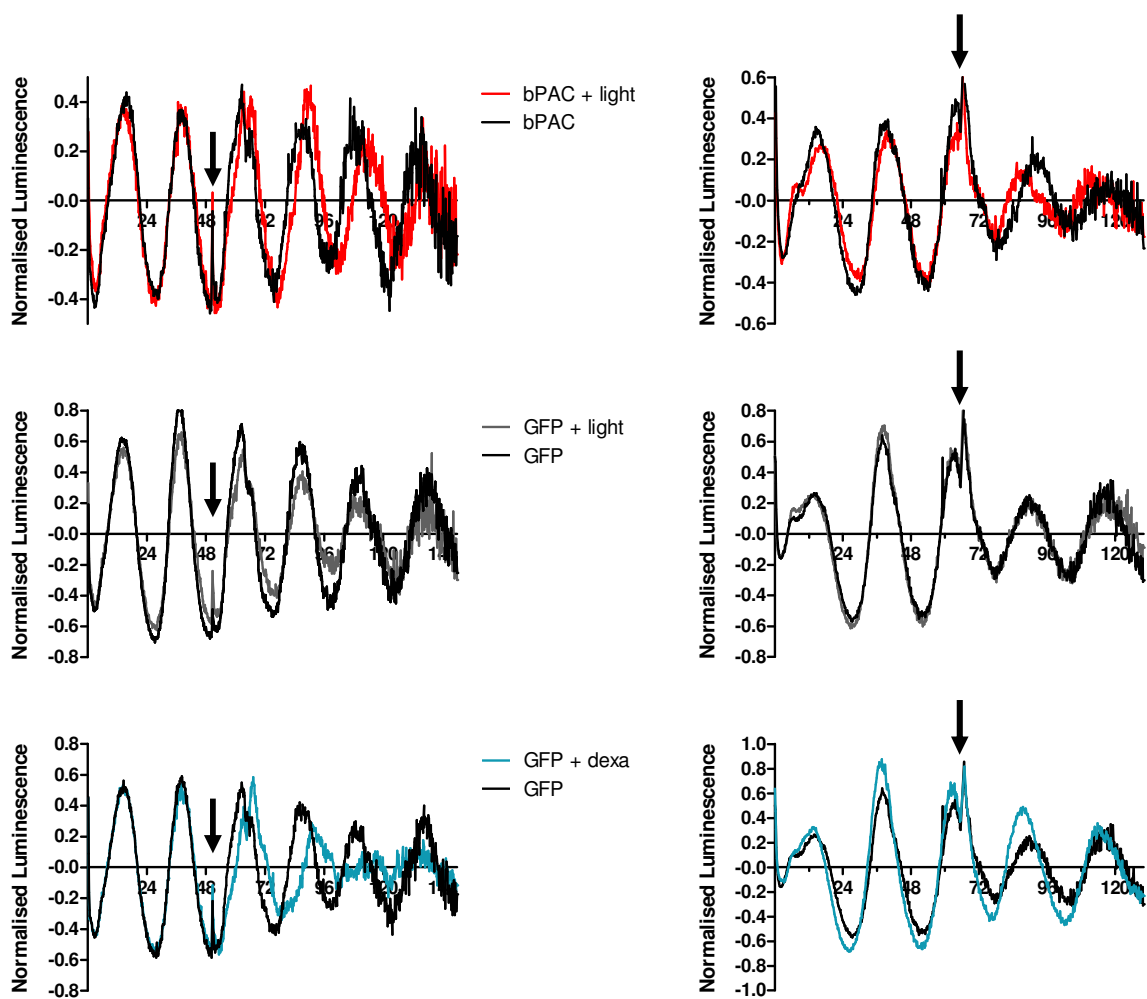
Fig. 3.5: Representative traces of cells having undergone stimulation at nadir (*left*) and peak (*right*) *Bmal1*. X-axis showing time after start of experiment (/h). Stimulation time point marked with an arrow. *Upper* Cells containing bPAC, the red trace having received illumination. *Middle* Cells containing GFP, the grey trace having received illumination. *Lower* Cells containing GFP, the blue trace having been treated with dexamethasone. All black traces received no stimulation.

To quantify the phase shifts, pre- and post-stimulation sine fits of the circadian oscillations were modeled. The following sections present the effects of stimulation on phase and period of post-stimulation circadian oscillations, leading to the construction of a phase response-curve.

3.4.1 Effect of stimulation on phase

In a first step, phase immediately prior to and after stimulation was calculated. **Fig 3.6** displays the phase change (/2π) for each condition as a function of pre-stimulation phase.
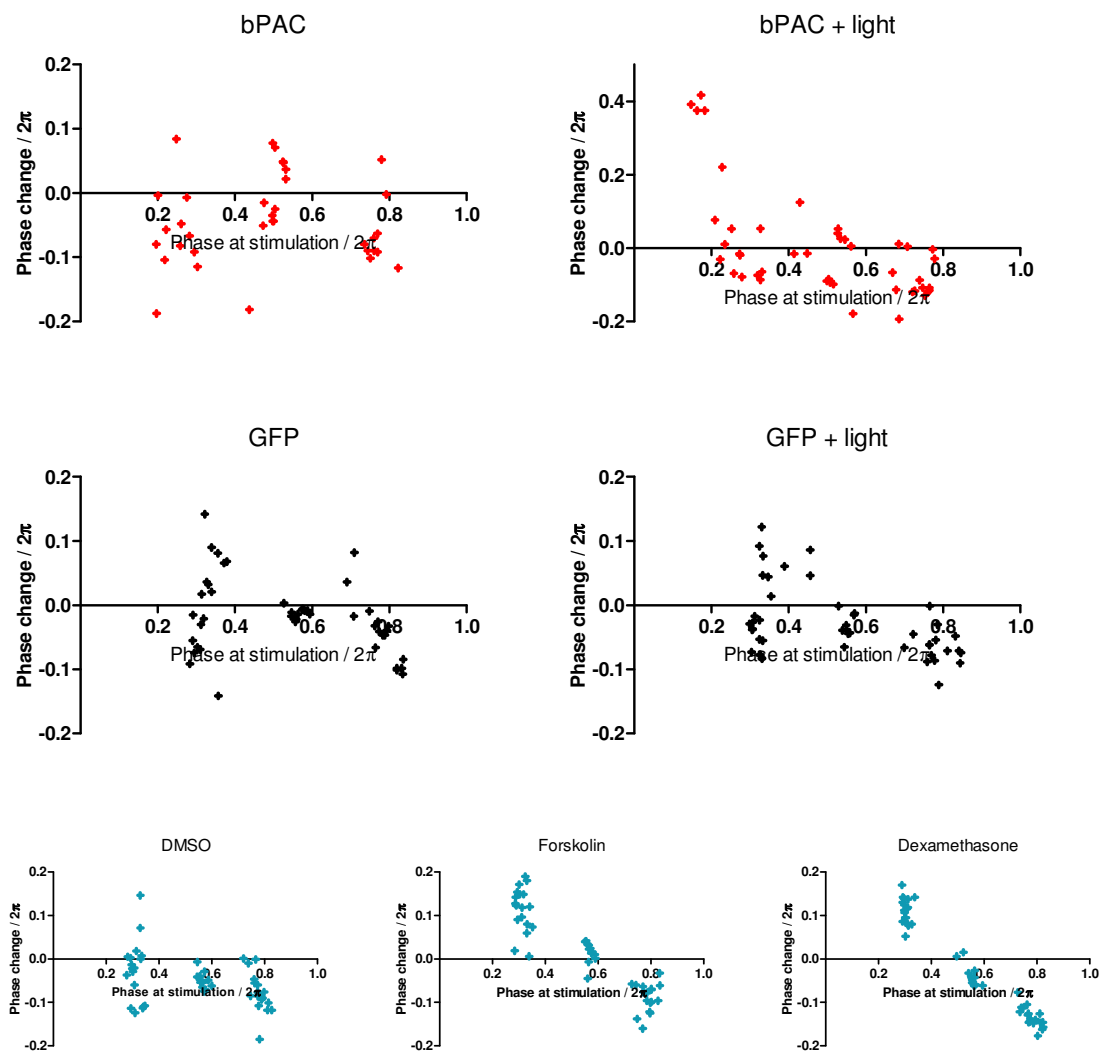
Fig. 3.6: Post-stimulation <u>phase change</u> of circadian oscillations as a function of pre-stimulation phase. Note that pre-stimulation phases (/2π) of 0.25 and 0.75 signify peak and nadir *Bmal1* expression respectively. Also note that a positive change in phase signifies a phase advance. Data from 8 independent experiments with n = 43, 45, 47, 45, 48, 47 and 48 data points respectively for the conditions (left - right, top - bottom).

By visual inspection, no phase-dependent effect of stimulation on phase of post-stimulation oscillation was evident for the negative control conditions using unilluminated samples (bPAC, GFP) as well as samples treated with a solvent control (DMSO). Contrarily, a clear phase dependence of post-stimulation phase was evident for the positive control samples treated with forskolin and dexamethasone. Here phase advances and delays were observed at peak and nadir *Bmal1* expression respectively. A similar but less clear pattern was observed for the illuminated samples containing bPAC (bPAC + light), whilst the control condition using illuminated samples containing GFP (GFP + light) yielded inconclusive results.

In order to further investigate the effect of stimulation on post-stimulation phase, net phase changes were calculated by subtracting the mean phase change of the appropriate control condition from the same experiment from the phase change of an individual well. Unilluminated cells containing bPAC served as controls for illuminated cells containing bPAC, whilst unilluminated cells containing GFP served as controls for all other conditions. The advantage of investigating net phase changes is that these can be attributed solely to the specific stimulation received. The resulting phase response diagram for net phase changes at peak and nadir *Bmal1* expression is displayed in **Fig. 3.7**.

At peak *Bmal1* expression mean net phase changes ($/2\pi$) were 0.203 ± 0.156, -0.023 ± 0.068, 0.114 ± 0.074 and 0.112 ± 0.045 for bPAC + light, GFP + light, GFP + forskolin and GFP + dexamethasone respectively. With 2π representing one full 24h cycle, these phase changes correspond to phase advances of ca. 5 h for illuminated cells containing bPAC and ca. 2.5 h for cells containing GFP treated with forskolin or dexamethasone.

At nadir *Bmal1* expression mean net phase changes ($/2\pi$) were -0.045 ± 0.058, -0.020 ± 0.038, -0.046 ± 0.055 and -0.089 ± 0.043 for bPAC + light, GFP + light, GFP + forskolin and GFP + dexamethasone respectively. These phase changes correspond to phase delays of ca. 1 h for illuminated cells containing bPAC as well as cells containing GFP treated with forskolin and of ca. 2 h for cells containing GFP treated with dexamethasone.

2-way ANOVA showed highly significant effects of stimulation time point, stimulation condition and interaction on variance ($p < 0.001$ for all). Importantly Bonferroni post-tests showed no statistical significant difference between the phase changes observed in unilluminated cells containing GFP at the two stimulation time points. For all other stimulation conditions the difference between the phase changes observed (i.e. phase advances vs. delays) was highly significant ($p < 0.001$).

Furthermore, the phase changes after stimulation could be compared against those observed in illuminated cells containing the GFP plasmid. Since the phase changes in this stimulation condition were not significantly affected by the stimulation time point, they most closely resembled a valid control condition. At peak *Bmal1* expression the phase advances observed for bPAC + light and GFP + forskolin/dexamethasone all reached statistical significance ($p < 0.001$). However at nadir *Bmal1* expression only the phase delays observed after treatment with dexamethasone reached statistical significance ($p < 0.05$).
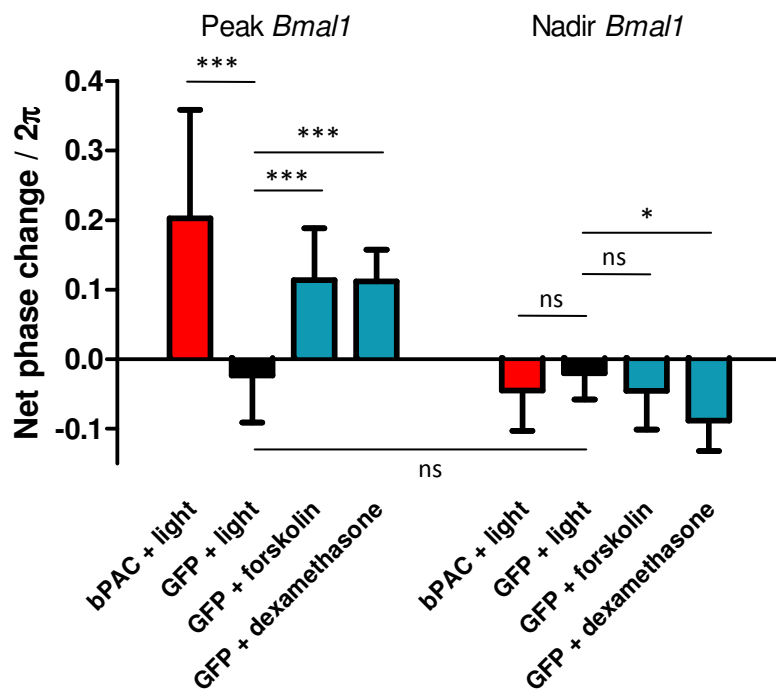
Fig. 3.7: Net phase changes ($/2\pi$) after stimulation at peak and at nadir *Bmal1* expression. Results plotted as mean + SD, n = 17 (peak) and 16 (nadir) for bPAC + light, 16 and 16 for GFP + light, 18 and 17 for GFP + forskolin, and 18 in each case for GFP + dexamethasone. Results for Bonferroni post-test after 2-way ANOVA displayed with $p < 0.05$, 0.01 and 0.001 denoted by *, ** and *** respectively.

A limitation of the depicted phase-response diagrams is that the post-stimulation phase used in their derivation is calculated by extrapolating post-stimulation sine fits backwards beyond their region of fitting. This method thus assumes an instant phase change of the treated samples which remains constant during the acclimatisation period until the region of fitting is reached. Whether this assumption holds true is unknown, hence further analyses were required to validate the observed phase-response relationships.

3.4.2 Effect of stimulation on period

The second key variable of any oscillation is its period. Again, using the modeled pre- and post-stimulation sine fits of the recorded circadian oscillations allowed for the comparison of periods prior to and after stimulation. **Fig. 3.8** displays the difference in pre- and post stimulation period for each condition as a function of pre-stimulation phase.
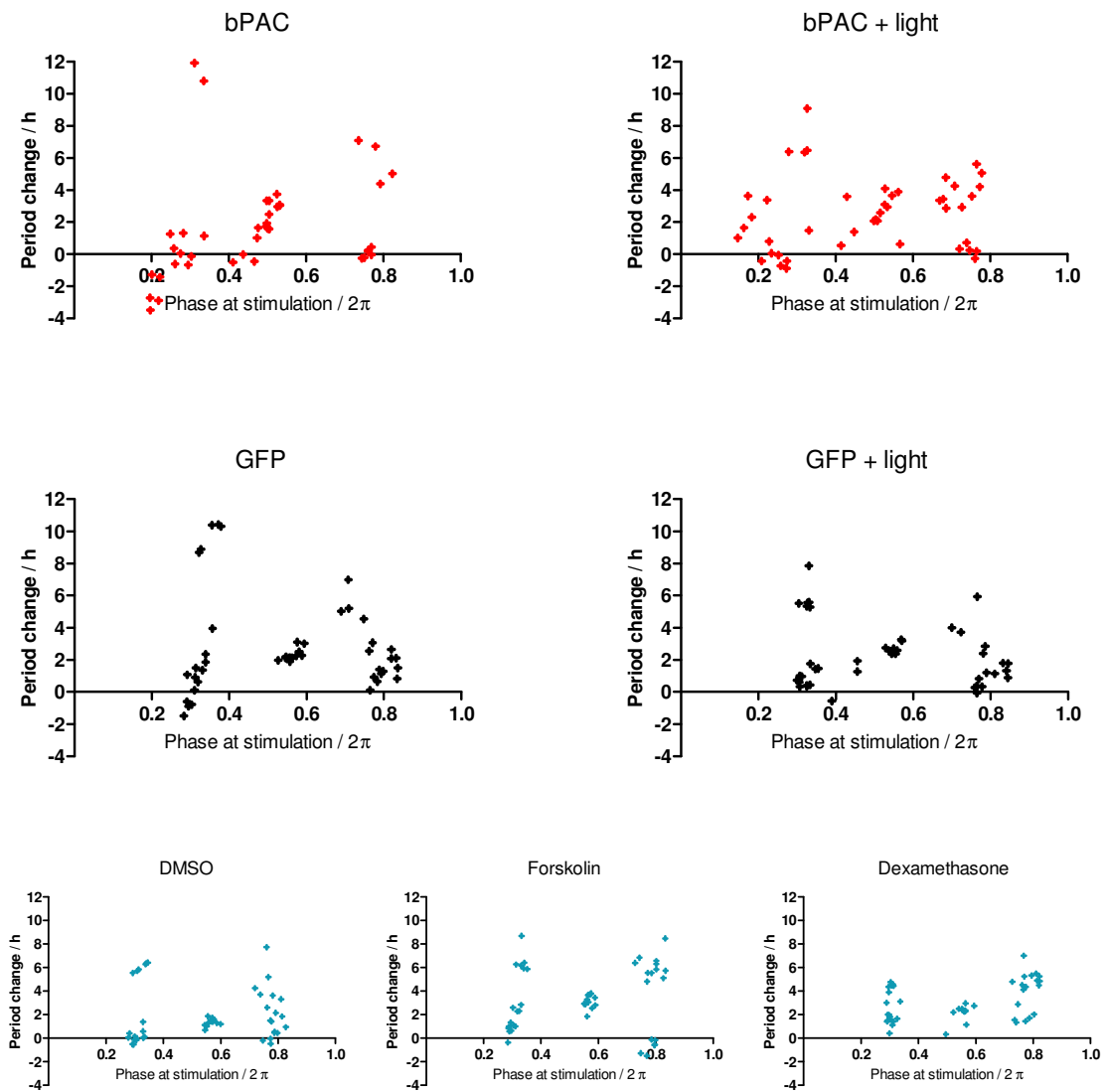
Fig. 3.8: Post-stimulation <u>period change</u> of circadian oscillations as a function of pre-stimulation phase. Data from 8 independent experiments with n = 43, 45, 47, 45, 48, 47 and 48 data points respectively for the conditions (left - right, top - bottom).

In general, longer periods were observed across all conditions after the stimulation procedure. However, in contrast to changes in phase (cf. **Fig. 3.6**), no dependency on pre-stimulation phase was apparent. The mean period changes across all experiments (n = 8) for each condition were thus pooled and the mean lengthening of the period (/h) for the different conditions calculated, as displayed in **Fig. 3.9**: 2.51 ± 1.44 (bPAC), 2.44 ± 0.73h (bPAC + light), 2.72 ± 0.99 (GFP), 2.21 ± 0.65 (GFP + light), 1.93 ± 0.76 (DMSO), 3.38 ± 0.95 (forskolin), 3.02 ± 0.54 (dexamethasone). 1-way ANOVA showed no significant difference between the different conditions (p = 0.939), with Bonferroni post-test also showing no significant differences between any column pairs. The observed lengthening of the period was thus independent of the individual stimulation conditions.
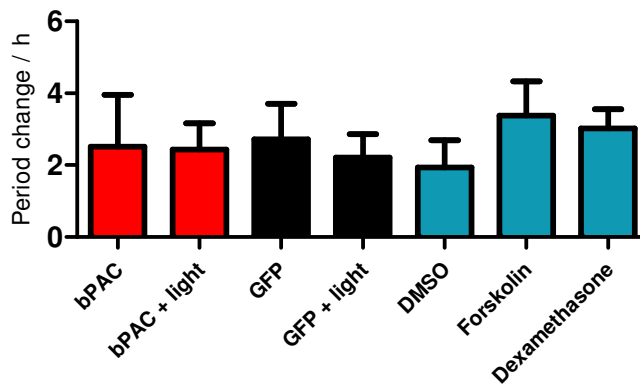
Fig. 3.9: Mean post-stimulation <u>period change</u> of circadian oscillations (n = 8, mean + SEM).

3.4.3 Quantifying phase shifts – adjusting for period changes

In section 3.4.1, phase changes (/2π) were calculated by subtracting the phase at stimulation of pre-stimulation sine fits from the extrapolated phase at stimulation of post-stimulation sine fits:

$$\Delta\varphi = \varphi_{post\text{-}stimulation\ signal}\ (t_{stimulation}) - \varphi_{pre\text{-}stimulation\ signal}\ (t_{stimulation})$$

An alternative method to quantify the phase response is by comparing extrapolated pre-stimulation sine fits and observed post-stimulation signals. In this case, a phase shift (/h) is defined as the time difference between the expected and the observed peak or nadir of *Bmal1* oscillations, whereby the phase shift is calculated at the phase corresponding to the phase at stimulation (e.g. stimulation at nadir *Bmal1* → phase shift calculated at the following nadir):

$$\Delta\varphi = t_{peak/nadir}\ (observed) - t_{peak/nadir}\ (expected)$$

However as outlined in the previous sections, both phase and period of the observed circadian oscillations were affected by the stimulation procedure. Challenges thus arise with this method when a simultaneous change in period is of the same order of magnitude as a phase shift. In this case, the observed phase shift can either be augmented or obscured. For example, a phase delay would be accentuated by an increased period, whilst a phase advance would conversely be diminished. Furthermore, the calculated phase shift would not be constant across time, e.g. a phase shift calculated at the first nadir after stimulation at nadir *Bmal1* would differ from one calculated at the second nadir. A methodical correction is therefore required which takes into account the individual period changes of each well. It was decided to adjust the calculated phase shift by subtracting the observed period change of the well in question:

$$\Delta\varphi_{adjusted} = \Delta\varphi - n \cdot \Delta\lambda$$

where *Δφ* is the phase shift as defined above, *Δλ* is the period change of an individual well and *n* is an integer equaling the number circadian cycles that have passed between stimulation and measurement of the phase shift.

In practice this means that phase delays driven by large increases in period are reduced, whilst phase advances that are counteracted by increased periods become more prominent. Furthermore, the time point of phase shift calculation is no longer important, as the formula corrects for the number of passed circadian cycles.

Using the definition for period adjusted phase shifts above, and again calculating net phase shifts by subtracting the mean phase shift of the appropriate control in an analogous fashion as described in section 3.4.1 yielded the phase response diagram shown in **Fig. 3.10**.

At peak *Bmal1* expression mean net phase shifts (/h) were 4.99 ± 4.25, -0.74 ± 2.17, 2.85 ± 2.23, 2.68 ± 1.62 for bPAC + light, GFP + light, GFP + forskolin and GFP + dexamethasone respectively. At nadir *Bmal1* expression mean net phase shifts (/h) were -1.42 ± 1.53, -0.47 ± 0.96, -1.06 ± 1.35, -2.37 ± 1.02 for bPAC + light, GFP + light, GFP + forskolin and GFP + dexamethasone respectively. Note that positive phase shifts correspond to phase advances whilst negative phase shifts correspond to phase delays.

Similarly to the results obtained for phase changes after stimulation, 2-way ANOVA showed highly significant effects of stimulation time point, stimulation condition and interaction on variance ($p < 0.001$ for all). The results for the Bonferroni post-tests are shown in **Fig. 3.10**.
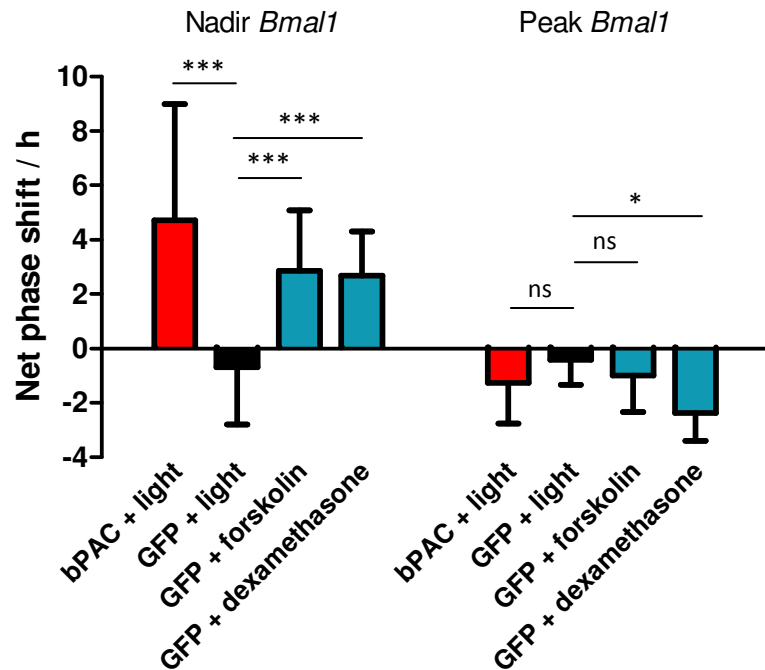
Fig. 3.10: Net adjusted phase shifts (/h) after stimulation at peak and at nadir *Bmal1* expression. Results plotted as mean + SD, n = 17 (peak) and 16 (nadir) for bPAC + light, 16 and 16 for GFP + light, 18 and 17 for GFP + forskolin, and 18 in each case for GFP + dexamethasone. Results for Bonferroni post-test after 2-way ANOVA displayed, $p < 0.05$, 0.01 and 0.001 denoted by *, ** and *** respectively.

Despite the different methods used in their construction, the phase diagrams displaying net phase changes (/2π) (**Fig. 3.7**) and net phase shifts (/h) (**Fig. 3.10**) were remarkably similar qualitatively: cells containing GFP were not phase shifted in a phase-dependent manner, whilst stimulated cells (illuminated cells containing bPAC or pharmacologically stimulated cells containing GFP) were phase advanced and delayed at peak and nadir *Bmal1* respectively.

A common theme to be observed in all phase response diagrams was the large variability of the phase shifts, raising questions about inter- and intra-experimental reproducibility of the phase response.

Nonetheless, circadian rhythms were successfully manipulated in a phase-dependent manner by both optogenetic and pharmacological means, with consistent results derived by two independent methods.

3.5 The role of the *Per1* in mediating phase shifts is unclear

In order to ascertain that the changes in wavelength and period observed after optogenetic stimulation were caused by an upregulation in clock genes, the expression of *Per1* was investigated in U2OS cells which had been synchronised for 2 h with 100 nM dexamethasone 12 h before stimulation. Judging by data from U2OS *Bmal1-Luc* cells which had undergone the same synchronisation procedure, this corresponds to the phase of peak *Bmal1* concentration (see **Fig. 3.5**), and the phase when the largest phase responses (phase advances) were inducible. Similarly as in non-synchronised cells, *Per1* expression was measured at the 0 and 2 h time points after stimulation (**Fig. 3.11**).
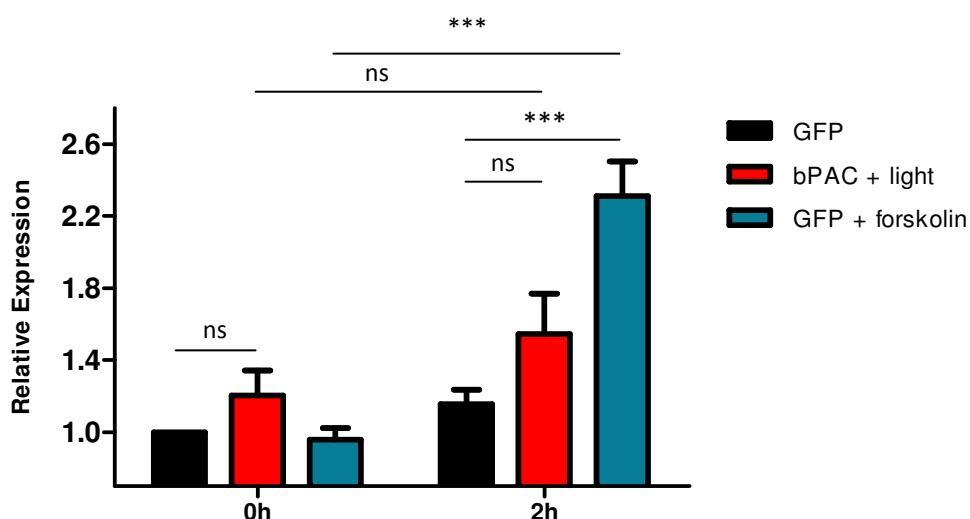
Fig. 3.11: Expression of *Per1* in synchronised U2OS cells, non-stimulated and 2 h after stimulation. Expression calculated relative to non-stimulated cells (t = 0) containing the GFP plasmid. Results plotted as mean + SEM, n = 4 independent experiments with 4 replicates each.

2-way ANOVA confirmed a significant effect of treatment ($p < 0.01$), time after stimulation ($p < 0.001$) and interaction ($p < 0.001$) on variance. Similarly as in non-synchronised cells, baseline *Per1* expression was not significantly different irrespective of plasmid load: 1.00 (GFP) vs. 1.20 ± 0.14 (bPAC) vs. 0.96 ± 0.06 (GFP + forskolin), $p > 0.05$ (Bonferroni post-test). 2 h after stimulation significant *Per1* upregulation was observed after treatment with forskolin compared to illuminated GFP controls (2.31 ± 0.19 vs. 1.16 ± 0.08, $p < 0.001$ (Bonferroni post-test)), however the numerically observed higher *Per1* expression after optogenetic stimulation of cells containing bPAC failed to reach statistical significance (1.55 ± 0.22, $p > 0.05$).

When comparing the 0 h and 2 h time points, a significant difference in *Per1* expression was again observed for cells treated with forskolin ($p < 0.001$ for Bonferroni post-test). No significant difference was detected for illuminated cells containing bPAC vs. non-stimulated bPAC controls ($p > 0.05$ for Bonferroni post-test), in part due to the high variance of *Per1* expression observed.

A simultaneously assembled time profile of *Per1* expression in hourly intervals for 4 h after stimulation is shown in **Fig. 3.12**. 2-way ANOVA testing showed a significant effect of plasmid used, time after stimulation and interaction on variance ($p < 0.0001$). In contrast to the data for non-synchronised cells, it showed no significant expressional changes in *Per1* in response to optogenetic stimulation at any post-stimulation time point ($p > 0.05$, Bonferroni post-test). Treatment with forskolin however still caused an upregulation of *Per1* with similar kinetics and of comparable magnitude as in non-synchronised cells ($p < 0.05$ at 1 h, $p < 0.001$ at 2 h/3 h/4 h, Bonferroni post-test).
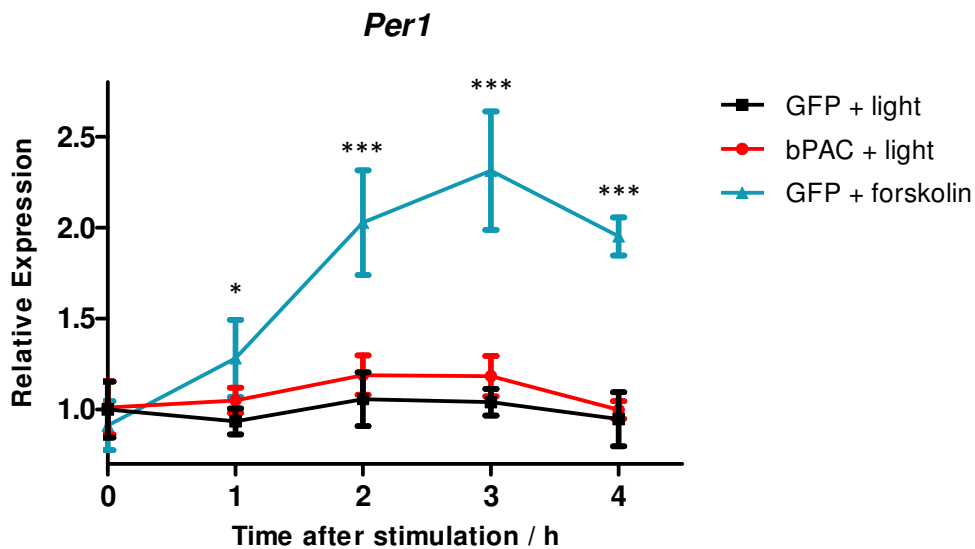
Fig. 3.12: Time profile of *Per1* expression in synchronised U2OS cells after stimulation. Expression calculated relative to non-stimulated cells (t = 0) containing the GFP plasmid. Results plotted as mean ± SD, n = 4.

With the role of *Per1* as a mediator of the observed phase shifts in U2OS *Bmal1-Luc* cells in question, exploratory analyses were carried out to determine whether stimulation elicited other transcriptional changes in synchronised cells. The immediate early gene *cFos* as well as the clock gene *Per2* were thus investigated.

3.6 Evidence for unspecific expressional changes in response to the stimulation procedure

A time profile of *cFos* was assembled, the immediate early gene serving as a marker of unspecific transcriptional changes in response to stimulation (**Fig. 3.13**). 2-way ANOVA revealed a significant effect of plasmid used and time after stimulation (both $p < 0.0001$) as well as interaction ($p < 0.05$) on variance. A strong initial upregulation after 1 h regardless of plasmid content or stimulation condition was observed, including illuminated cells containing GFP (i.e. the control condition). There was no detectable significant difference between the amount of upregulation: 2.71 ± 0.29 (GFP + light) vs. 2.84 ± 0.47 (bPAC + light) vs. 3.13 ± 0.56 (GFP + forskolin), $p > 0.05$ for all pairs tested (Bonferroni post-test). A late upregulation component of smaller magnitude was evident in cells containing bPAC that had received illumination and in cells containing GFP which had received forskolin when compared to illuminated control cells. This upregulation was significant at both 3 h and 4 h after stimulation: 1.30 ± 0.06 (GFP + light) vs. 1.89 ± 0.31 (bPAC + light, $p < 0.05$) vs. 2.00 ± 0.39 (GFP + forskolin, $p < 0.01$) at 3 h and 1.29 ± 0.24 (GFP + light) vs. 2.09 ± 0.33 (bPAC + light, $p < 0.01$) vs. 2.29 ± 0.18 (GFP + forskolin, $p < 0.001$) at 4 h. The initial upregulation of *cFos* across all conditions is thus related to the procedure involved in stimulation and unspecific, whilst the late upregulation can be attributed to the specific modes of stimulation.

Fig. 3.13: Time profile of *cFos* expression in synchronised U2OS cells after stimulation. Expression calculated relative to cells containing the GFP plasmid at t = 0. Results plotted as mean ± SD, n = 4.

Since *cFos* expression was noted to be numerically larger in non-stimulated cells containing bPAC in comparison to GFP controls, baseline *cFos* expression was determined in all experiments available involving synchronised cells. Cells containing bPAC were found to have a significantly elevated baseline *cFos* expression compared to cells containing GFP (1.47 ± 0.12 (SEM) vs. 1.00, $p = 0.0077$, n = 4 independent experiments with 4 replicates each). This finding was confirmed in non-synchronised cells (baseline *cFos* expression in cells containing bPAC relative to cells containing GFP 2.17 ± 0.62 (SEM, n = 3 independent experiments with 4 replicates each).

3.7 Delayed upregulation of *Per2* in sychronised cells

The time profile for *Per2* is shown in **Fig. 3.14**. 2-way ANOVA showed a significant effect of plasmid used ($p < 0.05$) and time after stimulation ($p < 0.0001$) on variance, but not of interaction ($p = 0.054$). A significant upregulation of *Per2* relative to illuminated control cells was only observed 4 h after stimulation for both optogenetically stimulated cells and pharmacologically stimulated cells: 1.11 ± 0.11 (GFP + light) vs. 1.31 ± 0.09 (bPAC + light, $p < 0.05$) and 1.43 ± 0.15 (GFP + forskolin, $p < 0.001$). Whilst more data for this time point from further experiments is lacking, it provides a possible link between optogenetic stimulation and the observed phase shifts in response to stimulation, offering a starting point for further experiments.
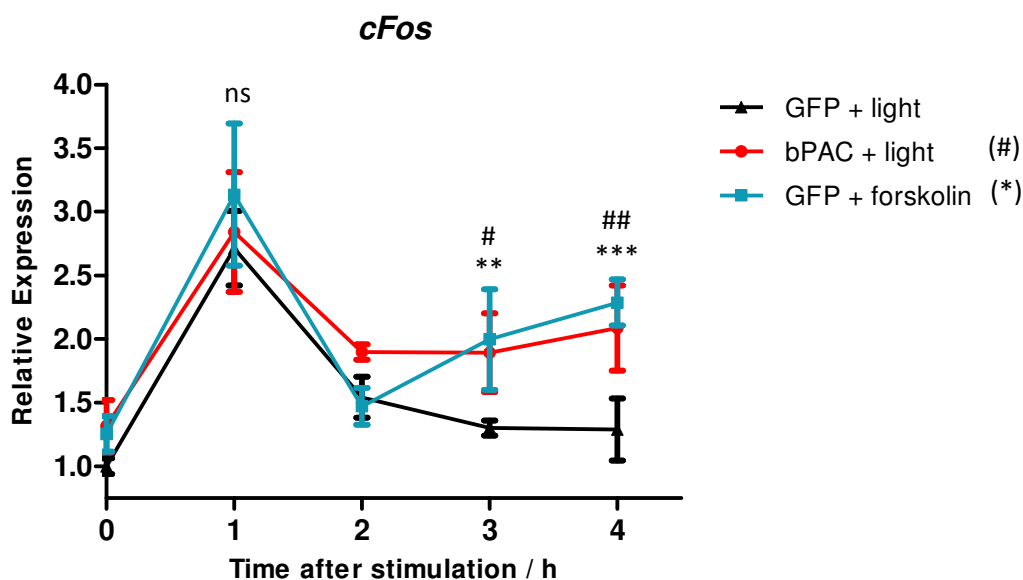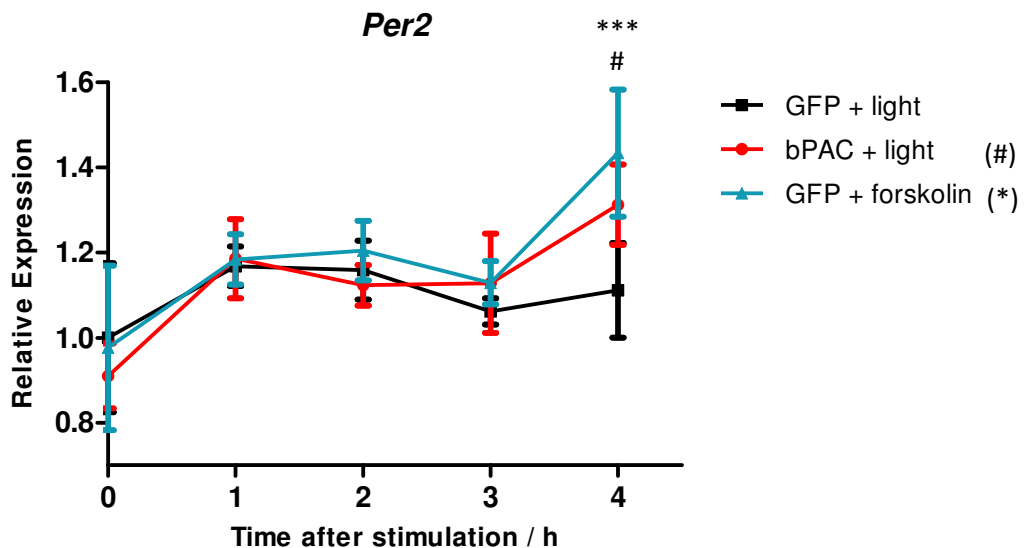

Fig. 3.14: Time profile of *Per2* expression in synchronised U2OS cells after stimulation. Expression calculated relative to non-stimulated cells (t = 0) containing the GFP plasmid. Results plotted as mean ± SD, n = 4.

4 Discussion

The aim of this study was to use an optogenetic approach involving the light-sensitive adenylyl cyclase bPAC to manipulate circadian rhythms in cell culture and to investigate the underlying transcriptional changes, particularly in clock gene expression.

The key findings of this study are the following: (i) the bPAC sequence was successfully cloned into a plasmid that could be delivered to cells using a simple transient transfection approach, (ii) in cells transfected with bPAC illumination caused rapid and significant increases in intracellular cAMP levels, (iii) in non-synchronised cells, this rise in cAMP led to upregulation of the clock gene *Per1*, (iv) in synchronised cells, optogenetic stimulation caused phase-dependent delays or advances to circadian rhythms, with phase response curves constructed by two independent methods yielding concordant results, (v) the role of the clock gene *Per1* in mediating these phase shifts is uncertain and (vi) the stimulation procedure used caused a lengthening of circadian period and induced unspecific transcriptional activation.

4.1 Magnitude and kinetics of cAMP increase after illumination

The experimental set up used to test optogenetic stimulation elicited convincing data for rapid and significant cAMP production. In lysates of cells containing bPAC, cAMP concentration was found to increase by a factor of ca. 150 upon illumination compared to non-illuminated controls. This is of the same order of magnitude as the 300-fold increase in enzymatic activity of bPAC reported in the original publication[271]. Comparisons of absolute cAMP concentrations or cAMP production rates against those reported in other publications are difficult as no normalisation against protein content was undertaken. Nonetheless the fold-change in cAMP concentration is a sufficient indicator to underline the functionality of the system.

The rise of cAMP in cells containing bPAC in response to illumination was fast – on the scale of seconds if a Michaelis-Menten fit is modeled (K_m = 35 s). Despite the limited temporal resolution of the results, this is in good agreement with the kinetic properties of bPAC reported, with a time constant of 23 s for cAMP production by purified bPAC observed *in vitro*[271]. The decay kinetics of cAMP after stimulation were not investigated in the presented work, but inferences can be made from the data reported in the literature. The decay of enzymatic activity after "lights-off" is found to be rapid, also on the scale of seconds (τ = 12 s for the active state of purified bPAC), however the decay kinetics of cAMP can be more complex, as they depend on the activity of endogenous cyclic nucleotide phosphodiesterases (PDEs).

The types of PDEs present, their expression levels and their substrate specificity vary in a tissue-specific manner, explaining why some cell systems return to baseline cAMP concentrations (or baseline physiology as a surrogate marker) faster than others, but always on the scale of minutes $(1 - 10 \text{ min})$[271,299]. Neuronal tissues for example display a high expression of different PDEs, whilst little is known about PDE expression in U2OS cells[299]. A minor uncertainty over the exact duration of elevated cAMP concentrations in response to illumination thus exists. However this does not constitute a relevant limitation – the described kinetics offer sufficiently precise temporal control, guaranteeing a temporally limited cAMP burst in illuminated cells containing bPAC.

In contrast, cells stimulated pharmacologically with forskolin were exposed to elevated cAMP concentrations for much longer: at pH > 6.5 in aqueous solution forskolin can isomerise to isoforskolin and both isomers are degraded by base-catalysed hydrolysis to forskolin D. At pH 7.4 and a temperature of 37 °C (the approximate experimental conditions used), the half-life of forskolin is reported to be 19.5 h, meaning cells stimulated with forskolin were exposed to physiologically relevant cAMP concentrations for well over a day under the assumption that in a cell model no further degradation pathways exist or degradation is not accelerated enzymatically[300]. Washing treated cells or tissue slices rapidly reverses the effects of forskolin[297], however this was decided against in order to avoid the perturbation of circadian processes associated with medium changes (in the case of forskolin treated cells) or with removal from the incubator/plate reader (in the case of cells from other stimulation conditions present on the same plate). The time scale of cAMP exposure therefore varied from < 30 min in the case of optogenetically stimulated cells to > 1 day in the case of pharmacologically stimulated cells.

A final point to mention concerns the intensity of illumination used in the experiments. Purified bPAC displays saturation kinetics when illuminated with increasing light intensity. If illuminated with monochromatic light (475 nm), the cAMP production rate plateaus above an intensity of ca. 20 μW/mm^{-2}. The absorption spectrum of bPAC peaks at 441 nm but only tails off at around 500 nm, meaning the polychromatic light source used for these experiments stimulated bPAC across a spectrum of wavelengths, the overall intensity equaling the integral over this range. This overall intensity was not quantified, but it can be safely assumed that under the stimulation conditions used, bPAC was operating at maximum capacity. Thus duration of illumination was the only variable determining the extent of cAMP exposure in optogenetically stimulated cells.

In summary, the kinetics of elevated cAMP in response to optogenetic stimulation resemble a square wave function with a short and brief cAMP burst, whilst those in response to pharmacological stimulation correspond to a gradual exponential decay with a more a tonic effect of cAMP exposure.

4.2 Baseline cAMP concentrations

An important point concerns the baseline enzymatic activity of bPAC in non-stimulated cells kept in the dark. Despite the level of enzymatic dark activity reported to be very low, it was nonetheless sufficient to cause slightly higher cAMP concentrations in cells containing bPAC compared to control cells in the original publication[271]. In the presented work, cAMP levels were not found to be significantly different in cells transfected with bPAC and in GFP controls. As a caveat, the ELISA used to measure cAMP concentrations was performing at the lower limit of its detection range despite the use of an acetylation step designed to improve its sensitivity. More than half of the measurements at baseline were outside the region of the standard curve across both conditions (bPAC and GFP), meaning there is considerable uncertainty about the true baseline cAMP concentrations. Use of a different ELISA kit with greater sensitivity at low cAMP concentrations or upscaling the experiment by using more cells are possible solutions to circumvent this problem. The evidence for potentially altered baseline cAMP concentrations and their implications will be discussed in section 4.8.

4.3 Magnitude and kinetics of *Period* gene transcriptional changes in non-synchronised cells

In non-synchronised cells, a rise in intracellular cAMP concentrations led to a significant upregulation of *Per1*, both in optogenetically as well as pharmacologically stimulated cells. This is in agreement with a wide body of evidence demonstrating the connection between the cAMP-PKA-CREB pathway and *Per1* expression (cf. sections 1.6 and 1.16).

The magnitude of *Per1* induction was relatively modest, with increases of approximately 40% and 70% for optogenetic and pharmacological stimulation respectively. This is lower than could have been expected from previous publications: for example, stimulation of rat fibroblasts with 10 μM forskolin (i.e., the identical concentration used for these experiments) elicits an 8-fold increase in *rPer1* expression after 1 h[284]. In the SCN of mice exposed to a 30 min light pulse

mPer1 transcripts increase around 5-fold[171,172]. With 10 μM forskolin a standard concentration used in many other published reports, a lack of intracellular cAMP and a resulting low transcription rate does not seem to be a likely cause for these results. A possible explanation could be an insufficient temporal resolution: *Per1* rises quickly but transiently in response to stimuli, with peak mRNA levels usually measured 60 – 90 min afterwards[13,171,172,284]. Thus it is possible that the peak of *Per1* transcripts is to be found between 1 h and 2h after stimulation, the time points investigated in the displayed time profile. One option to close this diagnostic blind spot would be to increase the frequency of sampling, e.g. by adding a 90-min time point to the time profile. A more elegant alternative would be the real-time monitoring of *Per1* transcription by a *Per1* promoter-driven luciferase reporter, similar to the *Bmal1-Luc* construct used in the experiments investigating circadian rhythms. Both a *hPer1-Luc* plasmid as well as a transgenic rat line harbouring such a construct have been created[275,301]. Indeed, experiments with a putative *hPer1-Luc* plasmid co-transfected with bPAC were carried out as part of the presented work, but were aborted due to doubts about the plasmid's identity as judged by functional behaviour and sequence analysis (data not shown). Whether an improved temporal resolution would have yielded higher measurable *Per1* transcript levels remains speculative, however, since 2 h as the time point of maximum *Per1* transcription after stimulation as reported here falls close to the published range. A further point to consider is that different cell lines can display slightly different *Per1* induction kinetics. For example in a glioblastoma cell line, *hPer1* induction as reported by a *hPer1-Luc* construct does not peak until 4 h after pharmacological stimulation[302]. Importantly, the role of phase as a chief contributor to the magnitude of *Per1* induction has to be considered as well. Since *Per1* is only upregulated in a phase-restricted manner during the subjective "night", statistically around half of the non-synchronised cells would have been stimulated at a phase when *Per1* was not inducible. This seems the most likely explanation for the modest *Per1* induction observed.

Comparing the magnitude and kinetics of *Per1* induction between the modes of stimulation, two key findings stand out: firstly, *Per1* transcription in optogenetically stimulated cells was transient. Only at the 2 h time point was the *Per1* transcript significantly elevated compared to control cells. In pharmacologically treated cells, *Per1* transcription remained significantly elevated until 4 h after stimulation. These contrasting kinetics likely reflect the exposure time to elevated cAMP concentrations of the stimulated cells as discussed in section 4.1: optogenetic stimulation led to a temporally limited cAMP burst and thus only a transient *Per1* upregulation, whilst forskolin was able to stimulate over a longer time and elicited a persistent *Per1* upregulation.

Alternatives to this persistent stimulation exist: if forskolin is washed out by a medium change 2 h after administration, *Per1* transcription returns to baseline levels by 4 h after stimulation[284]. No circadian disruption in connection with the medium change is reported in the quoted publication, however the medium used was serum-free. A similar strategy was not deemed feasible particularly for the plate reader experiments (i) due to the disruption associated with removal of plates from their equilibrated conditions and (ii) due to questions about long term viability of cells grown in serum-free medium.

Secondly *Per1* transcription in optogenetically stimulated cells was lower 2 h after stimulation compared to that observed in pharmacologically stimulated cells. Considering that the cAMP concentration in cell lysates of optogenetically stimulated cells was about 3-fold higher than after stimulation with forskolin, this is a surprising finding. Peak *Per1* transcription would be expected to correlate with cAMP concentration and be unaffected by duration of cAMP elevation. If anything, *Per1* transcription should thus have been higher in optogenetically stimulated cells. A possible explanation for this discrepancy could be a difference in the number of viable cells, despite all wells being seeded with the same number of cells to begin with, regardless of their destined stimulation condition. In this case cells transfected with bPAC would transcribe more *Per1* mRNA on a single-cell level but the overall amount of mRNA across all cells would be lower, as cells transfected with GFP would be more numerous. Whether this hypothesis holds true requires further analysis, e.g. using a live-dead stain.

Considering *Per2*, the time profile showed no evidence for an induction in response to elevated cAMP in non-synchronised cells. Putting this finding into context with how *Per2* responds to stimuli in other reports, several points stand out: *Per2* is inducible by a serum shock in rat fibroblast, however fails to respond acutely to treatment with forskolin or other pharmacological substances, similarly as observed here[13,282,284]. This is in contrast to how the gene behaves in the SCN in response to a light pulse, where it is upregulated during the early but not the late subjective night[84–86,171]. The kinetics of upregulation differ slightly from those seen for *Per1*, since *Per2* mRNA peaks later (ca. 2-3 h) after a light pulse. This leads to the question why *Per2* is inducible in the SCN but not in cell culture of peripheral cells. A possible explanation lies in the phase dependence of *Per2* inducibility, a characteristic seen in the SCN. The argument would run that the "non-synchronised" cells used in the experiment displayed residual synchrony, possibly as a result of the final medium change before the experiment was commenced[13]. If by chance the experiment was then carried out at the wrong phase (i.e. subjective "daytime" or "late night") a lack of *Per2* induction would be entirely expected.

A further point to consider is that differences may exist in the transcriptional control of clock genes in the SCN and in peripheral oscillators. In the SCN the central role of CREB in acutely mediating transcription in response to a light pulse has been extensively studied (see section 1.6). Similarly, the CRE in the *Per2* promoter has been demonstrated to be fully functional in non-SCN cells[223]. However, stimulation via the cAMP-PKA-CREB-pathway has diverging effects on *Per2* transcription in different cell models: for example, in murine chondrocytes stimulated with parathyroid hormone, *mPer2* induction depends on PKA and CRE[303]. On the other hand in human choriocarcinoma cells the *hPer2* promoter containing a functional CRE is not activated after treatment with forskolin[223]. This suggests that the *Per2* promoter displays tissue or signal-specific sensitivity to the cAMP-PKA-CREB-pathway. Section 1.9 describes how the *Per1* promoter can serve as an integrator of different clock input signals. Similar processes at the level of CREB or at the promoter level, e.g. due to additional response elements, are likely to govern the overall responsiveness of the *Per2* promoter to stimuli. This seems the most plausible explanation for the lack of *Per2* induction observed. A factor not deemed relevant for the lack of *Per2* induction was an insufficiently long observation time: the constructed 4 h time profile was comfortably long enough to capture a delayed induction of *Per2*, if there had been one to be observed.

4.4 Manipulation of circadian rhythms: effects on period and phase

Optogenetically or pharmacologically stimulated U2OS *Bmal1-Luc* cells displayed a clear phase response curve: at peak *Bmal1* transcription (corresponding to the late night) stimulation led to phase advances, at nadir *Bmal1* transcription (corresponding to the early night) stimulation led to phase delays, and at the halfway point in between no clear effect on phase was discernible. The shape of this phase response curve was exactly as anticipated from previous studies in both cells, tissue explants and organisms and has been established since the 1970-ies[125]. This validates the experimental set-up and methodology used.

The absolute magnitude of the phase shifts was of the same order of magnitude to those reported in previous publications investigating phase shifts *in vitro*: for example, rat SCN slices are phase advanced by 4-6 h when treated with cAMP/cGMP and by 3.5 h when treated with glutamate[161,276,304], mouse fibroblasts treated with a GRE-binding zinc finger protein are phase advanced or delayed by 1 h[286], whilst rat fibroblasts optogenetically stimulated by a light-sensitive $G_{\alpha s}$-protein coupled receptor are phase advanced or delayed by 6-8 h depending on the phase of stimulation[287].

A general observation to be made was the large inter-well and inter-experimental variability of the results. This accounts for the lack of statistical significance of the phase delays with the exception of the cells treated with dexamethasone. The large variability raises doubts about reproducibility and generalisability to other settings – not every experimental set-up will be able to compensate variability through the use of many replicates as was done here. Optimisation of the stimulation procedure will thus be required in order to extend the use of bPAC to other systems.

An interesting and unexpected observation was that the stimulation procedure caused a uniform lengthening of the phase of around 2-3 h regardless of the stimulation condition and regardless of the phase at stimulation. The cause of this period lengthening is not entirely clear. Since neither optogenetic stimulation nor pharmacological stimulation with forskolin or dexamethasone elicited significantly altered period responses to those seen in non-stimulated cells the effect does not seem to relate to elevated cAMP concentrations and its downstream signaling cascade/CRE-driven transcription, and not to increased *Period* transcription via glucocorticoid response elements. A possible explanation involves a temperature change of the medium during the stimulation procedure. Temperature rhythms are known to be able to sustain and reset circadian rhythms in peripheral oscillators[28,69]. A molecular link between temperature and the circadian clock is established for both transcriptional and posttranscriptional mechanisms:

On a transcriptional level, heat-shock factor 1 (HSF1) has been demonstrated to be a circadian transcription factor capable of controlling the expression of *Per2* and of synchronising circadian rhythms in peripheral oscillators via heat shock elements (HSEs) in the *Per2* promoter[305–307]. Furthermore mice which are deficient in *Hsf1* are observed to have longer circadian periods than their wildtype controls, whilst the inhibition of HSF1-driven transcription also lengthens circadian periods. This suggests not only an adaptive but a constituent role of the heat-shock pathway in the circadian clockwork[28,305]. The argument would therefore be that a temperature drop of the cell medium led to a decrease in HSF1-driven transcription and thus a longer period.

On a post-transcriptional level, circadian oscillations are influenced by cold-inducible RNA-binding protein (CIRP). CIRP expression levels increase with lower temperature and it binds to mRNA of circadian genes, most importantly *Clock*[308]. CIRP stabilises *Clock* mRNA and leads to an increased cytosolic fraction of the transcript, where it is translated into the CLOCK protein. Conversely in CIRP-depleted cells, cytosolic CLOCK levels decrease. Interestingly, *Clock* knockout mice (*Clock⁻/⁻*) display shorter periods than their wildtype counterparts, hence a possible link between lower temperatures and lengthened periods is the level of CLOCK expression[309].

The previous considerations would be consistent with a temperature drop of the cell culture during the stimulation procedure. This is of interest since most light sources emit heat energy as a by-product. On balance though, heat dissipation to the surroundings appear to dominate, calling for improved temperature control during the stimulation procedure.

Lastly, given the important role of PER and CRY stability in setting the pace of the TTL, one might speculate that the stimulation procedure affected the TTL at this molecular level, e.g. by delayed degradation of the proteins (cf. section 1.3). Further experiments with an optimised stimulation procedure with regard to temperature control are required in order to determine the exact cause of the lengthened periods.

4.5 Phase response curves: critical appraisal of methodology of construction

In the present study, two differing methods were used to analyse the phase response resulting from optogenetic or pharmacological stimulation. Both relied on the comparison of pre- and post-stimulation signals from the same well, thus yielding a phase response for each individual well. In order to put this phase response into context, the phase response relative to the mean phase response of the appropriate control condition was calculated. To avoid confusion, a terminological distinction between phase changes (/2π) and phase shifts (/h) was introduced.

The first method relied on extrapolating the post-stimulation signal backwards to the stimulation time point and to determine the change in phase between pre- and post-stimulation signal at this time point. An advantage of this method is that no correction for post-stimulation wavelength changes was necessary. It assumes an instant phase change upon stimulation which remains constant afterwards.

The second method relied on extrapolating the pre-stimulation signal beyond the stimulation time point and to determine the time difference between expected and observed defined phase points (nadirs or peaks of oscillation). A similar method has been described previously[287]. Due to the observed post-stimulation wavelength changes an extra calculation step was necessary to adjust the obtained phase shifts to the wavelength change of the individual well. One could argue that this correction renders the calculated phase shifts artificial and prone to error. Despite their differences, the two methods yielded remarkably consistent results. The phase response diagrams for phase changes (/2π, **Fig. 3.7**) and phase shifts (/h, **Fig. 3.10**) are virtually superimposable, underlining their respective validity.

A third possible method to interpret the data would have been the direct comparison of the post-stimulation signal of stimulated cells with those of the appropriate control cells, as used in other publications[286]. A considerable advantage of this method is the easy graphic demonstration of phase shifts. However, it was deemed unfeasible in the current experimental set-up for several reasons: firstly, even amongst the 6 wells on a plate receiving the same stimulation condition significant differences in period, phase, and post-stimulation wavelength change could be apparent. Thus no clear control curve exists. Secondly, comparisons between stimulated cells and control cells are only possible if these display the same wavelengths before and after stimulation as well as the identical phase at stimulation. These parameters vary between cells in different wells, hence a direct comparison of curves renders the resulting data meaningless as the inter-well differences are not controlled for.

In summary, whilst the methods used for the present analysis had their drawbacks, their key strength was that they account for inter-well variability.

4.6 Magnitude and kinetics of *Period* gene transcriptional changes in synchronised cells

In non-synchronised cells, optogenetic and pharmacological stimulation caused a significant upregulation of *Per1* (**Fig. 3.3**). Since *Per1* induction is thought to be a critical step in mediating phase shifts, its expression was also analysed in synchronised U2OS cells, the paradigm used in the construction of the phase response curve. Stimulation was carried out at the phase of peak *Bmal1* (i.e. nadir *Per1*) expression, which physiologically corresponds to the late night. At this phase, the largest phase responses in the form of phase advances were apparent in stimulated U2OS *Bmal1-Luc* cells (**Fig. 3.7** and **Fig. 3.10**). Furthermore, evidence for the role of *Per1* in mediating phase advances is strongest (cf. section 1.6).

It thus came as a surprise that optogenetic stimulation failed to elicit a robust *Per1* response in synchronised cells. *Per1* expression was numerically upregulated (**Fig. 3.11**), but this failed to reach statistical significance. In contrast, control cells that had been stimulated with forskolin displayed a highly significant *Per1* induction, which was numerically larger than that observed in non-synchronised cells (+130% vs. +70%, see. **Fig. 3.11** and **Fig. 3.3**). Inspection of the *Per1* response 2 h after stimulation showed that the same pattern was also evident in optogenetically stimulated cells (+55% in synchronised cells vs. +38% in non-synchronised cells).

Two factors contribute to the lack of statistical significance: firstly that the *Per1* expression in synchronised GFP control cells was larger than expected, and secondly that the variance in the *Per1* response of optogenetically stimulated cells was higher. The latter is caused in part by data from the *Per1* time profile (**Fig. 3.12**), where there was hardly any *Per1* upregulation seen, contributing to the data in **Fig. 3.11**. One could therefore argue that the variability of the effectiveness of optogenetic stimulation is a chief factor accounting for the lack of significance. A possible reason could be varying transfection efficiencies across the different experimental repeats.

A further point to consider is that in synchronised cells there might have been residual dexamethasone concentration and activity. The synchronisation procedure comprised a 2 h exposure to dexamethasone followed by a medium change. Since dexamethasone is lipophilic it diffuses into the cells, where it acts by binding to the GRE with high affinity. It is therefore questionable how much dexamethasone was removed by changing the medium. In this case, residual dexamethasone binding to the GRE in the *Per1* promoter would mean that baseline expression prior to stimulation was elevated, limiting additional *Per1* induction via the promoter's CRE. Whilst this hypothesis would account for the lack of *Per1* induction by optogenetic stimulation, it would not explain why forskolin elicited such a strong upregulation.

A final important point to consider regarding *Per1* is that the possibility has to be taken into account that the phase shifts observed were not in fact mediated by *Per1*, despite the evidence in the literature arguing to the contrary. Several strategies to interrogate the role of *Per1* are thinkable: it would be interesting whether changes on the protein level are detectable, i.e. whether PER1 concentration rises in response to optogenetic stimulation. The time point of measurement would have to be later though, as PER1 peaks around 2-3 h after *Per1*[174].Equally it would be possible to investigate whether the phase shifts observed can be blocked by interfering with *Per1* transcription or translation, e.g. by the application of antisense oligodeoxynucleotides or short interfering RNA (siRNA)[218]. Finally, as argued for in section 4.3, the use of a *Per1-Luciferase* construct (either as a plasmid or expressed in a cell line) would shed light on the acute behaviour of the gene in real-time[275].

When considering *Per2* in synchronised cells, it stands out that an upregulation observed was quite late (after 4 h). Even accounting for a delayed induction compared to *Per1*, this appears to be too late to conceivably display the behaviour of an immediate early gene which is directly induced by stimulation.

Furthermore, at the phase of stimulation (corresponding to the early morning) there is no convincing data suggesting *Per2* induction or a role in mediating phase shifts (cf. section 1.6). What seems most likely is that the effect observed was secondary to processes instigated prior, e.g. *de novo* produced transcription factors (like cFOS) acting on the *Per2* promoter. This hypothesis could be checked by blocking translation (e.g. through the application of cycloheximide) and repeating the experiment. Of greater interest would be to repeat the experiment at a phase where *Per1* transcription is high, corresponding to the early night. At this phase, the evidence for *Per2* induction is much stronger, although a potential dissociation between effects seen on the mRNA and protein level should be considered as a result of posttranslational modifications. In summary, further work is required to ascertain the behaviour of *Per2* in response to optogenetic stimulation and its potential role in mediating phase shifts.

4.7 *cFos* transcriptional changes as evidence for unspecific activation

In order to ascertain whether any transcriptional changes in response to optogenetic stimulation could be observed, a time profile of the immediate early gene *cFos* was assembled. Fast, strong and transient induction of *cFos* was observed in both stimulated and non-stimulated cells. Since *cFos* transcripts increase more rapidly (on the scale of 10 min, peaking after 30 min) in response to a stimulus than measurable with the used temporal resolution, it is likely the real peak of *cFos* was even higher[84,168]. There was no discernible difference between the stimulation conditions (with the caveat of the mentioned low temporal resolution), meaning the upregulation seen appears to stem from the procedure itself associated with stimulation. This involved the temporary removal of cell culture plates from an incubator or plate reader where they had been allowed to equilibrate with respect to temperature and atmosphere. After 15 min of illumination, and a further 5-15 min of administering the pharmacological stimulators as required, the cells were returned to their original location. Similarly as discussed in section 4.4, a change in temperature is a likely candidate driving the observed transcriptional changes[310,311], others being altered partial pressures of dissolved gases, pH of the cell culture or vibrations/motion. *cFos* in this case served as a marker gene for transcriptional changes that were unspecific to the individual stimulation condition and reflected disturbances during the stimulation procedure uncontrolled for. The late *cFos* upregulation component observed in both pharmacologically and optogenetically stimulated cells is of uncertain origin – a possible explanation could be that the rise reflects circadian oscillations triggered by stimulation.

In sections of the SCN, *cFos* transcription and expression is rhythmic, but little is known about rhythmicity in non-SCN cells[312]. Of note baseline *cFos* expression was elevated in cells containing bPAC compared to control cells. This suggests an adenylyl cyclase "dark" activity leading to relevantly elevated (but unmeasured) baseline cAMP concentrations, as will be discussed in the next section.

4.8 Effects of bPAC on baseline physiology

One of the reasons why bPAC was chosen for this study is its low enzymatic activity in the dark, since raised baseline cAMP concentrations might affect cellular physiology. In the current study, evidence for altered physiology is mixed:

Concerning transcriptional levels, baseline expression of clocks genes was not found to differ from controls, yet expression of *cFos* was significantly higher both in non-synchronised and synchronised cells. This observation is significant because cAMP exerts control on transcription via the PKA-CREB-pathway, and CREB-driven transcription controls a host of cellular processes besides the circadian cycle, e.g. cellular metabolism, neurotransmitter release, or neuronal differentiation[313]. It is therefore not surprising that several thousands of occupied CREB-binding sites close to promoters exist in diverse mammalian cell lines[314]. Further complexity arises as many CREB targets (such as *cFos*) are themselves transcription factors regulating other genes[315]. Therefore raised baseline cAMP concentrations due to the incorporation of bPAC could lead to wide-ranging and inadvertent physiological side effects, particularly if used in neuronal or endocrine cells. On the other hand a multitude of signaling pathways converge on CREB, the cAMP-PKA-cascade being just one of them[316]. Indeed the number of cAMP-responsive genes in a given cell line is considerably smaller (< 100) than the number of occupied CREB-binding sites. Furthermore, the profiles of inducible genes are highly tissue-specific as a result of tissue-specific CREB-binding and activation of further regulatory partners such as CBP, meaning different cell lines might be affected by altered baseline cAMP levels to a different degree[314,317]. Evidence from other publications using bPAC suggests that whether or not baseline cAMP concentration and cellular function is altered varies from study to study, meaning careful reassessment in each new experimental set-up is necessary[271,318–321].

Concerning key circadian parameters, period was not altered, whilst amplitude of circadian oscillations was lower in cells containing bPAC. The latter observation would be in agreement with chronically raised cAMP levels, however in such a case a *shorter* period should be observable[279]. This is not the case, arguing against cAMP levels raised significantly enough to alter circadian physiology. A possible explanation for the observed lower amplitude in oscillations might simply be fewer viable cells after transfection with bPAC and thus less luciferase activity, although this hypothesis was not tested by a live-dead stain.

On balance, it is reassuring that baseline expression of the clock genes and circadian period appeared to be unaffected by the presence of bPAC, indicating that overall circadian function of the cell model was unimpaired. This argues for baseline cAMP levels that, even if they might have been slightly raised, did not cross a physiologically relevant threshold for circadian processes. Should this problem arise in future investigations or in other cell models, a possible solution would be the use of a weaker promoter than the CMV promoter used here, yielding a lower bPAC expression. Alternatively it would be interesting to investigate whether intracellular spatial targeting of cAMP can reduce the side-effects of elevated baseline cAMP expression[322].

4.9 Modes of delivery of bPAC

In this study, it was chosen to deliver bPAC DNA to the cell model via transient transfection with a modified commercially available adeno-associated virus packaging plasmid containing the cloned bPAC DNA. The primary advantages of this method are its simplicity and its swiftness. A disadvantage is the dilution of plasmid DNA over time as transfected cells divide. This, together with suboptimal transfection efficiencies or plasmid degradation, means that bPAC DNA load might decrease to the extent that exposure to light would only lead to small increases in intracellular cAMP and thus dampened effects on transcription or other cellular processes.

For example, in the experiments investigating optogenetically induced phase shifts a time delay of up to 5 days between transfection and stimulation occurred. The high variability of results and the lack of statistical significance for cells transfected with bPAC, both in the experiments investigating clock gene expression as well as in those investigating the phase response, might be a direct consequence of insufficient bPAC DNA load. Alternatives to transient transfection exist, and going forwards from this study the next step for cell culture experiments would be the creation of a cell line stably expression bPAC, such as to circumvent the issue of uncertainty or

fluctuations in DNA quantity. For tissue culture or *in vivo* experiments use of a viral vector such as an adeno-associated viruses[321] or a lentivirus might be more feasible. Again, permanent expression by construction of transgenes would be preferable[272,318], aiming for tissue-specific expression in higher organisms by the use of tissue-specific promoters[273,319,320].

4.10 Optogenetic manipulation strategies of circadian rhythms

Few studies of optogenetically manipulated circadian rhythms have been reported: the one most closely resembling the presented work involved an optogenetically stimulated $G_{\alpha s}$-protein coupled receptor, also utilising the cAMP second messenger pathway to elicit changes in transcription and rhythmicity[287]. The phase response curve resembles the one constructed here, with similar orders of magnitude of the phase shifts observed. No survey of *Per1* transcription was carried out, however the authors report an upregulation of *Per2* (ca. +50%) and *Cry2* (ca. +120%) after 2 h of illumination at subjective dawn. Whilst the phase response curve is easily reconcilable with the data presented here, the transcriptional data is in disagreement. Particularly, at the reported time point no convincing evidence for the involvement of *Per2* in phase shifting exists.

Using a transgenic mouse model harbouring a SCN-directed channelrhodopsin as well as the PER2::LUC fusion protein, optogenetic manipulation of SCN neuron firing rates yielded phase responses *in vitro* and *in vivo* closely resembling those to light[288]. One can speculate whether delivery of bPAC to SCN neurons would have similar effects – limits could be posed by increased baseline cAMP concentrations, since cAMP has been described as a key constituent of the circadian clockwork[279]. Whether bPAC displays fast enough decay kinetics for the level of temporal control required in neurons would remain to be seen as well[271].

Whilst both an ion channel-based and a second messenger-based strategy for optogenetic control of circadian rhythms have been published, an intriguing angle of manipulation has thus far not been attempted or reported, namely the direct optogenetic control of the *Period* genes[267,268]. The advantage of this strategy would be that no unintended side effects of upstream signaling cascades would arise. Furthermore, it would allow for the precise dissection of the individual roles that upregulation of the two genes assume in causing phase shifts. Such an approach could help clarify a longstanding gap in knowledge in circadian physiology.

4.11 Limitations, critical appraisal and outlook

Several limitations of the experimental set up and manipulation strategies have been discussed in the previous sections, the most important being:

- the transient transfection method used to deliver bPAC is associated with varying DNA load between cells and over time, contributing to large variability of data obtained
- the stimulation strategy utilised the second messenger cAMP, which has pleiotropic effects, opening the possibility for off-target effects of stimulation which could potentially lead to wrong assumptions of causality
- the low but existent dark activity of bPAC potentially elevated baseline cAMP levels, which could potentially alter baseline intracellular physiology
- the stimulation procedure provided insufficient control of external conditions, most importantly temperature
- overall, the large variability of data raises doubts about reliability

Future work should thus focus on (i) experimental set ups in which bPAC is stably expressed to reduce inter- and intra-experimental variability, and (ii) improving the stimulation procedure, e.g. by stimulating using modern programmable LED-arrays[323] and ideally by engineering an illumination solution which circumvents the need for removal of cells from their incubator. If these challenges are overcome, selective delivery of bPAC and thus selective stimulation could for example be used to interrogate clock communication between different cell types residing within an organ or tissue, e.g. between astrocytes and neurons in the SCN or between the cells in the adrenal medulla and cortex[324–326]. It has to be kept in mind however, that for some experimental questions or in some set ups an optogenetic approach might fail or be unfeasible, e.g. due to complex illumination requirements, technical problems such as light scattering limiting spatial resolution, or when prolonged stimulation is desired. A chemogenetic approach should be considered in these cases, whereby an engineered receptor, e.g. a G-protein coupled receptor, is exclusively responsive to a small molecule ligand[327–329]. This technique involving so called DREADDs (designer receptors exclusively activated by designer drugs), bypasses some of the difficulties inherent in optogenetics, which were partly evident in the presented study.

Nonetheless, the study succeeded in optogenetically manipulating intracellular cAMP levels, clock gene transcription and circadian rhythms. Its novelty is underlined by the fact that it is only the second in the field utilising a second messenger-based approach to control circadian rhythms.

5 Summary

The daily light-dark cycle is the dominant rhythm governing most life on this planet, and most species have developed circadian clocks with an oscillatory period of ca. 24 h to track daytime. The molecular mechanism of circadian clocks in mammals consists of a transcriptional-translational feedback loop: in the positive arm the protein products of the clock genes *Bmal1* and *Clock* act as transcription factors on the clock genes *Period* and *Cryptochrome*. The protein products of these genes then form the negative arm, repressing *Bmal1* and *Clock's* transactivatory potential. Both *in vitro* and *in vivo* circadian clock rhythms are phase reset by diverse stimuli eliciting transcriptional changes in the *Period* genes following activation of the cAMP-PKA-CREB signaling cascade.

This study used an optogenetic approach involving the light-sensitive adenylyl cyclase bPAC from the marine and freshwater-dwelling bacterium *Beggiatoa* to manipulate circadian rhythms in human cell culture. For this purpose bPAC was cloned into a plasmid and delivered to cells by transient transfection. bPAC expressing cells were found to have an unaltered circadian phenotype. Upon illumination, a rapid increase in intracellular cAMP levels was observed. Furthermore, illumination caused phase-dependent delays and advances of cellular circadian rhythms. On a transcriptional level, the clock gene *Per1* was significantly upregulated in non-synchronised cells, whilst this upregulation was not significant in synchronised cells.

Limitations of the presented experiments include the large variability of data as well as a stimulation procedure providing insufficient control of external conditions. Lengthened circadian periods and unspecific transcriptional activation after illumination are likely to result from temperature fluctuations during the stimulation procedure. A further limitation of the used approach is the potential for altered baseline physiology due to elevated cAMP concentrations in cells expressing bPAC, since cAMP is a second messenger with pleiotropic effects.

Future work should thus focus on experimental set ups in which bPAC is stably expressed to reduce inter- and intra-experimental variability and to improve the stimulation procedure. Both are prerequisites for application of the technique in tissue culture or *in vivo*. Overall, the study succeeded in optogenetically manipulating intracellular cAMP levels, circadian gene transcription and circadian rhythms.

6 Literature

1. Paranjpe D, Sharma V. Evolution of temporal order in living organisms. *J Circadian Rhythm* 2005; 3: 7.

2. DeCoursey P, Walker J, Smith S. A circadian pacemaker in free-living chipmunks: essential for survival? *J Comp Physiol A* 2000; 186: 169–180.

3. Dodd AN, Salathia N, Hall A, et al. Cell biology: Plant circadian clocks increase photosynthesis, growth, survival, and competitive advantage. *Science* 2005; 309: 630–633.

4. Ouyang Y, Andersson CR, Kondo T, et al. Resonating circadian clocks enhance fitness in cyanobacteria. *Proc Natl Acad Sci U S A* 1998; 95: 8660–8664.

5. Yerushalmi S, Green RM. Evidence for the adaptive significance of circadian rhythms. *Ecol Lett* 2009; 12: 970–981.

6. Johnson CH, Zhao C, Xu Y, et al. Timing the day: What makes bacterial clocks tick? *Nat Rev Microbiol* 2017; 15: 232–242.

7. Bell-Pedersen D, Cassone VM, Earnest DJ, et al. Circadian rhythms from multiple oscillators: Lessons from diverse organisms. *Nat Rev Genet* 2005; 6: 544–556.

8. Aschoff J. Circadian Rhythms in Man. *Science* 1965; 148: 1427–1432.

9. Nobel Media AB. The Nobel Prize in Physiology or Medicine 2017, https://www.nobelprize.org/prizes/medicine/2017/summary/ (accessed 22 August 2020).

10. Yoo SH, Yamazaki S, Lowrey PL, et al. PERIOD2::LUCIFERASE real-time reporting of circadian dynamics reveals persistent circadian oscillations in mouse peripheral tissues. *Proc Natl Acad Sci U S A* 2004; 101: 5339–5346.

11. Durgan DJ, Hotze MA, Tomlin TM, et al. The intrinsic circadian clock within the cardiomyocyte. *Am J Physiol - Hear Circ Physiol* 2005; 289: H1530-1541.

12. Bollinger T, Leutz A, Leliavski A, et al. Circadian clocks in mouse and human CD4+ T cells. *PLoS One* 2011; 6: e29801.

13. Balsalobre A, Damiola F, Schibler U. A serum shock induces circadian gene expression in mammalian tissue culture cells. *Cell* 1998; 93: 929–937.

14. Welsh DK, Yoo SH, Liu AC, et al. Bioluminescence imaging of individual fibroblasts reveals persistent, independently phased circadian rhythms of clock gene expression. *Curr Biol* 2004; 14: 2289–2295.

15. Sinturel F, Gos P, Petrenko V, et al. Circadian hepatocyte clocks keep synchrony in the absence of a master pacemaker in the suprachiasmatic nucleus or other extrahepatic clocks. *Genes Dev* 2021; 35: 329–334.

16. Stephan FK, Zucker I. Circadian rhythms in drinking behavior and locomotor activity of rats are eliminated by hypothalamic lesions. *Proc Natl Acad Sci U S A* 1972; 69: 1583–1586.

17. Moore RY, Eichler VB. Loss of a circadian adrenal corticosterone rhythm following suprachiasmatic lesions in the rat. *Brain Res* 1972; 42: 201–206.

18. Welsh DK, Logothetis DE, Meister M, et al. Individual neurons dissociated from rat suprachiasmatic nucleus express independently phased circadian firing rhythms. *Neuron* 1995; 14: 697–706.

19. Liu C, Weaver DR, Strogatz SH, et al. Cellular construction of a circadian clock: Period determination in the suprachiasmatic nuclei. *Cell* 1997; 91: 855–860.

20. Colwell CS. Rhythmic coupling among cells in the suprachiasmatic nucleus. *J Neurobiol* 2000; 43: 379–388.

21. Long MA, Jutras MJ, Connors BW, et al. Electrical synapses coordinate activity in the suprachiasmatic nucleus. *Nat Neurosci* 2005; 8: 61–66.

22. Plano SA, Golombek DA, Chiesa JJ. Circadian entrainment to light-dark cycles involves extracellular nitric oxide communication within the suprachiasmatic nuclei. *Eur J Neurosci* 2010; 31: 876–882.

23. Honma S, Shirakawa T, Nakamura W, et al. Synaptic communication of cellular oscillations in the rat suprachiasmatic neurons. *Neurosci Lett* 2000; 294: 113–116.

24. Shirakawa T, Honma S, Katsuno Y, et al. Synchronization of circadian firing rhythms in cultured rat suprachiasmatic neurons. *Eur J Neurosci* 2000; 12: 2833–2838.

25. Yamaguchi S, Isejima H, Matsuo T, et al. Synchronization of Cellular Clocks in the Suprachiasmatic Nucleus. *Science* 2003; 302: 1408–1412.

26. Herzog ED, Aton SJ, Numano R, et al. Temporal Precision in the Mammalian Circadian System: A Reliable Clock from Less Reliable Neurons. *J Biol Rhythms* 2004; 19: 35–46.

27. Liu AC, Welsh DK, Ko CH, et al. Intercellular Coupling Confers Robustness against Mutations in the SCN Circadian Clock Network. *Cell* 2007; 129: 605–616.

28. Buhr ED, Yoo SH, Takahashi JS. Temperature as a universal resetting cue for mammalian circadian oscillators. *Science* 2010; 330: 379–385.

29. Welsh DK, Takahashi JS, Kay SA. Suprachiasmatic nucleus: Cell autonomy and network properties. *Annu Rev Physiol* 2009; 72: 551–577.

30. Abrahamson EE, Moore RY. Suprachiasmatic nucleus in the mouse: Retinal innervation, intrinsic organization and efferent projections. *Brain Res* 2001; 916: 172–191.

31. Leak RK, Card JP, Moore RY. Suprachiasmatic pacemaker organization analyzed by viral transynaptic transport. *Brain Res* 1999; 819: 23–32.

32. Moore RY, Speh JC. GABA is the principal neurotransmitter of the circadian system. *Neurosci Lett* 1993; 150: 112–116.

33. Moore RY, Lenn NJ. A retinohypothalamic projection in the rat. *J Comp Neurol* 1972; 146: 1–14.

34. Levine JD, Weiss ML, Rosenwasser AM, et al. Retinohypothalamic tract in the female albino rat: a study using horseradish peroxidase conjugated to cholera toxin. *J Comp Neurol* 1991; 306: 344–360.

35. Johnson RF, Moore RY, Morin LP. Loss of entrainment and anatomical plasticity after lesions of the hamster retinohypothalamic tract. *Brain Res* 1988; 460: 297–313.

36. Ebling FJP. The role of glutamate in the photic regulation of the suprachiasmatic nucleus. *Prog Neurobiol* 1996; 50: 109–132.

37. Hannibal J. Neurotransmitters of the retino-hypothalamic tract. *Cell Tissue Res* 2002; 309: 73–88.

38. Swanson LW, Cowan WM, Jones EG. An autoradiographic study of the efferent connections of the ventral lateral geniculate nucleus in the albino rat and the cat. *J Comp Neurol* 1974; 156: 143–163.

39.   Zhang DX, Rusak B. Photic sensitivity of geniculate neurons that project to the suprachiasmatic nuclei or the contralateral geniculate. *Brain Res* 1989; 504: 161–164.

40.   Harrington ME. The ventral lateral geniculate nucleus and the intergeniculate leaflet: Interrelated structures in the visual and circadian systems. *Neurosci Biobehav Rev* 1997; 21: 705–727.

41.   Hanna L, Walmsley L, Pienaar A, et al. Geniculohypothalamic GABAergic projections gate suprachiasmatic nucleus responses to retinal input. *J Physiol* 2017; 595: 3621–3649.

42.   Edelstein K, Amir S. The role of the intergeniculate leaflet in entrainment of circadian rhythms to a skeleton photoperiod. *J Neurosci* 1999; 19: 372–380.

43.   Freeman DA, Dhandapani KM, Goldman BD. The thalamic intergeniculate leaflet modulates photoperiod responsiveness in Siberian hamsters. *Brain Res* 2004; 1028: 31–38.

44.   Meyer-Bernstein EL, Morin LP. Differential serotonergic innervation of the suprachiasmatic nucleus and the intergeniculate leaflet and its role in circadian rhythm modulation. *J Neurosci* 1996; 16: 2097–2111.

45.   Moga MM, Moore RY. Organization of neural inputs to the suprachiasmatic nucleus in the rat. *J Comp Neurol* 1997; 389: 508–534.

46.   Glass JD, Grossman GH, Farnbauch L, et al. Midbrain raphe modulation of nonphotic circadian clock resetting and 5-HT release in the mammalian suprachiasmatic nucleus. *J Neurosci* 2003; 23: 7451–7460.

47.   Morin LP. Neuroanatomy of the extended circadian rhythm system. *Exp Neurol* 2013; 243: 4–20.

48.   Hermes MLHJ, Coderre EM, Buijs RM, et al. GABA and glutamate mediate rapid neurotransmission from suprachiasmatic nucleus to hypothalamic paraventricular nucleus in rat. *J Physiol* 1996; 496: 749–757.

49.   Kalsbeek A, Buijs RM, van Heerikhuize JJ, et al. Vasopressin-containing neurons of the suprachiasmatic nuclei inhibit corticosterone release. *Brain Res* 1992; 580: 62–67.

50.   Cheng MY, Bullock CM, Li C, et al. Prokineticin 2 transmits the behavioural circadian rhythm of the suprachiasmatic nucleus. *Nature* 2002; 417: 405–410.

51.   Schwartz WJ, Gross RA, Morton MT. The suprachiasmatic nuclei contain a tetrodotoxin-resistant circadian pacemaker. *Proc Natl Acad Sci U S A* 1987; 84: 1694–1698.

52.   Guo H, Brewer JMK, Champhekar A, et al. Differential control of peripheral circadian rhythms by suprachiasmatic-dependent neural signals. *Proc Natl Acad Sci U S A* 2005; 102: 3111–3116.

53.   Silver R, LeSauter J, Tresco PA, et al. A diffusible coupling signal from the transplanted suprachiasmatic nucleus controlling circadian locomotor rhythms. *Nature* 1996; 382: 810–813.

54.   Meyer-Bernstein EL, Jetton AE, Matsumoto SI, et al. Effects of suprachiasmatic transplants on circadian rhythms of neuroendocrine function in golden hamsters. *Endocrinology* 1999; 140: 207–218.

55.   Dibner C, Schibler U, Albrecht U. The mammalian circadian timing system: Organization and coordination of central and peripheral clocks. *Annu Rev Physiol* 2009; 72: 517–549.

56.   Kalsbeek A, Foppen E, Schalij I, et al. Circadian control of the daily plasma glucose rhythm: An interplay of GABA and glutamate. *PLoS One* 2008; 3: e3194.

57. Buijs RM, Wortel J, Van Heerikhuize JJ, et al. Anatomical and functional demonstration of a multisynaptic suprachiasmatic nucleus adrenal (cortex) pathway. *Eur J Neurosci* 1999; 11: 1535–1544.

58. Buijs RM, Chun SJ, Niijima A, et al. Parasympathetic and sympathetic control of the pancreas: A role for the suprachiasmatic nucleus and other hypothalamic centers that are involved in the regulation of food intake. *J Comp Neurol* 2001; 431: 405–423.

59. Buijs RM, La Fleur SE, Wortel J, et al. The suprachiasmatic nucleus balances sympathetic and parasympathetic output to peripheral organs through separate preautonomic neurons. *J Comp Neurol* 2003; 464: 36–48.

60. Vujović N, Davidson AJ, Menaker M. Sympathetic input modulates, but does not determine, phase of peripheral circadian oscillators. *Am J Physiol - Regul Integr Comp Physiol* 2008; 295: R355-360.

61. Cailotto C, Lei J, van der Vliet J, et al. Effects of nocturnal light on (clock) gene expression in peripheral organs: A role for the autonomic innervation of the liver. *PLoS One* 2009; 4: e5650.

62. Terazono H, Mutoh T, Yamaguchi S, et al. Adrenergic regulation of clock gene expression in mouse liver. *Proc Natl Acad Sci U S A* 2003; 100: 6795–6800.

63. Balsalobre A, Brown SA, Marcacci L, et al. Resetting of circadian time in peripheral tissues by glucocorticoid signaling. *Science* 2000; 289: 2344–2347.

64. Le Minh N, Damiola F, Tronche F, et al. Glucocorticoid hormones inhibit food-induced phase-shifting of peripheral circadian oscillators. *EMBO J* 2001; 20: 7128–7136.

65. Teclemariam-Mesbah R, Ter Horst GJ, Postema F, et al. Anatomical demonstration of the suprachiasmatic nucleus - Pineal pathway. *J Comp Neurol* 1999; 406: 171–182.

66. Kalsbeek A, Garidou ML, Palm IF, et al. Melatonin sees the light: Blocking GABA-ergic transmission in the paraventricular nucleus induces daytime secretion of melatonin. *Eur J Neurosci* 2000; 12: 3146–3154.

67. Bouatia-Naji N, Bonnefond A, Cavalcanti-Proença C, et al. A variant near MTNR1B is associated with increased fasting plasma glucose levels and type 2 diabetes risk. *Nat Genet* 2009; 41: 89–94.

68. Zawilska JB, Skene DJ, Arendt J. Physiology and pharmacology of melatonin in relation to biological rhythms. *Pharmacol Reports* 2009; 61: 383–410.

69. Brown SA, Zumbrunn G, Fleury-Olela F, et al. Rhythms of mammalian body temperature can sustain peripheral circadian clocks. *Curr Biol* 2002; 12: 1574–1583.

70. Stokkan KA, Yamazaki S, Tei H, et al. Entrainment of the circadian clock in the liver by feeding. *Science* 2001; 291: 490–493.

71. Damiola F, Le Minh N, Preitner N, et al. Restricted feeding uncouples circadian oscillators in peripheral tissues from the central pacemaker in the suprachiasmatic nucleus. *Genes Dev* 2000; 14: 2950–2961.

72. Lehman MN, Silver R, Gladstone WR, et al. Circadian rhythmicity restored by neural transplant. Immunocytochemical characterization of the graft and its integration with the host brain. *J Neurosci* 1987; 7: 1626–1638.

73. Ralph MR, Foster RG, Davis FC, et al. Transplanted suprachiasmatic nucleus determines circadian period. *Science* 1990; 247: 975–978.

74. Lowrey PL, Takahashi JS. Genetics of circadian rhythms in mammalian model organisms. *Adv Genet* 2011; 74: 175–230.

75. Shearman LP, Sriram S, Weaver DR, et al. Interacting molecular loops in the mammalian circadian clock. *Science* 2000; 288: 1013–1019.

76. Yagita K, Tamanini F, Van der Horst GTJ, et al. Molecular mechanisms of the biological clock in cultured fibroblasts. *Science* 2001; 292: 278–281.

77. Gekakis N, Staknis D, Nguyen HB, et al. Role of the CLOCK protein in the mammalian circadian mechanism. *Science* 1998; 280: 1564–1569.

78. Bunger MK, Wilsbacher LD, Moran SM, et al. Mop3 is an essential component of the master circadian pacemaker in mammals. *Cell* 2000; 103: 1009–1017.

79. Hogenesch JB, Gu YZ, Jain S, et al. The basic-helix-loop-helix-PAS orphan MOP3 forms transcriptionally active complexes with circadian and hypoxia factors. *Proc Natl Acad Sci U S A* 1998; 95: 5474–5479.

80. Yamaguchi S, Mitsui S, Miyake S, et al. The 5' upstream region of mPer1 gene contains two promoters and is responsible for circadian oscillation. *Curr Biol* 2000; 10: 873–876.

81. Hida A, Koike N, Hirose M, et al. The Human and Mouse Period1 Genes: Five Well-Conserved E-Boxes Additively Contribute to the Enhancement of mPer1 Transcription. *Genomics* 2000; 65: 224–233.

82. Tei H, Okamura H, Shigeyoshi Y, et al. Circadian oscillation of a mammalian homologue of the Drosophila period gene. *Nature* 1997; 389: 512–516.

83. Sun ZS, Albrecht U, Zhuchenko O, et al. RIGUI, a putative mammalian ortholog of the Drosophila period gene. *Cell* 1997; 90: 1003–1011.

84. Albrecht U, Sun ZS, Eichele G, et al. A differential response of two putative mammalian circadian regulators, mper1 and mper2, to light. *Cell* 1997; 91: 1055–1064.

85. Shearman LP, Zylka MJ, Weaver DR, et al. Two period homologs: Circadian expression and photic regulation in the suprachiasmatic nuclei. *Neuron* 1997; 19: 1261–1269.

86. Takumi T, Matsubara C, Shigeyoshi Y, et al. A new mammalian period gene predominantly expressed in the suprachiasmatic nucleus. *Genes to Cells* 1998; 3: 167–176.

87. Zylka MJ, Shearman LP, Weaver DR, et al. Three period homologs in mammals: Differential light responses in the suprachiasmatic circadian clock and oscillating transcripts outside of brain. *Neuron* 1998; 20: 1103–1110.

88. Takumi T, Taguchi K, Miyake S, et al. A light-independent oscillatory gene mPer3 in mouse SCN and OVLT. *EMBO J* 1998; 17: 4753–4759.

89. Griffin EA, Staknis D, Weitz CJ. Light-independent role of CRY1 and CRY2 in the mammalian circadian clock. *Science* 1999; 286: 768–771.

90. Kume K, Zylka MJ, Sriram S, et al. mCRY1 and mCRY2 are essential components of the negative limb of the circadian clock feedback loop. *Cell* 1999; 98: 193–205.

91. Chen R, Schirmer A, Lee Y, et al. Rhythmic PER Abundance Defines a Critical Nodal Point for Negative Feedback within the Circadian Clock Mechanism. *Mol Cell* 2009; 36: 417–430.

92. Sato TK, Yamada RG, Ukai H, et al. Feedback repression is required for mammalian circadian clock function. *Nat Genet* 2006; 38: 312–319.

93. Cao X, Yang Y, Selby CP, et al. Molecular mechanism of the repressive phase of the mammalian circadian clock. *Proc Natl Acad Sci U S A* 2021; 118: e2021174118.

94. Sato TK, Panda S, Miraglia LJ, et al. A functional genomics strategy reveals rora as a component of the mammalian circadian clock. *Neuron* 2004; 43: 527–537.

95. Preitner N, Damiola F, Luis-Lopez-Molina, et al. The orphan nuclear receptor REV-ERBα controls circadian transcription within the positive limb of the mammalian circadian oscillator. *Cell* 2002; 110: 251–260.

96. Guillaumond F, Dardente H, Giguère V, et al. Differential control of Bmal1 circadian transcription by REV-ERB and ROR nuclear receptors. *J Biol Rhythms* 2005; 20: 391–403.

97. Akashi M, Takumi T. The orphan nuclear receptor RORα regulates circadian transcription of the mammalian core-clock Bmal1. *Nat Struct Mol Biol* 2005; 12: 441–448.

98. Takahashi JS. Transcriptional architecture of the mammalian circadian clock. *Nat Rev Genet* 2017; 18: 164–179.

99. Lee C, Etchegaray JP, Cagampang FRA, et al. Posttranslational mechanisms regulate the mammalian circadian clock. *Cell* 2001; 107: 855–867.

100. Schmutz I, Wendt S, Schnell A, et al. Protein Phosphatase 1 (PP1) is a post-translational regulator of the Mammalian Circadian Clock. *PLoS One* 2011; 6: e21325.

101. Lee H, Chen R, Lee Y, et al. Essential roles of CKIdelta and CKIepsilon in the mammalian circadian clock. *Proc Natl Acad Sci U S A* 2009; 106: 21359–21364.

102. Lee HM, Chen R, Kim H, et al. The period of the circadian oscillator is primarily determined by the balance between casein kinase 1 and protein phosphatase 1. *Proc Natl Acad Sci U S A* 2011; 108: 16451–16456.

103. Vielhaber E, Eide E, Rivers A, et al. Nuclear Entry of the Circadian Regulator mPER1 Is Controlled by Mammalian Casein Kinase I ε. *Mol Cell Biol* 2000; 20: 4888–4899.

104. Akashi M, Tsuchiya Y, Yoshino T, et al. Control of Intracellular Dynamics of Mammalian Period Proteins by Casein Kinase I ε (CKIε) and CKIδ in Cultured Cells. *Mol Cell Biol* 2002; 22: 1693–1703.

105. Eide EJ, Woolf MF, Kang H, et al. Control of Mammalian Circadian Rhythm by CKIε-Regulated Proteasome-Mediated PER2 Degradation. *Mol Cell Biol* 2005; 25: 2795–2807.

106. Zhou M, Kim JK, Eng GWL, et al. A Period2 Phosphoswitch Regulates and Temperature Compensates Circadian Period. *Mol Cell* 2015; 60: 77–88.

107. Lamia KA, Sachdeva UM, Di Tacchio L, et al. AMPK regulates the circadian clock by cryptochrome phosphorylation and degradation. *Science* 2009; 326: 437–440.

108. Shirogane T, Jin J, Ang XL, et al. SCFβ-TRCP controls Clock-dependent transcription via casein kinase 1-dependent degradation of the mammalian period-1 (Per1) protein. *J Biol Chem* 2005; 280: 26863–26872.

109. Reischl S, Vanselow K, Westermark PO, et al. β-TrCP1-mediated degradation of PERIOD2 is essential for circadian dynamics. *J Biol Rhythms* 2007; 22: 375–386.

110. Yoo SH, Mohawk JA, Siepka SM, et al. Competing E3 ubiquitin ligases govern circadian periodicity by degradation of CRY in nucleus and cytoplasm. *Cell* 2013; 152: 1091–1105.

111. Meng QJ, Logunova L, Maywood ES, et al. Setting Clock Speed in Mammals: The CK1ε tau Mutation in Mice Accelerates Circadian Pacemakers by Selectively Destabilizing PERIOD Proteins. *Neuron* 2008; 58: 78–88.

112. Maywood ES, Chesham JE, Smyllie NJ, et al. The Tau Mutation of Casein Kinase ε Sets the Period of the Mammalian Pacemaker via Regulation of Period1 or Period2 Clock Proteins. *J Biol Rhythms* 2014; 29: 110–118.

113. Wilkins AK, Barton PI, Tidor B. The Per2 negative feedback loop sets the period in the mammalian circadian clock mechanism. *PLoS Comput Biol* 2007; 3: e242.

114. Masuda S, Narasimamurthy R, Yoshitane H, et al. Mutation of a PER2 phosphodegron perturbs the circadian phosphoswitch. *Proc Natl Acad Sci U S A* 2020; 117: 10888–10896.

115. Ripperger JA, Shearman LP, Reppert SM, et al. CLOCK, an essential pacemaker component, controls expression of the circadian transcription factor DBP. *Genes Dev* 2000; 14: 679–689.

116. Lavery DJ, Lopez-Molina L, Margueron R, et al. Circadian Expression of the Steroid 15 α-Hydroxylase (Cyp2a4) and Coumarin 7-Hydroxylase (Cyp2a5) Genes in Mouse Liver Is Regulated by the PAR Leucine Zipper Transcription Factor DBP. *Mol Cell Biol* 1999; 19: 6488–6499.

117. Lopez-Molina L, Conquet F, Dubois-Dauphin M, et al. The DBP gene is expressed according to a circadian rhythm in the suprachiasmatic nucleus and influences circadian behavior. *EMBO J* 1997; 16: 6762–6771.

118. Cho H, Zhao X, Hatori M, et al. Regulation of circadian behaviour and metabolism by REV-ERB-α and REV-ERB-β. *Nature* 2012; 485: 123–127.

119. Zhang R, Lahens NF, Ballance HI, et al. A circadian gene expression atlas in mammals: Implications for biology and medicine. *Proc Natl Acad Sci U S A* 2014; 111: 16219–16224.

120. Storch KF, Lipan O, Leykin I, et al. Extensive and divergent circadian gene expression in liver and heart. *Nature* 2002; 417: 78–83.

121. Panda S, Antoch MP, Miller BH, et al. Coordinated transcription of key pathways in the mouse by the circadian clock. *Cell* 2002; 109: 307–320.

122. Crosby P, Partch CL. New insights into non-transcriptional regulation of mammalian core clock proteins. *J Cell Sci* 2020; 133: jcs241174.

123. Reddy AB, Karp NA, Maywood ES, et al. Circadian Orchestration of the Hepatic Proteome. *Curr Biol* 2006; 16: 1107–1115.

124. Deery MJ, Maywood ES, Chesham JE, et al. Proteomic Analysis Reveals the Role of Synaptic Vesicle Cycling in Sustaining the Suprachiasmatic Circadian Clock. *Curr Biol* 2009; 19: 2031–2036.

125. Daan S, Pittendrigh CS. A Functional analysis of circadian pacemakers in nocturnal rodents - II. The variability of phase response curves. *J Comp Physiol* 1976; 106: 253–266.

126. Golombek DA, Rosenstein RE. Physiology of circadian entrainment. *Physiol Rev* 2010; 90: 1063–1102.

127. Berson DM, Dunn FA, Takao M. Phototransduction by retinal ganglion cells that set the circadian clock. *Science* 2002; 295: 1070–1073.

128. Melyan Z, Tarttelin EE, Bellingham J, et al. Addition of human melanopsin renders mammalian cells photoresponsive. *Nature* 2005; 433: 741–745.

129. Qiu X, Kumbalasiri T, Carlson SM, et al. Induction of photosensitivity by heterologous expression of melanopsin. *Nature* 2005; 433: 745–749.

130. Panda S, Sato TK, Castrucci AM, et al. Melanopsin (Opn4) requirement for normal light-induced circadian phase shifting. *Science* 2002; 298: 2213–2216.

131. Gompf HS, Fuller PM, Hattar S, et al. Impaired circadian photosensitivity in mice lacking glutamate transmission from retinal melanopsin cells. *J Biol Rhythms* 2015; 30: 35–41.

132. Mintz EM, Marvel CL, Gillespie CF, et al. Activation of NMDA receptors in the suprachiasmatic nucleus produces light-like phase shifts of the circadian clock in vivo. *J Neurosci* 1999; 19: 5124–5130.

133. Colwell CS, Menaker M. NMDA as Well as Non-NMDA Receptor Antagonists Can Prevent the Phase-Shifting Effects of Light on the Circadian System of the Golden Hamster. *J Biol Rhythms* 1992; 7: 125–136.

134. Meijer JH, Albus H, Weidema F, et al. The effects of glutamate on membrane potential and discharge rate of suprachiasmatic neurons. *Brain Res* 1993; 603: 284–288.

135. Mizoro Y, Yamaguchi Y, Kitazawa R, et al. Activation of AMPA receptors in the suprachiasmatic nucleus phase-shifts the mouse circadian clock in vivo and in vitro. *PLoS One* 2010; 5: e10951.

136. Colwell CS. NMDA-evoked calcium transients and currents in the suprachiasmatic nucleus: gating by the circadian system. *Eur J Neurosci* 2001; 13: 1420–1428.

137. Kim DY, Choi HJ, Kim JS, et al. Voltage-gated calcium channels play crucial roles in the glutamate-induced phase shifts of the rat suprachiasmatic circadian clock. *Eur J Neurosci* 2005; 21: 1215–1222.

138. Ding JM, Buchanan GF, Tischkau SA, et al. A neuronal ryanodine receptor mediates light-induced phase delays of the circadian clock. *Nature* 1998; 394: 381–384.

139. Prosser R, McArthur J, Gillette MU. cGMP induces phase shifts of a mammalian circadian pacemaker at night, in antiphase to cAMP effects. *Proc Natl Acad Sci U S A* 1989; 86: 6812–6815.

140. Ding JM, Chen D, Weber ET, et al. Resetting the biological clock: Mediation of nocturnal circadian shifts by glutamate and NO. *Science* 1994; 266: 1713–1717.

141. Yokota SI, Yamamoto M, Moriya T, et al. Involvement of calcium-calmodulin protein kinase but not mitogen-activated protein kinase in light-induced phase delays and Per gene expression in the suprachiasmatic nucleus of the hamster. *J Neurochem* 2001; 77: 618–627.

142. Golombek DA, Agostino P V., Plano SA, et al. Signaling in the mammalian circadian clock: The NO/cGMP pathway. *Neurochem Int* 2004; 45: 929–936.

143. Rosen LB, Ginty DD, Weber MJ, et al. Membrane depolarization and calcium influx stimulate MEK and MAP kinase via activation of Ras. *Neuron* 1994; 12: 1207–1221.

144. Obrietan K, Impey S, Storm DR. Light and circadian rhythmicity regulate MAP kinase activation in the suprachiasmatic nuclei. *Nat Neurosci* 1998; 1: 693–700.

145. Dziema H, Oatis B, Butcher GQ, et al. The ERK/MAP kinase pathway couples light to immediate-early gene expression in the suprachiasmatic nucleus. *Eur J Neurosci* 2003; 277: 29519–29525.

146. Butcher GQ, Dziema H, Collamore M, et al. The p42/44 mitogen-activated protein kinase pathway couples photic input to circadian clock entrainment. *J Biol Chem* 2002; 277: 29519–29525.

147. Tischkau SA, Gallman EA, Buchanan GF, et al. Differential cAMP gating of glutamatergic signaling regulates long-term state changes in the suprachiasmatic circadian clock. *J Neurosci* 2000; 20: 7830–7837.

148. Schak KM, Harrington ME. Protein kinase C inhibition and activation phase advances the hamster circadian clock. *Brain Res* 1999; 840: 158–161.

149. Jakubcakova V, Oster H, Tamanini F, et al. Light Entrainment of the Mammalian Circadian Clock by a PRKCA-Dependent Posttranslational Mechanism. *Neuron* 2007; 54: 831–843.

150. Lee B, Almad A, Butcher GQ, et al. Protein kinase C modulates the phase-delaying effects of light in the mammalian circadian clock. *Eur J Neurosci* 2007; 26: 451–462.

151. Antoun G, Cannon PB, Cheng HYM. Regulation of MAPK/ERK signaling and photic entrainment of the suprachiasmatic nucleus circadian clock by raf kinase inhibitor protein. *J Neurosci* 2012; 32: 4867–4877.

152. Masubuchi S, Gao T, O'Neill A, et al. Protein phosphatase PHLPP1 controls the light-induced resetting of the circadian clock. *Proc Natl Acad Sci U S A* 2010; 107: 1642–1647.

153. Doi M, Cho S, Yujnovsky I, et al. Light-inducible and clock-controlled expression of MAP kinase phosphatase 1 in mouse central pacemaker neurons. *J Biol Rhythms* 2007; 22: 127–139.

154. West AE, Chen WG, Dalva MB, et al. Calcium regulation of neuronal gene expression. *Proc Natl Acad Sci U S A* 2001; 98: 11024–11031.

155. Shaywitz AJ, Greenberg ME. CREB: A stimulus-induced transcription factor activated by a diverse array of extracellular signals. *Annu Rev Biochem* 1999; 68: 821–861.

156. von Gall C, Duffield GE, Hastings MH, et al. CREB in the mouse SCN: a molecular interface coding the phase-adjusting stimuli light, glutamate, PACAP, and melatonin for clockwork access. *J Neurosci* 1998; 18: 10389–10397.

157. Obrietan K, Impey S, Smith D, et al. Circadian regulation of cAMP response element-mediated gene expression in the suprachiasmatic nuclei. *J Biol Chem* 1999; 274: 17748–17756.

158. Ginty DD, Kornhauser JM, Thompson MA, et al. Regulation of CREB phosphorylation in the suprachiasmatic nucleus by light and a circadian clock. *Science* 1993; 260: 238–241.

159. Gau D, Lemberger T, Von Gall C, et al. Phosphorylation of CREB Ser142 regulates light-induced phase shifts of the circadian clock. *Neuron* 2002; 34: 245–253.

160. Wheaton KL, Hansen KF, Aten S, et al. The Phosphorylation of CREB at Serine 133 Is a Key Event for Circadian Clock Timing and Entrainment in the Suprachiasmatic Nucleus. *J Biol Rhythms* 2018; 33: 497–514.

161. Tischkau SA, Mitchell JW, Tyan SH, et al. Ca2+/cAMP response element-binding protein (CREB)-dependent activation of Per1 is required for light-induced signaling in the suprachiasmatic nucleus circadian clock. *J Biol Chem* 2003; 278: 718–723.

162. Sakamoto K, Norona FE, Alzate-Correa D, et al. Clock and light regulation of the CREB coactivator CRTC1 in the suprachiasmatic circadian clock. *J Neurosci* 2013; 33: 9021–9027.

163. Jagannath A, Butler R, Godinho SIH, et al. The CRTC1-SIK1 pathway regulates entrainment of the circadian clock. *Cell* 2013; 154: 1100–1111.

164. Stehle JH, Pfeffer M, Kühn R, et al. Light-induced expression of transcription factor ICER (inducible cAMP early repressor) in rat suprachiasmatic nucleus is phase-restricted. *Neurosci Lett* 1996; 217: 169–172.

165. Schwartz WJ, Aronin N, Sassone-Corsi P. Photoinducible and rhythmic ICER-CREM immunoreactivity in the rat suprachiasmatic nucleus. *Neurosci Lett* 2005; 385: 87–91.

166. Zmrzljak UP, Korenĉiĉ A, Košir R, et al. Inducible cAMP early repressor regulates the period 1 gene of the hepatic and adrenal clocks. *J Biol Chem* 2013; 288: 10318–10327.

167. Aronin N, Sagar SM, Sharp FR, et al. Light regulates expression of a Fos-related protein in rat suprachiasmatic nuclei. *Proc Natl Acad Sci U S A* 1990; 87: 5959–5962.

168. Kornhauser JM, Nelson DE, Mayo KE, et al. Photic and circadian regulation of c-fos gene expression in the hamster suprachiasmatic nucleus. *Neuron* 1990; 5: 127–134.

169. Kornhauser JM, Nelson DE, Mayo KE, et al. Regulation of jun-B messenger RNA and AP-1 activity by light and a circadian clock. *Science* 1992; 255: 1581–1584.

170. Field MD, Maywood ES, O'Brien JA, et al. Analysis of clock proteins in mouse SCN demonstrates phylogenetic divergence of the circadian clockwork and resetting mechanisms. *Neuron* 2000; 25: 437–447.

171. Yan L, Silver R. Differential induction and localization of mPer1 and mPer2 during advancing and delaying phase shifts. *Eur J Neurosci* 2002; 16: 1531–1540.

172. Shigeyoshi Y, Taguchi K, Yamamoto S, et al. Light-induced resetting of a mammalian circadian clock is associated with rapid induction of the mPer1 transcript. *Cell* 1997; 91: 1043–1053.

173. Schwartz WJ, Tavakoli-Nezhad M, Lambert CM, et al. Distinct patterns of Period gene expression in the suprachiasmatic nucleus underlie circadian clock photoentrainment by advances or delays. *Proc Natl Acad Sci U S A* 2011; 108: 17219–17224.

174. Yan L, Silver R. Resetting the brain clock: Time course and localization of mPER1 and mPER2 protein expression in suprachiasmatic nuclei during phase shifts. *Eur J Neurosci* 2004; 19: 1105–1109.

175. Akiyama M, Kouzu Y, Takahashi S, et al. Inhibition of light- or glutamate-induced *mPer1* expression represses the phase shifts into the mouse circadian locomotor and suprachiasmatic firing rhythms. *J Neurosci* 1999; 19: 1115–1121.

176. Wakamatsu H, Takahashi S, Moriya T, et al. Additive effect of mPer1 and mPer2 antisense oligonucleotides on light-induced phase shift. *Neuroreport* 2001; 12: 127–131.

177. Albrecht U, Zheng B, Larkin D, et al. mPer1 and mPer2 are essential for normal resetting of the circadian clock. *J Biol Rhythms* 2001; 16: 100–104.

178. Wollnik F, Brysch W, Uhlmann E, et al. Block of c-Fos and JunB Expression by Antisense Oligonucleotides Inhibits Light-induced-Phase Shifts of the Mammalian Circadian Clock. *Eur J Neurosci* 1995; 7: 388–393.

179. Shimomura K, Kornhauser JM, Wisor JP, et al. Circadian Behavior and Plasticity of Light-Induced c-fos Expression in SCN of tau Mutant Hamsters. *J Biol Rhythms* 1998; 13: 305–314.

180. Trávníčková Z, Sumová A, Peters R, et al. Photoperiod-dependent correlation between light-induced SCN c-fos expression and resetting of circadian phase. *Am J Physiol - Regul Integr Comp Physiol* 1996; 271: R825-831.

181. Ryseck RP, Bravo R. c-JUN, JUN B, and JUN D differ in their binding affinities to AP-1 and CRE consensus sequences: Effect of FOS proteins. *Oncogene* 1991; 6: 533–542.

182. Takeuchi J, Shannon W, Aronin N, et al. Compositional changes of AP-1 DNA-binding proteins are regulated by light in a mammalian circadian clock. *Neuron* 1993; 11: 825–836.

183. Schwartz WJ, Carpino A, De La Iglesia HO, et al. Differential regulation of fos family genes in the ventrolateral and dorsomedial subdivisions of the rat suprachiasmatic nucleus. *Neuroscience* 2000; 98: 535–547.

184. Motzkus D, Loumi S, Cadenas C, et al. Activation of human period-1 by PKA or CLOCK/BMAL1 is conferred by separate signal transduction pathways. *Chronobiol Int* 2007; 24: 783–792.

185. Bonsall DR, Lall GS. Protein kinase C differentially regulates entrainment of the mammalian circadian clock. *Chronobiol Int* 2013; 30: 460–469.

186. Bult A, Smale L. Distribution of Ca2+-dependent protein kinase C isoforms in the suprachiasmatic nucleus of the diurnal murid rodent, Arvicanthis niloticus. *Brain Res* 1999; 816: 190–199.

187. Ishida Y, Yagita K, Fukuyama T, et al. Constitutive expression and delayed light response of casein kinase Iε and Iδ mRNAs in the mouse suprachiasmatic nucleus. *J Neurosci Res* 2001; 64: 612–616.

188. Shimomura K, Menaker M. Light-Induced Phase Shifts in tau Mutant Hamsters. *J Biol Rhythms* 1994; 9: 97–110.

189. Agostino P V., Harrington ME, Ralph MR, et al. Casein kinase-1-epsilon (CK1ε) and circadian photic responses in hamsters. *Chronobiol Int* 2009; 26: 126–133.

190. Zhang Y, Takahashi JS, Turek FW. Critical period for cycloheximide blockade of light-induced phase advances of the circadian locomotor activity rhythm in golden hamsters. *Brain Res* 1996; 740: 285–290.

191. Harrington ME, Hoque S, Hall A, et al. Pituitary adenylate cyclase activating peptide phase shifts circadian rhythms in a manner similar to light. *J Neurosci* 1999; 19: 6637–6642.

192. Nielsen HS, Hannibal J, Knudsen SM, et al. Pituitary adenylate cyclase-activating polypeptide induces period1 and period2 gene expression in the rat suprachiasmatic nucleus during late night. *Neuroscience* 2001; 103: 433–441.

193. Chen D, Buchanan GF, Ding JM, et al. Pituitary adenylyl cyclase-activating peptide: A pivotal modulator of glutamatergic regulation of the suprachiasmatic circadian clock. *Proc Natl Acad Sci U S A* 1999; 96: 13468–13473.

194. Hannibal J, Ding JM, Chen D, et al. Pituitary Adenylate Cyclase-Activating Peptide (PACAP) in the Retinohypothalamic Tract: A Potential Daytime Regulator of the Biological Clock. *J Neurosci* 1997; 17: 2637–2644.

195. Lindberg PT, Mitchell JW, Burgoon PW, et al. Pituitary Adenylate Cyclase-Activating Peptide (PACAP)-Glutamate Co-transmission Drives Circadian Phase-Advancing Responses to Intrinsically Photosensitive Retinal Ganglion Cell Projections by Suprachiasmatic Nucleus. *Front Neurosci* 2019; 13: 1281.

196. Michel S, Itri J, Han JH, et al. Regulation of glutamatergic signalling by PACAP in the mammalian suprachiasmatic nucleus. *BMC Neurosci* 2006; 7: 15.

197. Butcher GQ, Lee B, Cheng HYM, et al. Light stimulates MSK1 activation in the suprachiasmatic nucleus via a PACAP-ERK/MAP kinase-dependent mechanism. *J Neurosci* 2005; 25: 5305–5313.

198. Golombek DA, Biello SM, Rendon RA, et al. Neuropeptide Y phase shifts the circadian clock in vitro via a Y2 receptor. *Neuroreport* 1996; 7: 1315–1319.

199. Lall GS, Biello SM. Attenuation of circadian light induced phase advances and delays by neuropeptide y and a neuropeptide Y Y1/Y5 receptor agonist. *Neuroscience* 2003; 119: 611–618.

200. Rusak B, Meijer JH, Harrington ME. Hamster circadian rhythms are phase-shifted by electrical stimulation of the geniculo-hypothalamic tract. *Brain Res* 1989; 493: 283–291.

201. Biello SM, Golombek DA, Schak KM, et al. Circadian phase shifts to neuropeptide Y in vitro: Cellular communication and signal transduction. *J Neurosci* 1997; 17: 8468–8475.

202. Huhman KL, Gillespie CF, Marvel CL, et al. Neuropeptide Y phase shifts circadian rhythms in vivo via a Y2 receptor. *Neuroreport* 1996; 7: 1249–1252.

203. Fukuhara C, Brewer JM, Dirden JC, et al. Neuropeptide Y rapidly reduces Period 1 and Period 2 mRNA levels in the hamster suprachiasmatic nucleus. *Neurosci Lett* 2001; 314: 119–22.

204. Smith BN, Sollars PJ, Dudek FE, et al. Serotonergic modulation of retinal input to the mouse suprachiasmatic nucleus mediated by 5-HT1B and 5-HT7 receptors. *J Biol Rhythms* 2001; 16: 25–38.

205. Bramley JR, Sollars PJ, Pickard GE, et al. 5-HT1B receptor-mediated presynaptic inhibition of GABA release in the suprachiasmatic nucleus. *J Neurophysiol* 2005; 19: 4034–4045.

206. Edgar DM, Dean RR, Dement WC, et al. Serotonin and the Mammalian Circadian System: II. Phase-Shifting Rat Behavioral Rhythms with Serotonergic Agonists. *J Biol Rhythms* 1993; 8: 17–31.

207. Christopher Ehlen J, Grossman GH, David Glass J. In vivo resetting of the hamster circadian clock by 5-HT7 receptors in the suprachiasmatic nucleus. *J Neurosci* 2001; 21: 5351–5357.

208. Horikawa K, Yokota S, Fuji K, et al. Nonphotic entrainment by 5-HT 1A/7 receptor agonists accompanies by reduced Per1 and Per2 mRNA levels in the suprachiasmatic nuclei. *J Neurosci* 2000; 20: 5867–5873.

209. McArthur AJ, Hunt AE, Gillette MU. Melatonin action and signal transduction in the rat suprachiasmatic circadian clock: Activation of protein kinase C at dusk and dawn. *Endocrinology* 1997; 138: 627–634.

210. Hunt AE, Al-Ghoul WM, Gillette MU, et al. Activation of MT2 melatonin receptors in rat suprachiasmatic nucleus phase advances the circadian clock. *Am J Physiol - Cell Physiol* 2001; 280: C110-118.

211. Kandalepas PC, Mitchell JW, Gillette MUG. Melatonin signal transduction pathways require E-Box-Mediated transcription of Per1 and Per2 to reset the SCN clock at dusk. *PLoS One* 2016; 11: e0157824.

212. Sack RL, Brandes RW, Kendall AR, et al. Entrainment of Free-Running Circadian Rhythms by Melatonin in Blind People. *N Engl J Med* 2000; 343: 1070–1077.

213. Piggins HD, Antle MC, Rusak B. Neuropeptides phase shift the mammalian circadian pacemaker. *J Neurosci* 1995; 15: 5612–5622.

214. Reed HE, Meyer-Spasche A, Cutler DJ, et al. Vasoactive intestinal polypeptide (VIP) phase-shifts the rat suprachiasmatic nucleus clock in vitro. *Eur J Neurosci* 2001; 13: 839–843.

215. Cutler DJ, Haraura M, Reed HE, et al. The mouse VPAC2 receptor confers suprachiasmatic nuclei cellular rhythmicity and responsiveness to vasoactive intestinal polypeptide in vitro. *Eur J Neurosci* 2003; 17: 197–204.

216. Nielsen HS, Hannibal J, Fahrenkrug J. Vasoactive intestinal polypeptide induces per1 and per2 gene expression in the rat suprachiasmatic nucleus late at night. *Eur J Neurosci* 2002; 15: 570–574.

217. Maywood ES, Mrosovsky N, Field MD, et al. Rapid down-regulation of mammalian Period genes during behavioral resetting of the circadian clock. *Proc Natl Acad Sci U S A* 1999; 96: 15211–15216.

218. Hamada T, Antle MC, Silver R. The role of Period1 in non-photic resetting of the hamster circadian pacemaker in the suprachiasmatic nucleus. *Neurosci Lett* 2004; 362: 87–90.

219. Biello SM, Golombek DA, Harrington ME. Neuropeptide Y and glutamate block each other's phase shifts in the suprachiasmatic nucleus in vitro. *Neuroscience* 1997; 77: 1049–1057.

220. McKinley Brewer J, Yannielli PC, Harrington ME. Neuropeptide Y differentially suppresses per1 and per2 mRNA induced by light in the suprachiasmatic nuclei of the golden hamster. *J Biol Rhythms* 2002; 17: 28–39.

221. Pickard GE, Weber ET, Scott PA, et al. 5HT(1B) receptor agonists inhibit light-induced phase shifts of behavioral circadian rhythms and expression of the immediate-early gene c- fos in the suprachiasmatic nucleus. *J Neurosci* 1996; 16: 8208–8220.

222. Mendoza J, Graff C, Dardente H, et al. Feeding cues alter clock gene oscillations and photic responses in the suprachiasmatic nuclei of mice exposed to a light/dark cycle. *J Neurosci* 2005; 25: 1514–1522.

223. Travnickova-Bendova Z, Cermakian N, Reppert SM, et al. Bimodal regulation of mPeriod promoters by CREB-dependent signaling and CLOCK/BMAL1 activity. *Proc Natl Acad Sci U S A* 2002; 99: 7728–7733.

224. Caldelas I, Challet E, Saboureau M, et al. Light and melatonin inhibit in vivo serotonergic phase advances without altering serotonergic-induced decrease of Per expression in the hamster suprachiasmatic nucleus. *J Mol Neurosci* 2005; 25: 53–63.

225. Schmutz I, Chavan R, Ripperger JA, et al. A specific role for the REV-ERBα-controlled L-type voltage-gated calcium channel Cav1.2 in resetting the circadian clock in the late night. *J Biol Rhythms* 2014; 29: 288–298.

226. Mathur A, Golombek DA, Ralph MR. cGMP-dependent protein kinase inhibitors block light-induced phase advances of circadian rhythms in vivo. *Am J Physiol - Regul Integr Comp Physiol* 1996; 270: R1031–R1036.

227. Weber ET, Gannon RL, Rea MA. cGMP-dependent protein kinase inhibitor blocks light-induced phase advances of circadian rhythms in vivo. *Neurosci Lett* 1995; 197: 227–230.

228. Plano SA, Agostino P V., de la Iglesia HO, et al. cGMP-phosphodiesterase inhibition enhances photic responses and synchronization of the biological circadian clock in rodents. *PLoS One* 2012; 7: e37121.

229. Tischkau SA, Weber ET, Abbott SM, et al. Circadian clock-controlled regulation of cGMP-protein kinase G in the nocturnal domain. *J Neurosci* 2003; 23: 7543–7550.

230. Gudi T, Casteel DE, Vinson C, et al. NO activation of fos promoter elements requires nuclear translocation of G-kinase I and CREB phosphorylation but is independent of map kinase activation. *Oncogene* 2000; 19: 6324–6333.

231. Oster H, Werner C, Magnone MC, et al. cGMP-dependent protein kinase II modulates mPer1 and mPer2 gene induction and influences phase shifts of the circadian clock. *Curr Biol* 2003; 13: 725–733.

232. Wang LM, Schroeder A, Loh D, et al. Role for the NR2B subunit of the N-methyl-D-aspartate receptor in mediating light input to the circadian system. *Eur J Neurosci* 2008; 27: 1771–1779.

233. Pennartz CMA, Hamstra R, Geurtsen AMS. Enhanced NMDA receptor activity in retinal inputs to the rat suprachiasmatic nucleus during the subjective night. *J Physiol* 2001; 532: 181–194.

234. Terajima H, Yoshitane H, Yoshikawa T, et al. A-to-I RNA editing enzyme ADAR2 regulates light-induced circadian phase-shift. *Sci Rep* 2018; 8: 14848.

235. Míková H, Kuchtiak V, Svobodová I, et al. Circadian Regulation of GluA2 mRNA Processing in the Rat Suprachiasmatic Nucleus and Other Brain Structures. *Mol Neurobiol* 2021; 58: 439–449.

236. Cheng HYM, Dziema H, Papp J, et al. The molecular gatekeeper Dexras1 sculpts the photic responsiveness of the mammalian circadian clock. *J Neurosci* 2006; 26: 129.

237. Rohling JHT, VanderLeest HT, Michel S, et al. Phase resetting of the mammalian circadian clock relies on a rapid shift of a small population of pacemaker neurons. *PLoS One* 2011; 6: e25437.

238. Maywood ES, Chesham JE, O'Brien JA, et al. A diversity of paracrine signals sustains molecular circadian cycling in suprachiasmatic nucleus circuits. *Proc Natl Acad Sci U S A* 2011; 108: 14306–14311.

239. Harmar AJ, Marston HM, Shen S, et al. The VPAC2 receptor is essential for circadian function in the mouse suprachiasmatic nuclei. *Cell* 2002; 109: 497–508.

240. Aton SJ, Colwell CS, Harmar AJ, et al. Vasoactive intestinal polypeptide mediates circadian rhythmicity and synchrony in mammalian clock neurons. *Nat Neurosci* 2005; 8: 476–483.

241. Maywood ES, Reddy AB, Wong GKY, et al. Synchronization and maintenance of timekeeping in suprachiasmatic circadian clock cells by neuropeptidergic signaling. *Curr Biol* 2006; 16: 599–605.

242. Patton AP, Edwards MD, Smyllie NJ, et al. The VIP-VPAC2 neuropeptidergic axis is a cellular pacemaking hub of the suprachiasmatic nucleus circadian circuit. *Nat Commun* 2020; 11: 3394.

243. To TL, Henson MA, Herzog ED, et al. A molecular model for intercellular synchronization in the mammalian circadian clock. *Biophys J* 2007; 92: 3792–3803.

244. An S, Irwin RP, Allen CN, et al. Vasoactive intestinal polypeptide requires parallel changes in adenylate cyclase and phospholipase C to entrain circadian rhythms to a predictable phase. *J Neurophysiol* 2011; 105: 2289–2296.

245. Hamnett R, Crosby P, Chesham JE, et al. Vasoactive intestinal peptide controls the suprachiasmatic circadian clock network via ERK1/2 and DUSP4 signalling. *Nat Commun* 2019; 10: 542.

246. Brancaccio M, Maywood ES, Chesham JE, et al. A Gq-Ca2+ Axis controls circuit-level encoding of circadian time in the suprachiasmatic nucleus. *Neuron* 2013; 78: 714–728.

247. Liu C, Reppert SM. GABA synchronizes clock cells within the suprachiasmatic circadian clock. *Neuron* 2000; 25: 123–128.

248. Albus H, Vansteensel MJ, Michel S, et al. A GABAergic mechanism is necessary for coupling dissociable ventral and dorsal regional oscillators within the circadian clock. *Curr Biol* 2005; 15: 886–893.

249. Plano SA, Agostino P V., Golombek DA. Extracellular nitric oxide signaling in the hamster biological clock. *FEBS Lett* 2007; 581: 5500–5504.

250. Best JD, Maywood ES, Smith KL, et al. Rapid resetting of the mammalian circadian clock. *J Neurosci*.

251. Watanabe K, Deboer T, Meijer JH. Light-induced resetting of the circadian pacemaker: Quantitative analysis of transient versus steady-state phase shifts. *J Biol Rhythms* 2001; 16: 564–573.

252. Asai M, Yamaguchi S, Isejima H, et al. Visualization of mPer1 transcription in vitro: NMDA induces a rapid phase shift of mPer1 gene in cultured SCN. *Curr Biol* 2001; 11: 1524–1527.

253. Nagano M, Adachi A, Nakahama KI, et al. An abrupt shift in the day/night cycle causes desynchrony in the mammalian circadian center. *J Neurosci* 2003; 23: 6141–6151.

254. Davidson AJ, Castanon-Cervantes O, Leise TL, et al. Visualizing jet lag in the mouse suprachiasmatic nucleus and peripheral circadian timing system. *Eur J Neurosci* 2009; 29: 171–180.

255. Nakamura W, Yamazaki S, Takasu NN, et al. Differential response of Period 1 expression within the suprachiasmatic nucleus. *J Neurosci* 2005; 25: 5481–5487.

256. Deisseroth K. Optogenetics: 10 years of microbial opsins in neuroscience. *Nat Neurosci* 2015; 18: 1213–1225.

257. Zhang F, Vierock J, Yizhar O, et al. The microbial opsin family of optogenetic tools. *Cell* 2011; 147: 1446–1457.

258. Nagel G, Ollig D, Fuhrmann M, et al. Channelrhodopsin-1: A light-gated proton channel in green algae. *Science* 2002; 296: 2395–2398.

259. Nagel G, Szellas T, Huhn W, et al. Channelrhodopsin-2, a directly light-gated cation-selective membrane channel. *Proc Natl Acad Sci* 2003; 100: 13940–13945.

260. Boyden ES, Zhang F, Bamberg E, et al. Millisecond-timescale, genetically targeted optical control of neural activity. *Nat Neurosci* 2005; 8(9):1263-: 1263–1268.

261. Lima SQ, Miesenböck G. Remote control of behavior through genetically targeted photostimulation of neurons. *Cell* 2005; 121: 141–152.

262. Aravanis AM, Wang LP, Zhang F, et al. An optical neural interface: in vivo control of rodent motor cortex with integrated fiberoptic and optogenetic technology. *J Neural Eng* 2007; 4: S143-156.

263. Christie JM, Gawthorne J, Young G, et al. LOV to BLUF: Flavoprotein contributions to the optogenetic toolkit. *Mol Plant* 2012; 5: 533–544.

264. Gao S, Nagpal J, Schneider MW, et al. Optogenetic manipulation of cGMP in cells and animals by the tightly light-regulated guanylyl-cyclase opsin CyclOp. *Nat Commun* 2015; 6: 8046.

265. Schröder-Lang S, Schwärzel M, Seifert R, et al. Fast manipulation of cellular cAMP level by light in vivo. *Nat Methods* 2007; 4: 39–42.

266. Beyer HM, Naumann S, Weber W, et al. Optogenetic control of signaling in mammalian cells. *Biotechnol J* 2015; 10: 273–283.

267. Konermann S, Brigham MD, Trevino AE, et al. Optical control of mammalian endogenous transcription and epigenetic states. *Nature* 2013; 500: 472–476.

268. Müller K, Naumann S, Weber W, et al. Optogenetics for gene expression in mammalian cells. *Biol Chem* 2015; 396: 145–152.

269. Stierl M, Penzkofer A, Kennis JTM, et al. Key residues for the light regulation of the blue light-activated adenylyl cyclase from Beggiatoa sp. *Biochemistry* 2014; 53: 5121–5130.

270. Ryu MH, Moskvin O V., Siltberg-Liberles J, et al. Natural and engineered photoactivated nucleotidyl cyclases for optogenetic applications. *J Biol Chem* 2010; 285: 41501–41508.

271. Stierl M, Stumpf P, Udwari D, et al. Light modulation of cellular cAMP by a small bacterial photoactivated adenylyl cyclase, bPAC, of the soil bacterium Beggiatoa. *J Biol Chem* 2011; 286: 1181–1188.

272. Hartmann A, Arroyo-Olarte RD, Imkeller K, et al. Optogenetic modulation of an adenylate cyclase in toxoplasma gondii demonstrates a requirement of the parasite cAMP for host-cell invasion and stage differentiation. *J Biol Chem* 2013; 288: 13705–13717.

273. Luyben TT, Rai J, Li H, et al. Optogenetic Manipulation of Postsynaptic cAMP Using a Novel Transgenic Mouse Line Enables Synaptic Plasticity and Enhances Depolarization Following Tetanic Stimulation in the Hippocampal Dentate Gyrus. *Front Neural Circuits* 2020; 14: 24.

274. Gancedo JM. Biological roles of cAMP: Variations on a theme in the different kingdoms of life. *Biol Rev* 2013; 88: 645–668.

275. Motzkus D, Maronde E, Grunenberg U, et al. The human PER1 gene is transcriptionally regulated by multiple signaling pathways. *FEBS Lett* 2000; 486: 315–319.

276. Prosser RA, Gillette MU. The mammalian circadian clock in the suprachiasmatic nuclei is reset in vitro by cAMP. *J Neurosci* 1989; 9: 1073–1081.

277. Prosser RA, Gillette MU. Cyclic changes in cAMP concentration and phosphodiesterase activity in a mammalian circadian clock studied in vitro. *Brain Res* 1991; 568: 185–192.

278.   Ferreyra GA, Golombek DA. Cyclic AMP and protein kinase A rhythmicity in the mammalian suprachiasmatic nuclei. *Brain Res* 2000; 858: 33–39.

279.   O'Neill JS, Maywood ES, Chesham JE, et al. cAMP-dependent signaling as a core component of the mammalian circadian pacemaker. *Science* 2008; 320: 949–953.

280.   O'Neill JS, Reddy AB. The essential role of cAMP/Ca 2+ signalling in mammalian circadian timekeeping. *Biochem Soc Trans* 2012; 40: 44–50.

281.   Doi M, Ishida A, Miyake A, et al. Circadian regulation of intracellular G-protein signalling mediates intercellular synchrony and rhythmicity in the suprachiasmatic nucleus. *Nat Commun* 2011; 2: 327.

282.   Balsalobre A, Marcacci L, Schibler U. Multiple signaling pathways elicit circadian gene expression in cultured Rat-1 fibroblasts. *Curr Biol* 2000; 10: 1291–1294.

283.   Akashi M, Nishida E. Involvement of the MAP kinase cascade in resetting of the mammalian circadian clock. *Genes Dev* 2000; 14: 645–649.

284.   Yagita K, Okamura H. Forskolin induces circadian gene expression of rPer1, rPer2 and dbp in mammalian rat-1 fibroblasts. *FEBS Lett* 2000; 465: 79–82.

285.   Nagoshi E, Saini C, Bauer C, et al. Circadian gene expression in individual fibroblasts: Cell-autonomous and self-sustained oscillators pass time to daughter cells. *Cell* 2004; 119: 693–705.

286.   Imanishi M, Nakamura A, Doi M, et al. Control of circadian phase by an artificial zinc finger transcription regulator. *Angew Chemie - Int Ed* 2011; 50: 9396–9399.

287.   Bailes HJ, Milosavljevic N, Zhuang L-Y, et al. Optogenetic interrogation reveals separable G-protein-dependent and -independent signalling linking G-protein-coupled receptors to the circadian oscillator. *BMC Biol* 2017; 15: 40.

288.   Jones JR, Tackenberg MC, McMahon DG. Manipulating circadian clock neuron firing rate resets molecular circadian rhythms and behavior. *Nat Neurosci* 2015; 18: 373–375.

289.   Vollmers C, Panda S, Di Tacchio L. A high-throughput assay for siRNA-based circadian screens in human U20S cells. *PLoS One* 2008; 3: e3457.

290.   Hoffmann J, Symul L, Shostak A, et al. Non-circadian expression masking clock-driven weak transcription rhythms in U2OS Cells. *PLoS One* 2014; 9: e102238.

291.   Gossen M, Freundlieb S, Bender G, et al. Transcriptional activation by tetracyclines in mammalian cells. *Science* 1995; 268: 1766–1769.

292.   Brown SA, Fleury-Olela F, Nagoshi E, et al. The period length of fibroblast circadian gene expression varies widely among human individuals. *PLoS Biol* 2005; 3: e338.

293.   Maier B, Wendt S, Vanselow JT, et al. A large-scale functional RNAi screen reveals a role for CK2 in the mammalian circadian clock. *Genes Dev* 2009; 23: 708–718.

294.   Addgene. Plasmid # 28134, http://n2t.net/addgene:28134 (accessed 12 January 2016).

295.   Cell Biolabs. pAAV-GFP Control Vector, https://www.cellbiolabs.com/sites/default/files/AAV-400-Map.jpg (accessed 2 July 2020).

296.   New England Biolabs. Tm Calculator, https://tmcalculator.neb.com/#!/batch (accessed 2 July 2020).

297.   Seamon KB, Padgett W, Daly JW. Forskolin: unique diterpene activator of adenylate cyclase in membranes and in intact cells. *Proc Natl Acad Sci U S A* 1981; 78: 3363–3367.

298. Pfaffl MW. A new mathematical model for relative quantification in real-time RT-PCR. *Nucleic Acids Res* 2001; 29: e45.

299. Azevedo MF, Faucz FR, Bimpaki E, et al. Clinical and molecular genetics of the phosphodiesterases (PDEs). *Endocr Rev* 2014; 35: 195–233.

300. Wang Y, Yin J, Weng W, et al. Kinetic study of the degradation of forskolin in aqueous systems by stability-indicating HPLC method and identification of its degradation products. *J Liq Chromatogr Relat Technol* 2016; 39: 44–49.

301. Yamazaki S, Numano R, Abe M, et al. Resetting central and peripheral circadian oscillators in transgenic rats. *Science* 2000; 288: 682–685.

302. Maronde E, Motzkus D. Oscillation of human period 1 (hPER1) reporter gene activity in human neuroblastoma cells in vivo. *Chronobiol Int* 2003; 20: 671–681.

303. Hinoi E, Ueshima T, Hojo H, et al. Up-regulation of per mRNA expression by parathyroid hormone through a protein kinase A-CREB-dependent mechanism in chondrocytes. *J Biol Chem* 2006; 281: 23632–23642.

304. Prosser RA, McArthur AJ, Gillette MU. cGMP induces phase shifts of a mammalian circadian pacemaker at night, in antiphase to cAMP effects. *Proc Natl Acad Sci U S A* 1989; 86: 6812–6815.

305. Reinke H, Saini C, Fleury-Olela F, et al. Differential display of DNA-binding proteins reveals heat-shock factor 1 as a circadian transcription factor. *Genes Dev* 2008; 22: 331–345.

306. Tamaru T, Hattori M, Honda K, et al. Synchronization of circadian Per2 rhythms and HSF1-BMAL1:clock interaction in mouse fibroblasts after Short-Term heat shock pulse. *PLoS One* 2011; 6: e24521.

307. Saini C, Morf J, Stratmann M, et al. Simulated body temperature rhythms reveal the phase-shifting behavior and plasticity of mammalian circadian oscillators. *Genes Dev* 2012; 26: 567–580.

308. Morf J, Rey G, Schneider K, et al. Cold-inducible RNA-binding protein modulates circadian gene expression posttranscriptionally. *Science* 2012; 338: 379–383.

309. DeBruyne JP, Noton E, Lambert CM, et al. A Clock Shock: Mouse CLOCK Is Not Required for Circadian Oscillator Function. *Neuron* 2006; 50: 465–477.

310. Colotta F, Polentarutti N, Staffico M, et al. Heat shock induces the transcriptional activation of c-fos protooncogene. *Biochem Biophys Res Commun* 1990; 168: 1013–1019.

311. Andrews GK, Harding MA, Calvet JP, et al. The heat shock response in HeLa cells is accompanied by elevated expression of the c-fos proto-oncogene. *Mol Cell Biol* 1987; 7: 3452–3458.

312. Sumová A, Trávníčková Z, Mikkelsen JD, et al. Spontaneous rhythm in c-Fos immunoreactivity in the dorsomedial part of the rat suprachiasmatic nucleus. *Brain Res* 1998; 801: 254–258.

313. Lonze BE, Ginty DD. Function and regulation of CREB family transcription factors in the nervous system. *Neuron* 2002; 35: 605–623.

314. Zhang X, Odom DT, Koo SH, et al. Genome-wide analysis of cAMP-response element binding protein occupancy, phosphorylation, and target gene activation in human tissues. *Proc Natl Acad Sci U S A* 2005; 102: 4459–4464.

315. Impey S, McCorkle SR, Cha-Molstad H, et al. Defining the CREB regulon: A genome-wide analysis of transcription factor regulatory regions. *Cell* 2004; 119: 1041–1054.

316. Mayr B, Montminy M. Transcriptional regulation by the phosphorylation-dependent factor creb. *Nature Reviews Molecular Cell Biology* 2001; 2: 599–609.

317. Cha-Molstad H, Keller DM, Yochum GS, et al. Cell-type-specific binding of the transcription factor CREB to the cAMP-response element. *Proc Natl Acad Sci U S A* 2004; 101: 13572–13577.

318. Efetova M, Petereit L, Rosiewicz K, et al. Separate roles of PKA and EPAC in renal function unraveled by the optogenetic control of cAMP levels in vivo. *J Cell Sci* 2013; 126: 778–788.

319. Jansen V, Alvarez L, Balbach M, et al. Controlling fertilization and cAMP signaling in sperm by optogenetics. *Elife* 2015; 4: e05161.

320. De Marco RJ, Groneberg AH, Yeh C-M, et al. Optogenetic elevation of endogenous glucocorticoid level in larval zebrafish. *Front Neural Circuits* 2013; 7: 82.

321. Zhang F, Tzanakakis ES. Optogenetic regulation of insulin secretion in pancreatic β-cells. *Sci Rep* 2017; 7: 1–10.

322. O'Banion CP, Vickerman BM, Haar L, et al. Compartmentalized cAMP Generation by Engineered Photoactivated Adenylyl Cyclases. *Cell Chem Biol* 2019; 26: 1393-1406.e7.

323. Gerhardt KP, Olson EJ, Castillo-Hair SM, et al. An open-hardware platform for optogenetics and photobiology. *Sci Rep* 2016; 6: 35363.

324. Tso CF, Simon T, Greenlaw AC, et al. Astrocytes Regulate Daily Rhythms in the Suprachiasmatic Nucleus and Behavior. *Curr Biol* 2017; 27: 1055–1061.

325. Brancaccio M, Patton AP, Chesham JE, et al. Astrocytes Control Circadian Timekeeping in the Suprachiasmatic Nucleus via Glutamatergic Signaling. *Neuron* 2017; 93: 1420-1435.e5.

326. Brancaccio M, Edwards MD, Patton AP, et al. Cell-autonomous clock of astrocytes drives circadian behavior in mammals. *Science* 2019; 363: 87–192.

327. Coward P, Wada HG, Falk MS, et al. Controlling signaling with a specifically designed Gi-coupled receptor. *Proc Natl Acad Sci U S A* 1998; 95: 352–357.

328. Conklin BR, Hsiao EC, Claeysen S, et al. Engineering GPCR signaling pathways with RASSLs. *Nat Methods* 2008; 5: 673–678.

329. Urban DJ, Roth BL. DREADDs (designer receptors exclusively activated by designer drugs): Chemogenetic tools with therapeutic utility. *Annu Rev Pharmacol Toxicol* 2015; 55: 399–417.

<u>Danksagung</u>

Abschließend möchte ich mich herzlich bei allen bedanken, die mich bei der Anfertigung dieser Dissertation unterstützt haben, und ohne die diese Arbeit nicht vollendet worden wäre.

Mein besonderer Dank gilt hierbei Prof. Dr. Henrik Oster für die Möglichkeit, diese Doktorarbeit in seinem Institut anzufertigen. Seiner exzellenten wissenschaftlichen Betreuung, der konstruktiven Denkanstöße und der kritischen Durchsicht ist das Gelingen dieser Arbeit zu verdanken.

Ein weiterer besonderer Dank gilt Dr. Anthony Tsang, welcher mir nachts (und tags) als Betreuer für wissenschaftliche Fragen und technische Unterstützung im Labor zu Verfügung stand.

Auch danke ich der Arbeitsgruppe Chronophysiologie für acht schöne und abwechslungsreiche Monate als Teil des Teams.

Zu guter Letzt geht ein großes Dankeschön an meine Frau, Dr. Larissa Schuchardt, für ihre moralische Unterstützung während des Schreibprozesses und das Korrekturlesen der Arbeit.

Lebenslauf

Name	Blaum
Vorname	Christopher Matthias
Geburtsdatum	16.07.1988 in Krefeld
Staatsangehörigkeit	deutsch

Berufliche Laufbahn

Seit 11/2017   Universitäres Herz- & Gefäßzentrum Hamburg
                    Klinik und Poliklinik für Kardiologie

07/2017   Approbation

Universitätslaufbahn

10/2010 – 06/2017   Universität zu Lübeck
                    Studium der Humanmedizin

Abschluss   1. Abschnitt der ärztlichen Prüfung   09/2012   1,5
                    2. Abschnitt der ärztlichen Prüfung   10/2015   1,0
                    3. Abschnitt der ärztlichen Prüfung   05/2017   1,0
                    Gesamtnote Ärztliche Prüfung   1,17 (sehr gut)

Praktisches Jahr   Innere Medizin (Universitätsklinikum Schleswig-Holstein, Lübeck)
05/2016 – 04/2017   Chirurgie (Sana Klinik Lübeck)
                    Pädiatrie (Great North Children's Hospital, Newcastle, Sana Klinik Eutin)

Promotion   Experimenteller Teil, ehemals Institut für Chronophysiologie der
11/2015 – 06/2016   Medizinischen Klinik I der Universität zu Lübeck

2006 – 2010   Jesus College, Cambridge University, UK
                    Studium der Naturwissenschaften (Schwerpunkt Chemie)
                    abgeschlossen mit dem Master of Science, MSci (Class I)

Schulbildung

2004 – 2006   Oundle School, Oundle (UK)
                    A Levels   Chemistry, Physics, Mathematics, Latin, Geography
                    AS Level   Further Mathematics
                    anerkannt als Allgemeine dt. Hochschulreife
                    Gesamtnote   1,0

1998 – 2004   Mataré Gymnasium, Meerbusch

Veröffentlichungen

Christopher Blaum, Anthony H.K. Tsang, Henrik Oster:

Optogenetische Steuerung zirkadianer Rhythmen

oder wie man durch Licht die innere Uhr verstellt

Posterpräsentation bei Uni im Dialog, Lübeck, Juni 2016